MATHEMATICAL MODELS OF BRUCELLOSIS INFECTION

PATTARAPAN KUMPAI

A Thesis Submitted to the Graduate School of Naresuan University
in Partial Fulfillment of the Requirements
for the Doctor of Philosophy Degree in Mathematics
March 2024

This thesis entitled "Mathematical models of Brucellosis infection"

by Pattarapan Kumpai

has been approved by the Graduate School as partial fulfillment of the requirements for the Doctor of Philosophy Degree in Mathematics of Naresuan University

Oral Defense Committee

..... Chair

(Associate Professor Sayan Kaennakham, Ph.D.)

..... Advisor

(Associate Professor Chairat Modnak, Ph.D.)

..... Internal Examiner

(Associate Professor Supaporn Suksern, Ph.D.)

..... Internal Examiner

(Associate Professor Ratchada Viriyapong, Ph.D.)

..... External Examiner

(Assistant Professor Benjawan Rodjanadid, Ph.D.)

Approved

.....

(Associate Professor Krongkarn Chootip, Ph.D.)

Dean of the Graduate School

13 MAR 2024

ACKNOWLEDGEMENT

First and foremost, I am extremely grateful to my advisor, Associate Professor Chairat Modnak, for his invaluable advice, continuous support, and patience during my Ph.D. studies. His constant guidance and feedback helped me throughout the entire research and thesis writing process.

Furthermore, I would like thank my thesis committees, Associate Professor Sayan Kaennakham, Associate Professor Supaporn Suksern, Associate Professor Ratchada Wiriyapong and Assistant Professor Benjawan Rodjanadid for their interest in my work and their valuable comments and suggestions.

I would like to extend my sincere thanks to the Science Achievement Scholarship of Thailand (SAST) for their support in financing my doctoral studies. Additionally, I would like to thank the Department of Mathematics, Faculty of Science at Naresuan University for facilitating places and others that are useful to support this thesis.

Finally, I would like to express my gratitude to my parents and friends for their encouragement and support throughout my studies. It is their kindness and support that has made my time at the university both enriching and wonderful.

Pattarapan Kumpai

Title	MATHEMATICAL MODELS OF BRUCELLOSIS INFECTION
Author	Pattarapan Kumpai
Advisor	Associate Professor Chairat Modnak, Ph.D.
Academic Paper	Ph.D. Dissertation in Mathematics, Naresuan University, 2023.
Keywords	Brucellosis, Mathematical model, Optimal control theory, Bifurcation analysis, Bovine-tuberculosis, Cost-effectiveness, Co-infection disease.

ABSTRACT

In this thesis, we present a bison brucellosis model with both direct and indirect transmissions from infected animals, including the chronic state, and the bacteria in the environment. Additionally, we assume that some of the recovered animals have temporary immunity. We derive the basic reproduction number, conduct equilibrium analysis, perform numerical simulations, and sensitivity analysis of the basic reproduction number in term of some parameters. Furthermore, an optimal control study is carried out to explore strategies involving culling, animal vaccination, and bacteria elimination. Our results show that the combined implementation of these three controls yields a significant reduction in the total number of both chronic and infectious animals. Meanwhile, we also formulate and analyze a deterministic mathematical model to describe the transmission dynamics of the brucellosis-bovine tuberculosis epidemic in animals. We first analyze two submodels, brucellosis and bovine tuberculosis submodels, and then investigate the basic reproduction number and perform equilibrium analysis for each one. Besides, we proceed to analyze the full brucellosis-bovine tuberculosis model and extend our model to an optimal control problem. The model includes culling infected animals and elimination of *Brucella* and *Mycobacterium Bovis* in the environment as control variables to minimize the total number of infected animals while minimizing the implementation costs. Finally, we compute the average cost-effectiveness ratio (ACER) and the incremental cost-effectiveness ratio (ICER) to examine the cost-effectiveness of all possible combinations of the three control measures. Our

findings indicate that the most cost-effective control strategy involves the implementation of a combined approach using all available controls. Additionally, in the final segment of our study, we engage in data fitting and compare our model with others. Through parameter adjustments, we demonstrate our capability to align our model with provided data.

LIST OF CONTENTS

Chapter **Page**

LIST OF CONTENTS (CONT.)

Chapter **Page**

LIST OF TABLES

Table **Page**

LIST OF FIGURES

Figure **Page**

LIST OF FIGURES (CONT.)

Figure **Page**

LIST OF FIGURES (CONT.)

Figure **Page**

LIST OF FIGURES (CONT.)

Figure **Page**

LIST OF FIGURES (CONT.)

Figure **Page**

CHAPTER I

INTRODUCTION

Zoonotic diseases have the potential to infect humans through either direct contact with infected animals or indirect means like contaminated food, water, or the environment. These diseases pose substantial public health concerns [1]. Brucellosis, recognized by various names such as undulant fever, Mediterranean fever, or Malta fever, is classified as a zoonotic disease. The transmission of this infection primarily occurs through direct or indirect interaction with infected animals or their byproducts [2]. Additionally, brucellosis can give rise to noteworthy economic and welfare challenges within livestock populations [3]. The disease is attributed to various bacteria within the *Brucella* family, which generally display an inclination to infect specific animal species. Nevertheless, it is important to note that many *Brucella* species possess the ability to infect diverse animal species as well [4]. Presently, this genus encompasses several distinct members, including *Brucella abortus* in cattle, *B. melitensis* in sheep and goats, *B. suis* in swine, *B. ovis* in livestock, *B. canis* in dogs, *B. ceti* and *B. pinnipedialis* in marine mammals, *B. neotomae* and *B. microti* in wild rodents, alongside a few other organisms that remain only partially understood [5]. The typical mode of Brucella transmission is from animal to animal through contact, often following an abortion event [2]. Elevated levels of the bacteria are usually present in the birth fluids of infected animals [4]. Moreover, the bacteria can be detected in the milk, blood, urine, and semen of afflicted animals [6]. Consequently, animals may contract the bacteria through oral ingestion, direct contact with mucous membranes (such as the eyes, nose, mouth), or openings in the skin. *Brucella* can also be transmitted through contaminated objects (fomites), such as equipment, clothing, shoes, hay, feed, or water [6]. The bacteria can survive outside the host animal in the environment for several months, especially in cool and moist conditions [4]. Nevertheless, it is highly susceptible to destruction by sunlight, high temperatures, and desiccation [7]. Moreover, brucellosis leads to substantial economic losses for farmers due to diminished animal production, including instances of abortion, stillbirth,

sterility, longer calving intervals, and reduced milk yields [8, 9]. In humans and animals, brucellosis ecology can be divided as acute (0-2 months), sub-acute (3-12 months), and chronic (more than 12 months) [10]. Moreover, it is worth noting that animals in the chronic state show no clinical signs of the disease and the majority of these animals would not be pregnant [11].

Mathematical models are used to analyze brucellosis outbreaks in some animal species. Moreover, they can be useful for a better understanding of disease dynamics and can be used as tools to seek effective control strategies for brucellosis. In 2013, Qiang Hou et al. [12] studied the transmission dynamics of sheep brucellosis in Inner Mongolia. They purposed a dynamic model for the sheep-human transmission of brucellosis, involving sheep population, human population, and brucella in the environment. In 2014, Gui-Quan Sun and Zi-ke Zhang [13] presented a sheep brucellosis model with immigration and proportional birth to include both direct and indirect transmission with infected animals, and the bacteria of the environment. In the same year, Ming-Tao et al. [14] presented a mathematical model that focused on the disease transmission between cattle and sheep populations on the same farm. The study shows that prohibiting mixed feeding in a public farm should remove mixed cross infection between sheep and cattle. In 2015, Emmanuel Abatih et al. [15] proposed a model for the transmission dynamics of brucellosis among bison. The model contains three subclasses; susceptible, infected, and recovered individuals. In 2017, Yang et al. [16] presented a nonlinear modeling framework to investigate the transmission dynamics of brucellosis, incorporating both the spatial and seasonal variations. In 2018, Lolika et al. [17] proposed an extended model in [15] to include an additional epidemiological class that accounts for animals in chronic state, a seasonal variation on disease transmission pathway, and time-dependent culling effort. In 2020, Nyerere et al. [18] presented a mathematical model for the impacts of different control options on the transmission dynamics of brucellosis. They focused on livestock vaccination, gradual culling through the slaughter of seropositive cattle and small ruminants, environmental hygiene and sanitation, and personal protection. However, this study did not include the animal recovered class with a waning vaccine or temporary immunity. In 2022, Stephen Abagna et al. [19] studied the transmission dynamics and control of bovine brucellosis in a herd of cattle.

We see that many papers have considered brucellosis in animals such as cattle and sheep, and there are only a few focused on bison. Also, there are studies mentioned before that environmental factors can cause both direct and indirect transmissions of brucellosis in a bison population. Thus, we have developed and extended the model of Lokika et al. [17]. We will investigate environmental factors as one of our interests, which will be relevant for places such as wildlife sanctuaries and national parks. Therefore, we have incorporated the subclass of *Brucella* present in the environment into our model. Since vaccination usually results in clinical disease elimination, we will also include vaccination control in our study. Also, we assume that some recovered animals can lose their immunity and are susceptibles to the disease since not many researchers have included this fact in their studies. We also conduct a rigorous analysis of the trivial and non-trivial equilibria of the system and establish their existence and stability where possible. Meanwhile, we perform an optimal control study for the model and seek effective strategies that best balance the outcomes of the controls in reducing the disease. Our modeling, simulation, and analysis focus on the complex interplay among the animal hosts, the vaccinated class, the chronic infectious bison, the environmental pathogen, and the recovered animals (temporary immunity).

On the other hand, bovine tuberculosis are major zoonotic diseases worldwide [20]. Bovine tuberculosis is a chronic bacterial disease of animals caused by the bacterium *Mycobacterium bovis* [21, 22]. It is a major infectious disease that mostly affects cattle, but it can also infect other domesticated animals and certain wildlife populations [22]. Hence, bovine tuberculosis has an important economic impact and threatens livelihoods [23]. In developed countries, Bovine tuberculosis is still common and significant economic losses can occur from livestock deaths, chronic disease, and trade restrictions. In some situations, this disease could also be a serious threat to endangered species [21]. Infected animals expel bacteria in milk, feces, respiratory secretions, and, less frequently, other bodily fluids [24]. It is possible to contract the disease through direct contact with infected domestic or wild animals or indirectly by ingesting contaminated material [22]. Cattle are infected by inhaling droplets (aerosol) that contain the bacteria. Furthermore, calves can be infected by ingesting colostrum or milk from infected cows [22, 24].

Bovine tuberculosis and brucellosis are significant zoonotic diseases of

global economic and public health importance, particularly in developing countries. These diseases further strain public health systems and hinder efforts to enhance livestock production and export [20]. The rapid expansion and intensification of livestock production are anticipated to lead to an increased prevalence of both brucellosis and bovine tuberculosis [25]. In Morocco, both diseases are endemic zoonoses in ruminants, impacting both animal and human health [25]. Furthermore, these two diseases are noteworthy milk-borne zoonoses, showing varying degrees of prevalence among Ethiopian cattle [26]. In Burkina Faso's Sahel and Hauts-Bassins regions, brucellosis and bovine tuberculosis are present on cattle farms, exhibiting high herd prevalence. Given the potential transmission of these diseases to humans through the consumption or handling of milk or meat from infected animals, this situation holds critical implications for public health [27]. Moreover, both diseases are easily transmissible to humans through the consumption of animal products like raw dairy or close contact with infected animals or animal tissues [26].

In 2008, Simeon and colleagues reported a case of co-infection involving brucellosis and tuberculosis in cattle slaughtered at the Bodija abattoir in Ibadan, Nigeria. This incident resulted in six animals being afflicted by both brucellosis and bovine tuberculosis [65]. In 2013, Gorisch et al. monitored 126 buffalo in South Africa for tuberculosis and brucellosis infections. It was noted that buffalo co-infected with both pathogens exhibited the highest mortality rates [29]. Additionally, Folitse et al. conducted a study in 2014 involving the testing of 444 cattle for tuberculosis and brucellosis using the single comparative intradermal tuberculin and Rose Bengal plate tests in Dormaa and Kintampo Districts, Brong Ahafo region, Ghana. According to their findings, a cow older than 5 years had both diseases, yielding a prevalence estimate of 0.23% [30].

Numerous mathematical models have been proposed to study the transmission of brucellosis only [12–19, 31–36], as illustrated above. Additionally, several mathematical models have been proposed and analyzed in bovine tuberculosis only [37–47]. As an illustration, in 2016, Patrick B. Phepa et al. [41] studied the transmission dynamics of bovine tuberculosis (BTB) in both buffalo and cattle populations. In the same year, Tasmi et al. [46] discussed a model for the transmission of badger tuberculosis with vaccination. In 2017, Mahamat Fayiz Abakar

et al. [47] established a mathematical model for BTB transmission in cattle and humans in Morocco to provide a general understanding of BTB. However, these studies did not focus on the co-infection of brucellosis and bovine tuberculosis within a single host population.

Recently, Lolika et al. [48] introduced a framework for modeling co-infection of brucellosis and tuberculosis. They incorporated all pertinent biological factors and considered culling of infected animals as the primary intervention strategy. Furthermore, they conducted an optimal control study to assess the impact of culling infectious animals on the prevalence of both infections. Nonetheless, this study did not take into account the influence of *Brucella* and *Mycobacterium bovis* in the environment.

In our thesis, we have developed a co-infection model that encompasses both brucellosis and bovine tuberculosis infections, while also incorporating additional environmental factors. Concurrently, we undertake an optimal control analysis of the model, with the goal of identifying the most effective strategies to mitigate disease transmission. Our approach initiates with the formulation of a comprehensive mathematical model that captures the dynamics of co-infection and the associated environmental variables. Following this, we carry out analyses of disease dynamics. Lastly, we conduct numerical simulations to explore an optimal control problem, aiming to pinpoint cost-effective measures for disease management. Moreover, we engage in real data fitting and compare our model with other existing models to further enhance the depth of our investigation.

This thesis is organized as follows: Chapter 2, we introduce lemmas and theories important for our model. Additionally, we present some interesting mathematical models related to the transmission of brucellosis and bovine tuberculosis. The establishment and analysis of the mathematical model for Brucellosis infection in bison were presented in Chapter 3. Furthermore, in Chapter 4, we develop and scrutinize a mathematical model for the co-infection of brucellosis and bovine tuberculosis, along with exploring the optimal cost-effective control strategies for this model. A discussion and conclusion are given in Chapter 5.

CHAPTER II

PRELIMINARIES

2.1 Lemma and theories

2.1.1 The basic reproduction number

The next-generation matrix is a method used to derive the basic reproduction number for a compartmental model of the spread of infectious diseases. It calculates the basic reproduction number by dividing the population into n compartments. Let $x = (x_1, ..., x_n)^t$, where each $x_i \geq 0$ represents the number of individuals in each compartment, whereas m compartments correspond to infected individuals. Moreover $X_s = \left\{ x \geq 0 : x_i = 0,\ i = 1, ..., m \right\}$ is defined as the set of all disease free states. Let $\mathcal{F}_i(x)$ be the rate at which new infections emerge in compartment i. $\mathcal{V}_i^+(x)$ denotes the rate of people entering the compartment i, and $\mathcal{V}_i^-(x)$ denotes the rate of people leaving the compartment i. The disease transmission model consists of nonnegative initial conditions together with the following system of equations:

$$\frac{dx_i}{dt} = f_i(x) = \mathcal{F}_i(x) - \mathcal{V}_i(x) \tag{2.1.1}$$

where $\mathcal{V}_i(x) = \mathcal{V}_i^-(x) - \mathcal{V}_i^+(x)$ and the functions satisfy assumptions (A1)–(A5) described below.

(A1) If $x \geq 0$, then $\mathcal{F}_i$, $\mathcal{V}_i^+$, $\mathcal{V}_i^- \geq 0$ for $i = 1, ..., m$.

(A2) If $x_i = 0$, then $\mathcal{V}_i^- = 0$. In particular, if $x \in X_s$ then $\mathcal{V}_i^- = 0$ for $i = 1, \ldots, m$.

(A3) $\mathcal{F}_i > 0$ if $i > m$.

(A4) If $x \in X_s$, then $\mathcal{F}_i(x) = 0$ and $\mathcal{V}_i^+(x) = 0$ for $i = 1, ..., m$.

(A5) If $\mathcal{F}(x)$ is set to zero, then all eigenvalues of $Df(x_0)$ have a negative real part. Here, $Df(x_0)$ represents the derivative $[\partial f_i / \partial x_j]$ evaluated at the disease-free equilibrium point x_0, i.e., the Jacobian matrix.

Let x_0 be the disease-free equilibrium point of (2.1.1), and let $f_i(x)$ satisfy (A1)–(A5). We have F and V as $m \times m$ matrices defined by:

$$F = \left[\frac{\partial \mathcal{F}_i}{\partial x_j}(x_0)\right] \quad \text{and} \quad V = \left[\frac{\partial \mathcal{V}_i}{\partial x_j}(x_0)\right] \; for \; 1 \leq i, j \leq m.$$

The matrix FV^{-1} is referred to as the next-generation matrix for the model. The basic reproduction number, denoted as $(\mathcal{R}_0)$, for the model is the spectral radius of FV^{-1}.

Theorem 2.1.1. [49] *Consider the disease transmission model given by* (2.1.1) *with* $f(x)$ *satisfying condition* $(A1)$–$(A5)$. *If* x_0 *is a disease-free equilibrium of model, then* x_0 *is locally asymptotically stable if* $\mathcal{R}_0 < 1$, *but unstable if* $\mathcal{R}_0 > 1$.

2.1.2 The stability of continuous systems by Routh-Hurwitz criteria

Given the characteristic equation of Jacobian matrix at steady state as

$$P(\lambda) = \lambda^n + a_1\lambda^{n-1} + \cdots + a_{n-1}\lambda + a_n,$$

where the coefficients a_i are real constants, $i = 1, 2, ..., n$, define the n Hurwitz matrices using the coefficients a_i of the characteristic polynomial as below:

$$H_1 = (a_1), H_2 = \begin{bmatrix} a_1 & 1 \\ a_3 & a_2 \end{bmatrix}, H_3 = \begin{bmatrix} a_1 & 1 & 0 \\ a_3 & a_2 & a_1 \\ a_5 & a_4 & a_3 \end{bmatrix}$$

and

$$H_n = \begin{bmatrix} a_1 & 1 & 0 & 0 & \cdots & 0 \\ a_3 & a_2 & a_1 & 1 & \cdots & 0 \\ a_5 & a_4 & a_3 & a_2 & \cdots & 0 \\ \vdots & \vdots & \vdots & \vdots & \cdots & \vdots \\ 0 & 0 & 0 & 0 & \cdots & a_n \end{bmatrix},$$

where $a_j = 0$ if $j > n$. All of the roots of the polynomial $P(\lambda)$ are negative or have negative real part if and only if the determinants of all Hurwitz matrices are positive that is:

$$\det H_j > 0, j = 1, 2, \ldots, n.$$

When $n = 2$, the Routh-Hurwitz criteria simplifies to $\det H_1 = a_1 > 0$ and

$$\det H_2 = \det \begin{bmatrix} a_1 & 1 \\ 0 & a_2 \end{bmatrix} = a_1 a_2 > 0$$

or $a_1 > 0$ and $a_2 > 0$.

For characteristic equation of degree $n = 2, 3, 4$ and 5, the Routh-Hurwitz criteria are summarized below.

$n = 2$; $a_1 > 0$ and $a_2 > 0$

$n = 3$; $a_1 > 0, a_3 > 0$ and $a_1 a_2 > a_3$

$n = 4$; $a_1 > 0, a_3 > 0, a_4 > 0$ and $a_1 a_2 a_3 > a_3^2 + a_1^2 a_4$

$n = 5$; $a_i > 0$, $i = 1, 2, 3, 4, 5$, $a_1 a_2 a_3 > a_3^2 + a_1^2 + a_4$ and
$(a_1 a_4 - a_5)(a_1 a_2 a_3 - a_3^2 - a_1^2 a_4) > a_5 (a_1 a_2 - a_3)^2 + a_1 a_5^2$.

2.1.3 Forward-backward bifurcation

Theorem 2.1.2. [50] *Consider the following general system of ordinary differential equations with the parameter ϕ:*

$$\frac{dx}{dt} = f(x, \phi), \quad f : \mathbb{R}^n \times \mathbb{R} \to \mathbb{R}^n \quad \text{and } f \in \mathbb{C}^2(\mathbb{R}^n \times \mathbb{R}). \tag{2.1.2}$$

Without loss of generality, it is assumed that 0 is an equilibrium for system (2.1.2) for all values of the parameter ϕ, that is $f(0, \phi) \equiv 0$ for all ϕ. Assume that

(A1) $A = D_x f(0,0) = \left(\frac{\partial f_i}{\partial x_j}(0,0)\right)$ *is linearisation of system (2.1.2) around the equilibrium 0 with ϕ evaluated at 0. Zero is a simple eigenvalue of A and all other eigenvalues of A have negative real parts:*

(A2) Matrix A has a non-negative right eigenvector w and a left eigenvector v corresponding to the zero eigenvalue.

Let f_k be the k^{th} component of f and

$$\begin{aligned} a &= \sum_{k,i,j=1}^{n} v_k w_i w_j \frac{\partial^2 f_k}{\partial x_i \partial x_j}(0,0), \\ b &= \sum_{k,i=1}^{n} v_k w_i \frac{\partial^2 f_k}{\partial x_i \partial \phi}(0,0). \end{aligned} \tag{2.1.3}$$

The local dynamics of (2.1.2) around 0 are totally governed by a and b.

(i.) $a > 0, b > 0$. *When* $\phi < 0$ *with* $|\phi| \ll 1$, 0 *is locally asymptotically stable, and there exists a positive unstable equilibrium; when* $0 < \phi \ll 1$, 0 *is unstable and there exists a negative and locally asymptotically stable equilibrium;*

(ii.) $a < 0, b < 0$. *When* $\phi < 0$ *with* $|\phi| \ll 1$, 0 *is unstable; when* $0 < \phi \ll 1$, 0 *is locally asymptotically stable, and there exists a positive unstable equilibrium;*

(iii.) $a > 0, b < 0$. *When* $\phi < 0$ *with* $|\phi| \ll 1$, 0 *is unstable, and there exists a locally asymptotically stable negative equilibrium; when* $0 < \phi \ll 1$, 0 *is stable, and a positive unstable equilibrium appears;*

(iv.) $a < 0, b > 0$. *When* ϕ *changes from negative to positive,* 0 *changes its stability from stable to unstable. Correspondingly a negative unstable equilibrium becomes positive and locally asymptotically stable.*

Corollary 2.1.3. [50] *When* $a > 0$ *and* $b > 0$, *the bifurcation at* $\phi = 0$ *is subcritical (backward).*

2.1.4 The global asymptotic stability of the disease-free equilibrium

Lemma 2.1.4. [51] *Consider a model system written in the form*

$$\frac{dX_1}{dt} = F(X_1, X_2)$$
$$\frac{dX_2}{dt} = G(X_1, X_2), \qquad G(X_1, 0) = 0,$$

where $X_1 \in \mathbb{R}^m$ *denotes (its components) the number of uninfected individuals and* $X_2 \in \mathbb{R}^n$ *denotes (its components) the number of infected individuals including latent, infectious, etc;* $U_0 = (X^*, 0)$ *denotes the disease-free equilibrium of this system. And assume,*

(H1) For $\frac{dX_1}{dt} = F(X_1^*, 0)$, X_1^* *is globally asymptotically stable ;*

(H2) $G(X_1, X_2) = AX_2 - \hat{G}(X_1, X_2)$, $\hat{G}(X_1, X_2) \geq 0$ *for* $(X_1, X_2) \in \Omega$, *where the Jacobian* $A = \dfrac{\partial G(X_1^*, 0)}{\partial X_2}$ *is an M-matrix (the off-diagonal elements of* A *are nonnegative) and* Ω *is the region where the model makes biological sense.*

Then the disease-free equilibrium $U_0 = (X_1^*, 0)$ *is globally asymptotically stable for* $R_0 < 1$.

2.1.5 The global asymptotic stability of the endemic equilibrium

Lemma 2.1.5. [52] *Consider a dynamical system* $\frac{dX}{dt} = f(X)$, *where* $f : \Omega \to \mathbb{R}^n$ *is a* C^1 *function and* $\Omega \subset \mathbb{R}^n$ *is a simply connected domain. Assume that there exists a compact absorbing set* $K \subset \Omega$ *and the system has a unique equilibrium point* X^* *is globally asymptotically stable in* Ω *if* $\bar{q}_2 < 0$, *where*

$$\bar{q}_2 = \limsup_{t\to\infty} \sup_{X_0 \in K} \frac{1}{t} \int_0^1 m(B(X(s, X_0)))ds. \tag{2.1.4}$$

In (2.1.4), B *is a matrix-valued function defined as*

$$B = Q_f Q^{-1} + Q J^{[2]} Q^{-1},$$

where $Q(X)$ *is a* $\binom{n}{2} \times \binom{n}{2}$ *matrix-valued* C^1 *function in* Ω, Q_f *is the derivative of* Q *(entry-wise) along the direction of* f, *and* $J^{[2]}$ *is the second additive compound matrix of the Jacobian* $J(X) = Df(X)$. *If* $J = (a_{ij})$ *is a* 4×4 *matrix, then* $J^{[2]}$ *is given by* [53],

$$J^{[2]} = \begin{bmatrix} a_{11}+a_{22} & a_{23} & a_{24} & -a_{13} & -a_{14} & 0 \\ a_{32} & a_{11}+a_{33} & a_{34} & a_{12} & 0 & -a_{14} \\ a_{42} & a_{43} & a_{11}+a_{44} & 0 & a_{12} & a_{13} \\ -a_{31} & a_{21} & 0 & a_{22}+a_{33} & a_{34} & -a_{24} \\ -a_{41} & 0 & a_{21} & a_{43} & a_{22}+a_{44} & a_{23} \\ 0 & -a_{41} & a_{31} & -a_{42} & a_{32} & a_{33}+a_{44} \end{bmatrix}. \tag{2.1.5}$$

Meanwhile, $m(B)$ *is the Lozinskiĭ measure of* B *with respect to a matrix norm; i.e.,*

$$m(B) = \lim_{h\to 0^+} \frac{\|I + hB\| - 1}{h},$$

where I *represents the identity matrix.*

2.1.6 The Arithmetic Mean - Geometric Mean Inequality

Theorem 2.1.6. [54] *Let $a_1, a_2, \ldots, a_n$ be positive numbers. Then,*

$$\frac{a_1 + a_2 + \cdots + a_n}{n} \geq \sqrt[n]{a_1 a_2 \cdots a_n}.$$

Equality holds if and only if $a_1 = a_2 = \cdots = a_n$.

2.1.7 LaSalle's invariance principle

Theorem 2.1.7. [55] *Let $\Omega \subset D$ be a compact set that is positively invariant with respect to $\dot{x} = f(x)$, $x \in D$. Let $V : D \to \mathbb{R}$ be a continuously differentiable function such that $\dot{V}(x) \leq 0$ in Ω. Let E be the set of all points in Ω where $\dot{V}(x) = 0$. Let M be the largest invariant set in E. Then every solution starting in Ω approaches M as $t \to \infty$.*

2.1.8 Sensitivity analysis

The normalized forward sensitivity index is used to calculate sensitivity indices of the basic reproduction number with respect to the parameters [56, 57].

Definition 2.1.8. [58] The normalized forward sensitivity index of R_0 that depends differentiability on a parameter P is defined by

$$\Upsilon_P^{R_0} = \frac{\partial R_0}{\partial P} \times \frac{P}{R_0}. \tag{2.1.6}$$

2.1.9 Optimal control

Optimal control is a powerful method for solving dynamic optimization problems, when the problem are expressed in continuous time. This primary method was developed by Pontryagin et al. in 1962 [59].

Lenhatrt and Workman in 2007 [60] consider $u(t)$ as the control and $x(t)$ as the state. The state variable is governed by a differential equation involving the control variable:

$$x^{'}(t) = g(t, x(t), u(t)).$$

An optimal control problem consists of finding piecewise control $u(t)$ and the associated state variable $x(t)$ to maximize (minimize) the given objective funtional,

$$J(u) = max(min) \int_{t_0}^{t_1} f(t, x(t), u(t))dt,$$

subject to

$$x^{'}(t) = g(t, x(t), u(t)),$$
$$x(t_0) = x_0 \quad \text{and} \quad x(t_1) \quad \text{free.}$$

Such a maximizing (minimizing) control is called an optimal control. By $x(t)$ free, it means that the value of $x(t)$ is unrestricted; f and g are continuous differentiable functions in all three arguments. Thus, the control will always be piecewise continuous and the associated states will always be piecewise differentiable.

The principal technique for an optimal control problem is to solve a set of "necessary conditions" that an optimal control and corresponding state must satisfy. The necessary conditions are generated from the Hamiltonian H, which is defined as follow;

$$H(t, x, u, \lambda) = f(t, x, u) + \lambda g(t, x, u).$$

Since, we want to maximize (minimize) H with respect to u at u^*, and the necessary conditions can be written in terms of the Hamiltonian:

$$\frac{\partial H}{\partial u} = 0 \ \text{ at } \ u^* \Longrightarrow f_u + \lambda g_u = 0 \qquad \text{(optimality condition)},$$
$$\lambda^{'} = -\frac{\partial H}{\partial x} \Longrightarrow \lambda^{'} = -(f_x + \lambda g_x) \qquad \text{(adjoint equation)},$$
$$\lambda(t_1) = 0 \qquad \text{(transversality condition)},$$

where the dynamics of the state equation is

$$x^{'} = g(t, x, u) = \frac{\partial H}{\partial \lambda}, \quad x(t_0) = x_0.$$

Therefore, we can solve the optimal control problem by the following scheme;

1. Form the Hamiltonian for the problem.

2. Set up the adjoint differential equations, transversality boundary conditions and optimality conditions. Now there are three unknowns, u^*, x^* and λ.

3. Eliminate u^* by using the optimality equation $H_u = 0$, that is, solve u^* in terms of x^* and λ.

4. Solve differential equations for x^* and λ with boundary conditions, substituting u^* in the differential equations with the expression for the optimal control from the previous step.

5. After finding the optimal state and adioint, solve the optimal control.

2.2 Literature reviews

In this section, we will introduce intriguing mathematical models associated with epidemics of brucellosis and bovine tuberculosis.

Mathematical modeling of brucellosis

In 2013, Qiang Hou et al. [12] studied the transmission dynamics of sheep brucellosis in Inner Mongolia. They purposed a dynamic model for the sheep-human transmission of brucellosis, involving sheep population, human population, and brucella in the environment. The results show that vaccinating and disinfecting both young and adult sheep are appropriate and effective strategies to control brucellosis in Inner Mongolia of China. This model classifies the sheep population into four compartments: the susceptible compartment $S(t)$, the exposed compartment $E(t)$, the infectious compartment $I(t)$, and the vaccinated compartment $V(t)$. Additionally, it classifies the human population into three groups: the susceptible group $S_h(t)$, acute infections $I_{ah}(t)$, and chronic infections $I_{ch}(t)$. Furthermore, let $B(t)$ denote the number of infectious unit in the environment. The flow diagram of the model is shown in Figure 1.

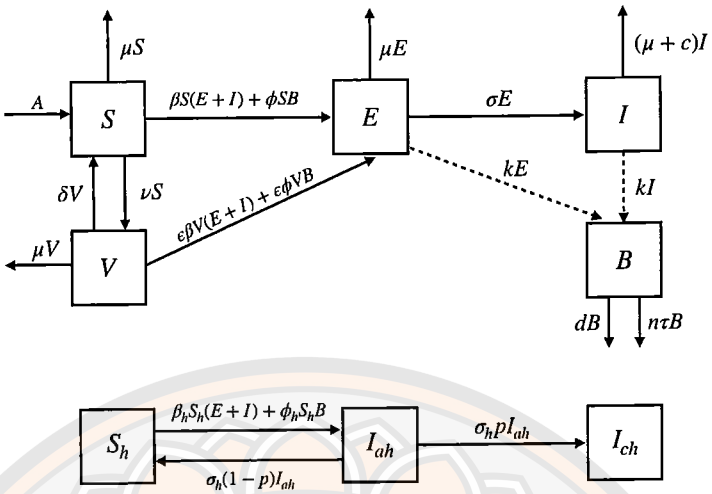

Figure 1 Flowchart of sheep brucellosis transmission [12].

The system of ordinary differential equations of their model is as follows:

$$
\begin{aligned}
\frac{dS}{dt} &= A - \beta S(E+I) - \phi SB - (\mu + v)S + \delta V, \\
\frac{dV}{dt} &= vS - (\mu + \delta)V - \epsilon\beta V(E+I) - \epsilon\phi VB, \\
\frac{dE}{dt} &= \beta(S + \epsilon V)(E+I) + \phi(S + \epsilon V)B - (\sigma + \mu)E, \\
\frac{dI}{dt} &= \sigma E - (\mu + c)I, \\
\frac{dB}{dt} &= k(E+I) - (d + n\tau)B, \\
\frac{dS_h}{dt} &= -\beta_h S_h(E+I) - \phi_h S_h B + \sigma_h(1-p)I_{ah}, \\
\frac{dI_{ah}}{dt} &= \beta_h S_h(E+I) + \phi_h S_h B - \sigma_h I_{ah}, \\
\frac{dI_{ch}}{dt} &= \sigma_h p I_{ah}.
\end{aligned}
$$

Notation:

A	is the recruitment rate of the sheep population.
μ	is the rate of sheep natural elimination.
c	is the elimination rate caused by brucellosis.
δ	is the rate of sheep loss of vaccination.
v	is the sheep vaccination rate.
β	is the sheep-to-sheep transmission rate.

ϵ	is the invalid vaccination rate.
ϕ	is the Brucella-to-susceptible sheep transmission rate.
σ	is the rate of clinical outcome of exposed sheep.
k	is the Brucella shedding rate by exposed and infected sheep.
d	is the decaying rate of brucella in the environment.
n	is the disinfection times.
τ	is the effective disinfection rate.
β_h	is the transmission rate from sheep to humans.
ϕ_h	is the transmission rate from brucella to human.
$\sigma_h p$	is the transfer rate from acute infections to chronic infections.
$\sigma_h(1-p)$	is the transfer rate from acute infections to susceptible population.

In 2014, Gui-Quan Sun, & Zi-ke Zhang [13] presented a sheep brucellosis model with immigration and proportional birth to include both direct and indirect transmission with infected animals, and the bacteria of the environment. In addition, this paper confirmed that elimination, vaccination and disinfection are the useful control strategies. The model's flowchart is depicted in Figure 2.

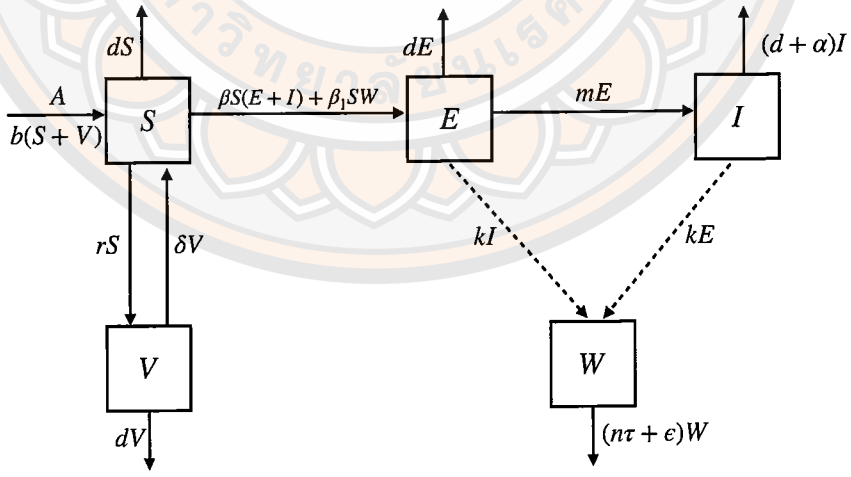

Figure 2 Diagram depicting the dynamic transmission of brucellosis among sheep [13].

The model is given by the following system of ordinary differential equa-

tions:

$$\begin{aligned}
\frac{dS}{dt} &= A + b(S+V) + \delta V - (d+r)S - \beta S(E+I) - \beta_1 SW, \\
\frac{dE}{dt} &= \beta S(E+I) + \beta_1 SW - (d+m)E, \\
\frac{dI}{dt} &= mE - (d+\alpha)I, \\
\frac{dV}{dt} &= rS - (\delta+d)V, \\
\frac{dW}{dt} &= k(I+E) - (n\tau+\epsilon)W.
\end{aligned}$$

Notation:

S	is the number of susceptible individuals.
V	is the number of vaccinated individuals.
E	is the number of exposed individuals.
I	is the number of infected individuals.
W	is the quantity of sheep brucella in the environment.
A	is the immigration rate of sheep.
b	is the birth rate of sheep.
d	is the removed rate of sheep.
δ	is the rate of sheep losing immunity from vaccination.
r	is the vaccination rate of sheep.
m	is the transfer rate of sheep from exposed to infectious compartment.
α	is the disease-related elimination rate.
k	is the shedding rate from exposed and infectious sheep into the environment.
ϵ	is the natural death rate of brucella in the environment.
β	is the transmission rate from exposed and infectious sheep to susceptible sheep.
β_1	is the transmission rate from brucella to susceptible sheep.
n	is the disinfection number.
τ	is the efficient disinfection rate.

In the same year, Ming-Tao et al. [14] presented a mathematical model that focused on the disease transmission between cattle and sheep populations on the same farm. In their model, $S_1(t), E_1(t), I_1(t), R_1(t)$ and $S_2(t), E_2(t), I_2(t), R_2(t)$

represent susceptible, exposed, infectious, vaccinated cattle and sheep at time t, respectively. Moreover, $V_1(t)$ and $V_2(t)$ represent the quantity of cattle brucella and sheep brucella in the environment at time t, respectively. The flow diagram of the model is shown in Figure 3.

The system of ordinary differential equations of their model is as follows:

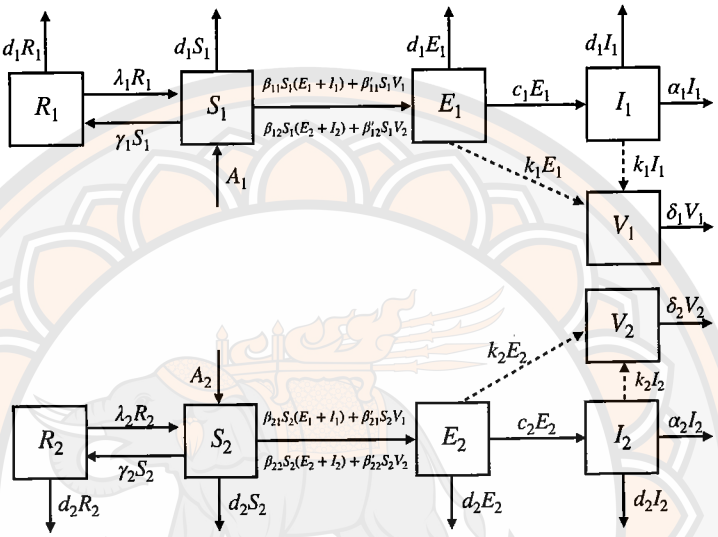

Figure 3 Transmission diagram on the dynamical transmission of brucellosis between cattle and sheep in public farm [14].

$$\frac{dS_i}{dt} = A_i - (d_i + \gamma_i)S_i + \lambda_i R_i - \sum_{j=1}^{2}\left(\beta_{ij}S_i(E_j + I_j) + \beta'_{ij}S_iV_j\right)$$

$$\frac{dE_i}{dt} = \sum_{j=1}^{2}\left(\beta_{ij}S_i(E_j + I_j) + \beta'_{ij}S_iV_j\right) - (d_i + c_i)E_i,$$

$$\frac{dI_i}{dt} = c_iE_i - (d_i + \alpha_i)I_i,$$

$$\frac{dR_i}{dt} = \gamma_iS_i - (\lambda_i + d_i)R_i,$$

$$\frac{dV_i}{dt} = k_i(E_i + I_i) - \delta_iV_i,$$

where $i = 1, 2$.

Notation:

A_1 is the recruitment rate of cattle population.

A_2 is the recruitment rate of sheep population.

d_1 is the natural mortality rate of cattle.

d_2 is the natural mortality rate of sheep.

λ_1 is the loss rate of vaccination immunity of cattle.

λ_2 is the loss rate of vaccination immunity of sheep.

γ_1 is the vaccination rate of cattle.

γ_2 is the vaccination rate of sheep.

c_1 is the clinical outcome rate of exposed cattle.

c_2 is the clinical outcome rate of exposed sheep.

α_1 is the disease-related elimination rate of cattle.

α_2 is the disease-related elimination rate of sheep.

k_1 is the brucella shedding rate by exposed and infected cattle.

k_2 is the brucella shedding rate by exposed and infected sheep.

δ_1 is the decaying rate of cattle brucella in the environment.

δ_2 is the decaying rate of sheep brucella in the environment.

β_{11} is the transmission rate from exposed and infected cattle to susceptible cattle.

β_{21} is the transmission rate from exposed and infected cattle to susceptible cattle.

β_{22} is the transmission rate from exposed and infected cattle to susceptible sheep.

β_{12} is the transmission rate from exposed and infected sheep to susceptible cattle.

β_{22} is the transmission rate from exposed and infected sheep to susceptible sheep.

β'_{11} is the transmission rate from cattle brucella of the environment to susceptible cattle.

β'_{21} is the transmission rate from cattle brucella of the environment to susceptible sheep.

β'_{12} is the transmission rate from sheep brucella of the environment to susceptible cattle.

β'_{22} is the transmission rate from sheep brucella of the environment to susceptible sheep.

In 2015, Emmanuel Abatih et al. [15] proposed a model for the transmission dynamics of brucellosis among bison. The model contains three subclasses; susceptible (S), infected (I), and recovered individuals (R). Figure 4 displays the flow diagram of the model.

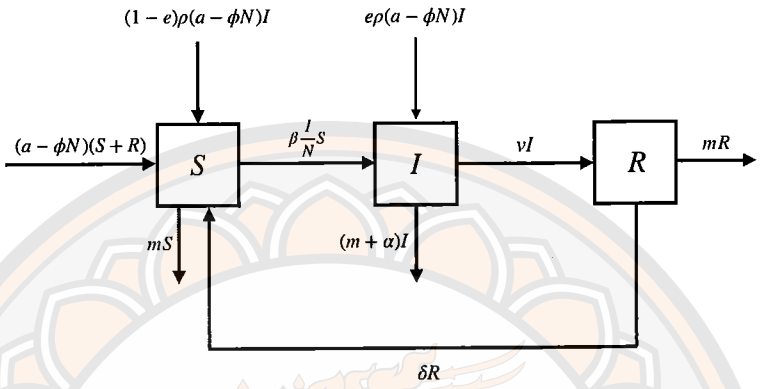

Figure 4 Flow diagram of the transmission dynamics of brucellosis among bison [15].

The model is given by the following system of ordinary differential equations:

$$\begin{aligned}
\frac{dS}{dt} &= (a-\phi N)[S+R+I\rho(1-e)] - mS + \delta R - \beta\frac{I}{N}S, \\
\frac{dI}{dt} &= \beta\frac{I}{N}S + e\rho(a-\phi N)I - (\alpha+m+v)I, \\
\frac{dR}{dt} &= vI - (m+\delta)R.
\end{aligned}$$

Notation:

- S is the number of susceptible individuals.
- I is the number of infected individuals.
- R is the number of recovered individuals.
- a is the birth rate.
- ϕ is the density dependent reduction in birth.
- m is the per capita disease free death rate.
- α is the disease related death rate.
- δ is the rate of loss of resistance.

v is the recovery rate.

β is the disease transmission rate.

e is the proportion of vertical transmission.

ρ is the reduction of fecundity in infectious bison.

N is the number of susceptible, infected and recovered individuals.

In 2017, Yang et al. [16] presented a nonlinear modeling framework to investigate the transmission dynamics of brucellosis, incorporating both the spatial and seasonal variations. They introduced a two-patch model that animals in each patch had distinct populations and infection characteristics. The study found that if animals living in patch 1 immigrated to patch 2, prevention and intervention efforts should be devoted to animals in patch 2 to control brucellosis outbreaks.

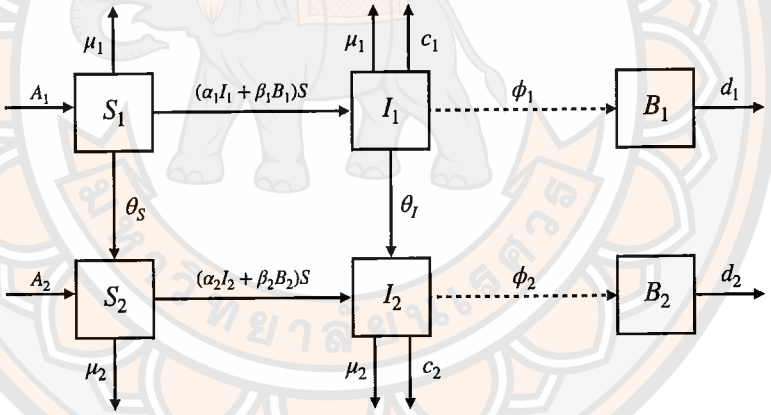

Figure 5 Flowchart illustrating the dynamics of brucellosis [16].

The following system of ordinary differential equations describe the brucellosis transmission dynamics:

$$\dot{S}_1(t) = A_1 - (\alpha_1 I_1 + \beta_1 B_1)S_1 - (\theta_S + \mu_1)S_1,$$
$$\dot{I}_1(t) = (\alpha_1 I_1 + \beta_1 B_1)S_1 - (\theta_I + c_1 + \mu_1)I_1,$$
$$\dot{B}_1(t) = \phi_1 I_1 - d_1 B_1,$$
$$\dot{S}_2(t) = A_2 - (\alpha_2 I_2 + \beta_2 B_2)S_2 - \mu_2 S_2 + \theta_S S_1,$$
$$\dot{I}_2(t) = (\alpha_2 I_2 + \beta_2 B_2)S_2 - (\mu_2 + c_2)I_2 + \theta_I I_1,$$

$$\dot{B}_2(t) = \theta_2 I_2 - d_2 B_2.$$

Notation:

S_j $(j = 1, 2)$	is the number of susceptible individuals.
I_j $(j = 1, 2)$	is the number of infectious individuals.
B_j $(j = 1, 2)$	is the population of the free-living pathogen (i.e., Brucella).
A_j $(j = 1, 2)$	is the constant recruitment rate for animals in each patch.
μ_j $(j = 1, 2)$	is the natural animal death rate.
α_j $(j = 1, 2)$	is the host-to-host disease transmission rates.
β_j $(j = 1, 2)$	is the environment-to-host disease transmission rates.
c_j^{-1} $(j = 1, 2)$	is the mean infectious period for animals in each patch.
ϕ_j $(j = 1, 2)$	is the pathogen shedding rate.
d_j $(j = 1, 2)$	is the pathogen removal rate that includes the effects of both the natural decay and the decontamination practices.
θ_S $(j = 1, 2)$	is the migration rate of susceptible animals from patch 1 to patch 2.
θ_I $(j = 1, 2)$	is the migration rate of infectious animals from patch 1 to patch 2.

In the 2018, Lolika et al. [17] proposed an extended model in [15] to incorporate an additional epidemiological class that accounts for animals in chronic state. Additionally, they introduced a non-autonomous bison-brucellosis model integrating seasonal variations and time-dependent culling effort. Figure 6 shows the model's flow diagram.

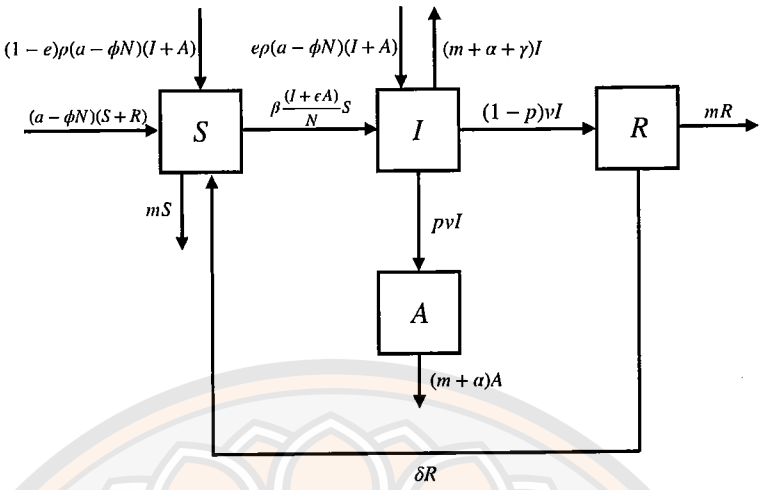

Figure 6 Flow diagram of the dynamics of brucellosis infection in bison population with vertical transmission and culling [17].

The model is given by the following system of ordinary differential equations:

$$\begin{aligned}
\frac{dS}{dt} &= (a-\phi N)[S+R+(I+A)\rho(1-e)] - mS + \delta R - \frac{\beta(I+\epsilon A)S}{N}, \\
\frac{dI}{dt} &= \frac{\beta(I+\epsilon A)S}{N} + e\rho(a-\phi N)(I+A) - (m+\alpha+\gamma+v)I, \\
\frac{dA}{dt} &= pvI - (m+\alpha)A, \\
\frac{dR}{dt} &= (1-p)vI - (m+\delta)R.
\end{aligned}$$

Notation:

- S is the number of susceptible individuals.
- I is the number of infected individuals.
- A is the number of chronic infected individuals.
- R is the number of recovered individuals.
- a is the recruitment rate.
- ϕ is the density dependent reduction in birth.
- m is the natural mortality rate.
- α is the disease related death rate.
- δ is the rate of loss of resistance.

υ is the recovery rate.

β is the disease transmission rate.

e is the proportion of vertical transmission.

ρ is the reduction of fecundity in infectious bison.

p is the proportion of symptomatic animals that become chronic.

ϵ is the modification factor.

γ is the culling rate.

In 2020, Nyerere et al. [18] presented a mathematical model for the impacts of different control options on the transmission dynamics of brucellosis. They focused on livestock vaccination, gradual culling through the slaughter of seropositive cattle and small ruminants, environmental hygiene and sanitation, and personal protection. The study recommends that the combination of vaccination, gradual culling of seropositive cattle and small ruminants, environmental hygiene, and personal protection in humans should be implemented. The flowchart representing the model can be seen in Figure 7.

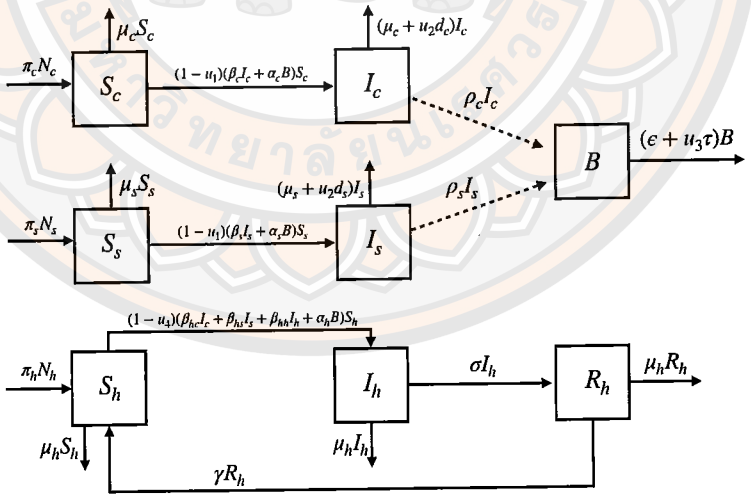

Figure 7 A schematic diagram for direct and indirect transmission of brucellosis in cattle, small ruminant, and human populations [18].

The system of ordinary differential equations of their model is as follows:

$$\frac{dS_c}{dt} = \pi_c N_c - ((1-u_1(t))(\beta_c I_c + \alpha_c B) + \mu_c)S_c,$$
$$\frac{dI_c}{dt} = (1-u_1(t))(\beta_c I_c + \alpha_c B)S_c - (\mu_c + u_2(t)d_c)I_c,$$
$$\frac{dS_s}{dt} = \pi_s N_s - ((1-u_1(t))(\beta_s I_s + \alpha_s B) + \mu_s)S_s,$$
$$\frac{dI_s}{dt} = (1-u_1(t))(\beta_s I_s + \alpha_s B)S_s - (\mu_s + u_2(t)d_s)I_s,$$
$$\frac{dS_h}{dt} = \pi_h N_h + \gamma R_h - ((1-u_4(t))(\beta_{hc}(t)I_c + \beta_{hs}I_s + \beta_{hh}(t)I_h + \alpha_h B) + \mu_h)S_h,$$
$$\frac{dI_h}{dt} = (1-u_4(t))(\beta_{hc}I_c + \beta_{hs}I_s + \beta_{hh}I_h + \alpha_h B)S_h - (\sigma + \mu_h + d_h)I_h,$$
$$\frac{dR_h}{dt} = \sigma I_h - (\gamma + \mu_h)R_h,$$
$$\frac{dB}{dt} = \rho_c I_c + \rho_s I_s - (\epsilon + u_3(t)\tau)B.$$

Notation:

S_h	is the number of susceptible humans.
I_h	is the number of infected human.
R_h	is the number of recovered humans.
S_c	is the number of susceptible cattle.
I_c	is the number of infected cattle.
S_s	is the number of susceptible small ruminants.
I_s	is the number of infected small ruminants.
B	is the number of Brucella bacteria load per unit volume in the environment.
π_c	is the per capita cattle birth rate.
π_h	is the per capita human birth rate.
σ	is the human recovery rate.
μ_h	is the per capita human natural death rate.
β_c	is the transmission rate within cattle.
α_c	is the transmission rate of Brucella from the environment to cattle.
α_s	is the transmission rate of Brucella from the environment to small ruminant.
α_h	is the transmission rate of Brucella from the environment to human.
β_{hc}	is the rate of transmission from cattle to humans.
β_{hs}	is the rate of transmission from small ruminants to humans.
π_s	is the per capita birth rate of small ruminants.

β_s is the transmission rate within small ruminant.

μ_s is the per capita natural death rate of small ruminants.

τ is the rate of environmental hygiene and sanitation.

ϵ is the decaying rate of Brucella in the environment.

d_c is the culling rate of seropositive cattle.

d_s is the culling rate of seropositive small ruminants.

$u_1(t)$ is the measure of the effectiveness of the S19 and Rev1 vaccines for cattle and small ruminants.

$u_2(t)$ is the measure of the effectiveness of gradual culling of seropositive animals.

$u_3(t)$ is the measure of effectiveness of environmental hygiene.

$u_4(t)$ is the measure of the effectiveness of personal protection in humans.

In 2022, Stephen Abagna et al. [19] studied the transmission dynamics and control of bovine brucellosis in a herd of cattle. The cattle population is divided into five compartments: susceptible (S), infected (I), recovered (R), vaccinated (V), and biosecured (B). The biosecured class (B) represents cattle that are unable to contract bovine brucellosis due to comprehensive adherence to biosecurity protocols. Figure 8 shows the model's flow diagram.

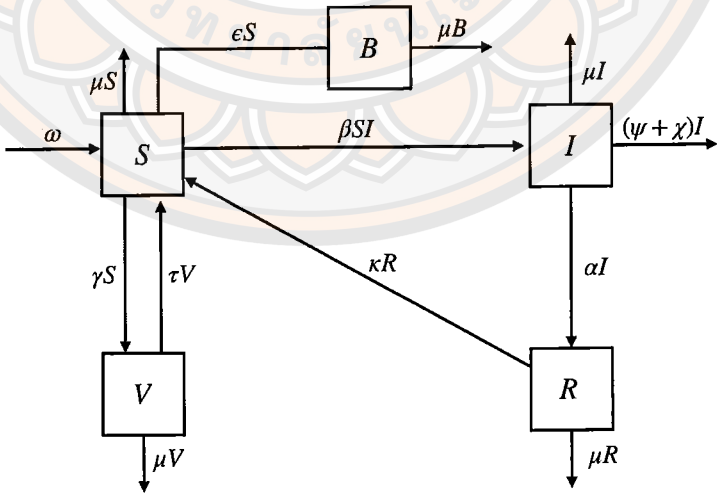

Figure 8 Schematic diagram of the transmission dynamics of bovine brucellosis in cattle with biosecurity [19].

The model is given by the following system of ordinary differential equations:

$$\begin{aligned}
\frac{dS}{dt} &= \omega - \beta SI - (\mu + \gamma + \epsilon)S + \kappa R + \tau V, \\
\frac{dI}{dt} &= \beta SI - (\mu + \psi + \alpha + \chi)I, \\
\frac{dR}{dt} &= \alpha I - (\mu + \kappa)R, \\
\frac{dB}{dt} &= \epsilon - \mu B, \\
\frac{dV}{dt} &= \gamma S - (\mu + \tau)V.
\end{aligned}$$

Notation:

- β is the rate at which infected cattle transmit Brucella infections.
- ω is the rate at which cattle are recruited into the susceptible class.
- μ is the rate at which cattle die naturally in each compartment.
- γ is the rate at which susceptible cattle are vaccinated.
- τ is the rate at which vaccinated cattle lose temporal immunity.
- ψ is the rate at which cattle die as a result of Brucella infections.
- χ is the rate at which infected cattle are culled.
- α is the rate at which cattle recover from Brucella infections.
- κ is the rate of waning of recovery-derived immunity.
- ϵ is the rate at which susceptibles enter the biosecured compartment.

Mathematical modeling of bovine tuberculosis

In 2016, Patrick B. Phepa et al. [41] studied the transmission dynamics of bovine tuberculosis (BTB) in both buffalo and cattle populations. The model incorporates cross-infection and contaminated environment transmission routes. Figure 9 displays the flow diagram of the model.

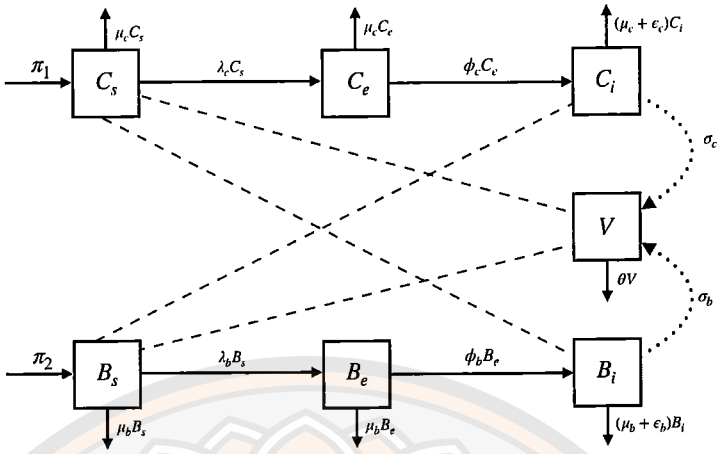

Figure 9 The flowchart of the transmission dynamics of bovine tuberculosis in buffalo and cattle population [41].

The system of ordinary differential equations of their model is as follows:

$$\begin{aligned}
\frac{dC_s}{dt} &= \pi_1 - \lambda_c C_s - \mu_c C_s, \\
\frac{dC_e}{dt} &= \lambda_c C_s - \phi_c C_e - \mu_c C_e, \\
\frac{dC_i}{dt} &= \phi_c C_e - (\mu_c + \epsilon_c) C_i, \\
\frac{dV}{dt} &= \sigma_c C_i + \sigma_b B_i - \theta V, \\
\frac{dB_s}{dt} &= \pi_2 - \lambda_b B_s - \mu_b B_s, \\
\frac{dB_e}{dt} &= \lambda_b B_s - \phi_b B_e - \mu_b B_e, \\
\frac{dB_i}{dt} &= \phi_b B_e - (\mu_b + \epsilon_b) B_i,
\end{aligned}$$

where $\lambda_c = \frac{\beta_c C_i}{N_c} + \frac{\beta_{cb} B_i}{N_b} + \frac{\psi_c V}{K}$ and $\lambda_b = \frac{\beta_b B_i}{N_b} + \frac{\beta_{bc} C_i}{N_c} + \frac{\psi_b V}{K}$.

Notation:

N_c is the population size of cattle.

N_b is the population size of buffalo.

C_s is the number of susceptible cattle.

C_e is the number of exposed cattle.

C_i is the number of infected cattle.

B_s is the number of susceptible buffalo.

B_e is the number of exposed buffalo.

B_i is the number of infected buffalo.

V is the quantity of infectious M. bovis in the environment.

σ_c, σ_b is the pathogen shedding rate.

θ is the pathogen decay rate.

K is the maximum carrying capacity of M. bovis in the environment.

β_c is the transmission rate with the infected cattle.

β_{cb} is the transmission rate with the infected baffalo.

ψ_c is the transmission rate with the contaminated environment.

ϕ_c is the progresses rate from the exposed cattle to the infectious class.

μ_c is the natural death rate of the cattle.

ϵ_c is the disease related death rate of the cattle.

π_1 is the recruitment rate of cattle.

β_b is the transmission rate with the infected baffalo.

β_{bc} is the transmission rate with the infected cattle.

ψ_b is the transmission rate with the contaminated environment.

ϕ_b is the progresses rate from the exposed baffalo to the infectious class.

π_2 is the recruitment rate of baffalo.

μ_b is the natural death rate of the baffalo.

ϵ_b is the disease related death rate of the baffalo.

In the same year, Tasmi et al. [46] discussed a model for the transmission of badger tuberculosis with vaccination. The badger population is divided into five compartments: susceptible badgers (S), vaccinated susceptible badgers (S_t), exposed badgers (E), vaccinated exposed badgers (E_t), and infectious badgers (I). Let N be the total population of badger. The flow diagram of the model is shown in Figure 10.

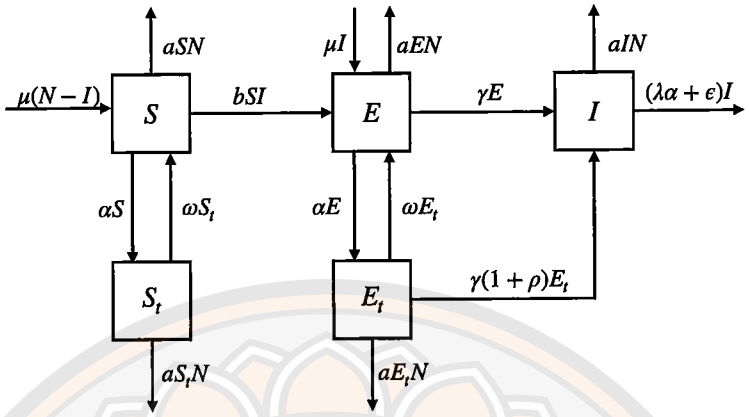

Figure 10 Transmission diagram of tuberculosis in badger [46].

The system of ordinary differential equations of their model is as follows:

$$\begin{aligned}
\frac{dS}{dt} &= \mu(N-I) + \omega S_t - bSI - aSN - \alpha S, \\
\frac{dS_t}{dt} &= \alpha S - aS_tN - \omega S_t, \\
\frac{dE}{dt} &= \mu I + \omega E_t + bSI - (aN + \gamma + \alpha)E, \\
\frac{dE_t}{dt} &= \alpha E - (aN + \omega + \gamma(1+\rho))E_t, \\
\frac{dI}{dt} &= \gamma E + \gamma(1+\rho)E_t - aIN - (\lambda\alpha + \epsilon)I.
\end{aligned}$$

Notation:

- μ is the birth rate of badger.
- α is the rate of vaccination.
- ω is the rate of drop out vaccination.
- a is coefficient of logistic.
- b is coefficient of contact between susceptible badger with infected badger badger.
- γ is the rate of transition of badger from the incubation period became infected.
- ρ is the effect of vaccination in exposed badger.
- λ is the effect of vaccination in infected badger.
- ϵ is the rate of death from disease.

In 2017, Mahamat Fayiz Abakar et al. [47] established a mathematical model for BTB transmission in cattle and humans in Morocco to provide a general understanding of BTB. The cattle population is divided into three mutually exclusive compartments: susceptible cattle (S_C), exposed cattle with latent BTB, which test positive to the tuberculin test but do not exhibit visible lesions (E_C), and infected cattle with active BTB, displaying tuberculosis lesions (I_C). Hence, the total cattle population (N_C) is the sum of the populations of susceptible (S_C), exposed (E_C), and infected (I_C) cattle. The human population consists of four mutually exclusive compartments: susceptible humans (S_H), exposed humans with latent BTB reacting to the Mantoux test (E_H), infected humans with active BTB (I_H), and humans who have recovered from BTB, possessing temporary immunity (R_H). The total human population (N_H) is the sum of the populations of susceptible (S_H), exposed (E_H), infected (I_H), and recovered (R_H) individuals. Figure 11 shows the model's flow diagram.

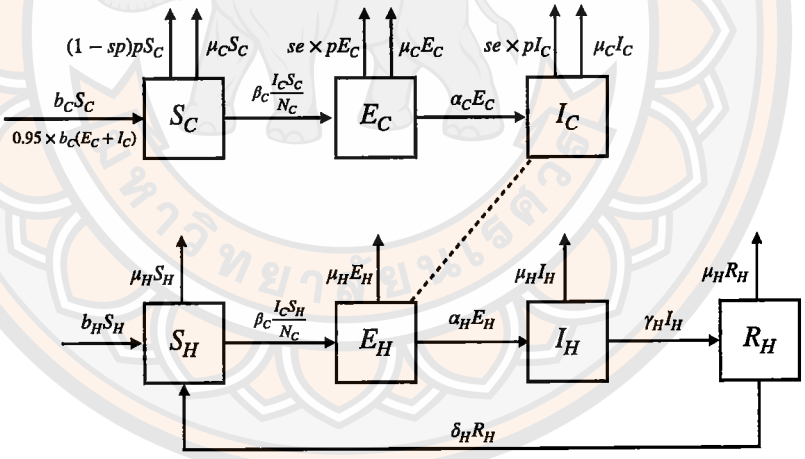

Figure 11 Schematic diagram of the BTB cattle-human transmission model for Morocco [47].

The model is given by the following system of ordinary differential equations:

$$\frac{dS_C}{dt} = b_C S_C + (0.95 \times b_C(E_C + I_C)) - \beta_C \frac{I_C S_C}{N_C} - \mu_C S_C - (1 - sp)pS_C,$$
$$\frac{dE_C}{dt} = \beta_C \frac{I_C S_C}{N_C} - \alpha_C E_C - \mu_C - se \times pE_C,$$

$$\frac{dI_C}{dt} = \alpha_C E_C - \mu_C I_C - se \times pI_C,$$
$$\frac{dS_H}{dt} = b_H S_H - \beta_H \frac{I_C S_H}{N_C} - \mu_H S_H,$$
$$\frac{dE_H}{dt} = \beta_H \frac{I_C S_H}{N_C} - \alpha_H E_H - \mu_H E_H,$$
$$\frac{dI_H}{dt} = \alpha_H E_H - \gamma_H I_H - \mu_H I_H,$$
$$\frac{dR_H}{dt} = \gamma_H I_H - \delta_H R_H - \mu_H R_H.$$

Notation:

b_C	is the birth rate of cattle.
β_C	is the transmission rate of cattle to cattle.
μ_C	is the mortality rate of cattle.
α_C	is the inverse of cattle incubation period.
p	is the proportion of tested animals.
sp	is the specificity of the test.
se	is the sensitivity of the test.
b_H	is the birth rate of humans.
β_H	is the rate of transmission from cattle to humans.
μ_H	is the natural mortality rate of humans.
α_H	is the inverse of human incubation period.
γ_H	is the rate of success in treating humans.
δ_H	is the loss of immunity in humans.

Mathematical modeling of brucellosis-tuberculosis co-infection

In 2021, Lolika et al. [48] developed a modeling framework for brucellosis-tuberculosis co-infection that incorporates all relevant biological factors, with culling of infectious animals as the primary intervention strategy. Let S, I_{11}, I_{22} and I_{12} denote proportions of the susceptible, animals singly infected with brucellosis, animals singly infected with tuberculosis and dually infected animals, respectively. Figure 12 displays the flow diagram of the model.

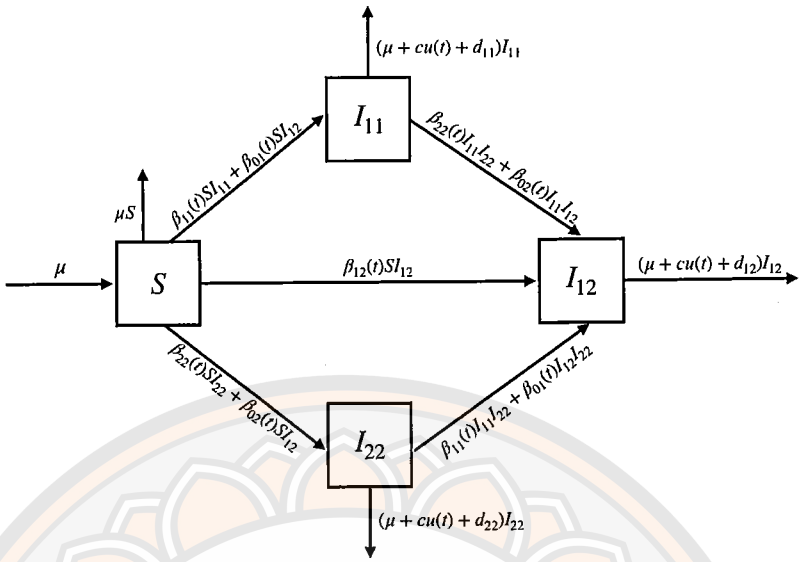

Figure 12 The flowchart of the transmission dynamics of brucellosis tuberculosis co-infection [48].

Their model is governed by the following system of equations:

$$\begin{aligned}
\frac{dS}{dt} &= \mu - (\beta_{11}(t)I_{11} + \beta_{01}I_{12} + \beta_{22}I_{22} + \beta_{02}(t)I_{12} + \beta_{12}(t)I_{12})\,S - \mu S,\\
\frac{dI_{11}}{dt} &= (\beta_{11}(t)I_{11} + \beta_{01}(t)I_{12})\,S - (\beta_{22}(t)I_{22} + \beta_{02}(t)I_{12})\,I_{11} - (\mu + cu(t)) + d_{11})I_{11},\\
\frac{dI_{22}}{dt} &= (\beta_{22}(t)I_{22} + \beta_{02}(t)I_{12})\,S - (\beta_{11}(t)I_{11} + \beta_{01}(t)I_{12})\,I_{22} - (\mu + cu(t)) + d_{22})I_{22},\\
\frac{dI_{12}}{dt} &= \beta_{12}(t)I_{12}S + (\beta_{22}(t)I_{22} + \beta_{02}(t)I_{12})\,I_{11} + (\beta_{11}(t)I_{11} + \beta_{01}(t)I_{12})\,I_{22}\\
&\quad - (\mu + cu(t)) + d_{12})I_{12}.
\end{aligned}$$

Note that the transmission rate of brucellosis is denoted by $\beta_{11}(t)$, while those singly infected with tuberculosis transmit the disease at a rate represented by $\beta_{22}(t)$. These rates are defined as:

$$\beta_{ii}(t) = \widetilde{\beta}_{ii}\left[1 + a_{ii}\sin\left(\frac{2\pi t}{12}\right)\right], \quad i = 1, 2.$$

Furthermore, co-infected animals are assumed to transmit both infections at rate $\beta_{12}(t)$, given by

$$\beta_{12}(t) = \widetilde{\beta}_{12}\left[1 + a_{12}\sin\left(\frac{2\pi t}{12}\right)\right],$$

Additionally, co-infected animals can transmit either brucellosis or tuberculosis at rates $\beta_{01}(t)$ and $\beta_{02}(t)$, respectively. These rates are defined as:

$$\beta_{0i}(t) = \widetilde{\beta}_{0i}\left[1 + a_{0i}\sin\left(\frac{2\pi t}{12}\right)\right], \quad i = 1, 2.$$

Here, $\widetilde{\beta}_{ii}$, $\widetilde{\beta}_{12}$, and $\widetilde{\beta}_{0i}$ denote the basic contact rate without seasonal forcing, while $0 \leq a_{ii}, a_{12}, a_{0i} \leq 1$ represent the magnitude of seasonal fluctuations.

Notation:

μ	is the constant rate of entry for new animals into the susceptible class.
c	is the culling rate.
d_{11}	is the mortality rate related to brucellosis.
d_{22}	is the mortality rate related to tuberculosis.
d_{12}	is the disease related mortality rate for dual infected animals.
$u(t)$	is the control function.

CHAPTER III

MATHEMATICAL MODELS OF BRUCELLOSIS INFECTION IN BISON

3.1 Model formulation

In this section, we classify the bison population into four compartments: the susceptible $S(t)$, the infectious $I(t)$, the chronic (still can infect others) $A(t)$, and the recovered (with temporary immunity) $R(t)$ at time t. The total bison population at time t is $N(t) = S(t) + I(t) + A(t) + R(t)$. Moreover, $W(t)$ is the concentration of Brucella in the environment.

The parameter a denotes birth rate, and ϕ is the density-dependent reduction in births. The natural mortality rate for the bison population is denoted by m, and the natural death rate of Brucella in the environment is denoted by d. The parameter e is the proportion of vertical transmission rate, and ρ is the reduction of fecundity in infectious bison such that $\rho \leq 1$. Therefore ρe is the reduced birth rate. Note that $(a - \phi N)$ is the total birth rate of the susceptible and recovered class. Our flow diagram in Figure 13 shows that the recruitment rate of the susceptible class can come from infectious and chronic classes at the overall per capita birth rate of $\rho(1 - e)(a - \phi N)$ and the recovered class at the rate of δ due to waning immunity. Now, susceptible individuals can be infected from both direct and indirect transmissions. The direct transmission comes from contacting the infectious and chronic states at a rate of β_1. Besides, we denote the indirect transmission by β_2. Therefore, $\beta_1 \left(\frac{I+\epsilon A}{N}\right) S$ is the direct infection rate from the infected and chronic states to the susceptible bison, and $\beta_2 SW$ is the indirect infection from the Brucella in the environment. We assume the bison in the infectious individuals has more bacteria load than the bison in the chronic state, and thus ϵ is the modification factor such that $\epsilon < 1$. Some susceptible individuals can enter the recovered individual with a vaccination rate of ϕ_1, whereas the immunity waning rate is δ. Besides, α and γ are the disease-related death rate and the culling rate, respectively. The infected population recovery rate is v in

which a fraction of this denoted by p moves to the chronic state and $(1-p)$ moves to the recovered class. In the environment, the Brucella shedding rate from the infectious and the chronic individuals are ξ_1 and ξ_2, respectively. Furthermore, ϕ_2 is the elimination rate of Brucella in the environment. The model flow diagram is represented in Figure 13.

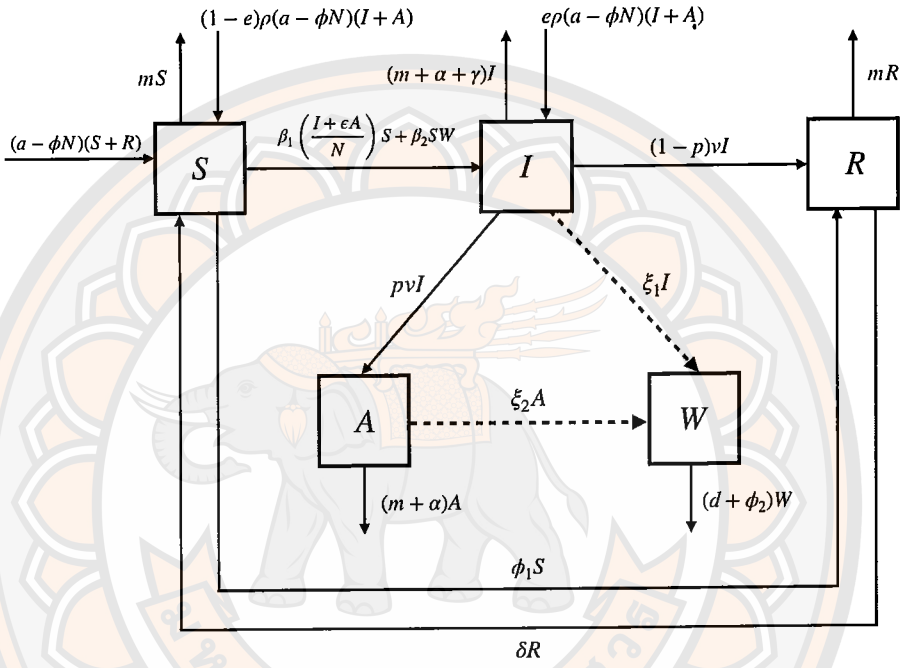

Figure 13 The flowchart of the transmission dynamics of brucellosis in bison. The solid arrows represent transfer orientation of bison population (the transitions between compartments). The dashed arrows represent incoming of Brucella to environment discharged by I and A.

The model is given by the following system of differential equations:

$$\begin{aligned}
\frac{dS}{dt} &= (a-\phi N)(S+R) + (1-e)\rho(a-\phi N)(I+A) + \delta R \\
&\quad - \left(\beta_1\left(\frac{I+\epsilon A}{N}\right)S + \beta_2 SW\right) - (m+\phi_1)S \\
\frac{dI}{dt} &= \beta_1\left(\frac{I+\epsilon A}{N}\right)S + \beta_2 SW + e\rho(a-\phi N)(I+A) \\
&\quad - (v+m+\alpha+\gamma)I \\
\frac{dA}{dt} &= pvI - (m+\alpha)A \\
\frac{dR}{dt} &= (1-p)vI + \phi_1 S - (m+\delta)R \\
\frac{dW}{dt} &= \xi_1 I + \xi_2 A - (d+\phi_2)W.
\end{aligned} \tag{3.1.1}$$

The model has initial conditions given by :

$$S(0) \geq 0, I(0) \geq 0, A(0) \geq 0, R(0) \geq 0, W(0) \geq 0.$$

3.2 Positivity of solution

Theorem 3.2.1. *The solutions $S(t), I(t), A(t), R(t)$ and $W(t)$ of the system are nonnegative for $t \geq 0$.*

Proof. : Let the initial data $S(0) \geq 0, I(0) \geq 0, A(0) \geq 0, R(0) \geq 0$ and $W(0) \geq 0$. We prove that $S(t)$ is positive. Assume that there exists a first time $t_1 : S(t_1) = 0, S'(t_1) < 0$ and $S(t) > 0, I(t) > 0, A(t) > 0, R(t) > 0, W(t) > 0$ for $0 < t < t_1$. By the first equation of (3.1.1), we have

$$\begin{aligned}
\frac{dS(t_1)}{dt} &= (a-\phi N)(S(t_1)+R(t_1)) + (1-e)\rho(a-\phi N)(I(t_1)+A(t_1)) + \delta R(t_1) \\
&\quad - \left(\beta_1\left(\frac{I(t_1)+\epsilon A}{N}\right)S(t_1) + \beta_2 S(t_1)W(t_1)\right) - (m+\phi_1)S(t_1) \\
&= (a-\phi N)(R(t_1)) + (1-e)\rho(a-\phi N)(I(t_1)+A(t_1)) + \delta R(t_1) \\
&> 0,
\end{aligned}$$

which leads to a contradiction, implying that $S(t)$ remains positive.

Next, we prove that $I(t)$ is positive. Assume that there exists a first time

$t_2 : I(t_2) = 0, I'(t_2) < 0$ and $S(t) > 0, I(t) > 0, A(t) > 0, R(t) > 0, W(t) > 0$ for $0 < t < t_2$. By the second equation of (3.1.1), we have

$$\begin{aligned}\frac{dI(t_2)}{dt} &= \beta_1 \left(\frac{I(t_2) + \epsilon A(t_2)}{N} \right) S(t_2) + \beta_2 S(t_2) W(t_2) + e\rho(a - \phi N)(I(t_2) + A(t_2)) \\ &\quad - (v + m + \alpha + \gamma) I(t_2) \\ &= \beta_1 \left(\frac{\epsilon A(t_2)}{N} \right) S(t_2) + \beta_2 S(t_2) W(t_2) + e\rho(a - \phi N) A(t_2) > 0,\end{aligned}$$

which leads to a contradiction, implying that $I(t)$ remains positive.

Next, we will show $A(t)$ is positive. Assume that there exists a first time $t_3 : A(t_3) = 0, A'(t_3) < 0$ and $S(t) > 0, I(t) > 0, A(t) > 0, R(t) > 0, W(t) > 0$ for $0 < t < t_3$. Consider the third equation of (3.1.1), we have

$$\begin{aligned}\frac{dA(t_3)}{dt} &= pvI(t_3) - (m + \alpha) A(t_3) \\ &= pvI(t_3) > 0,\end{aligned}$$

which is a contradiction, meaning that A remains positive.

Then, we will prove that $R(t)$ is positive. Assume that there exists a first time $t_4 : R'(t_4) = 0, R(t_4) < 0$ and $S(t) > 0, I(t) > 0, A(t) > 0, R(t) > 0, W(t) > 0$ for $0 < t < t_4$. In the fourth equation of (3.1.1), we have

$$\begin{aligned}\frac{dR(t_4)}{dt} &= (1 - p)vI(t_4) + \phi_1 S(t_4) - (m + \delta) R(t_4) \\ &= (1 - p)vI(t_4) + \phi_1 S(t_4) > 0,\end{aligned}$$

which is a contradiction. This means that $R(t)$ remains positive.

Next, we will show $W(t)$ is positive. Assume that there exists a first time $t_5 : W(t_5) = 0, W'(t_5) < 0$ and $S(t) > 0, I(t) > 0, A(t) > 0, R(t) > 0, W(t) > 0$ for $0 < t < t_5$. Consider the last equation of (3.1.1), we have

$$\begin{aligned}\frac{dW(t_5)}{dt} &= \xi_1 I(t_5) + \xi_2 A(t_5) - (d + \phi_2) W(t_5) \\ &= \xi_1 I(t_5) + \xi_2 A(t_5) > 0,\end{aligned}$$

which is a contradiction, meaning that W remains positive.

Therefore, all solutions of model (3.1.1) are nonnegative whenever $t \geq 0$. □

3.3 Boundary of solution

We determine the boundary of solutions of the system of (3.1.1)

Since $N = S + I + A + R$, then

$$\begin{aligned}
\frac{dN}{dt} &= \frac{dS}{dt} + \frac{dI}{dt} + \frac{dA}{dt} + \frac{dR}{dt} \\
&= (a - \phi N)(S + R) + \rho(a - \phi N)(I + A) - m(S + I + A + R) \\
&\quad - (\alpha + \gamma)I - \alpha A \\
&\leq (a - \phi N)(S + R) + \rho(a - \phi N)(I + A) - m(S + I + A + R) \\
&= (a - \phi N)(S + R + \rho I + \rho A) - mN \\
&\leq (a - \phi N)(S + R + I + A) - mN \\
&= (a - \phi N)N - mN.
\end{aligned}$$

By integration both sides, we have

$$\begin{aligned}
\int_0^t \frac{dN}{((a - \phi N) - m)N} &\leq \int_0^t 1dt \\
\int_0^t \left(\frac{1}{(a-m)N}\right) dN - \int_0^t \frac{\phi}{(a-m)(\phi N - (a-m))} dN &\leq t \\
\ln\left[\frac{N(t)(\phi N(0) - (a-m))}{N(0)(\phi N(t) - (a-m))}\right] &\leq (a-m)t \\
\frac{N(t)(\phi N(0) - (a-m))}{N(0)(\phi N(t) - (a-m))} &\leq e^{(a-m)t}
\end{aligned}$$

then

$$\begin{aligned}
N(t) &\leq \frac{e^{(a-m)t}N(0)(\phi N(t) - (a-m))}{\phi N(0) - (a-m)} \\
N(t) &\leq \frac{e^{(a-m)t}N(0)\phi N(t)}{\phi N(0) - (a-m)} - \frac{(a-m)e^{(a-m)t}N(0)}{\phi N(0) - (a-m)} \\
N(t) - \frac{e^{(a-m)t}N(0)\phi N(t)}{\phi N(0) - (a-m)} &\leq -\frac{(a-m)e^{(a-m)t}N(0)}{\phi N(0) - (a-m)} \\
\frac{\phi N(0)N(t) - (a-m)N(t) - e^{(a-m)t}N(0)\phi N(t)}{\phi N(0) - (a-m)} &\leq -\frac{(a-m)e^{(a-m)t}N(0)}{\phi N(0) - (a-m)} \\
\left(\phi N(0) - (a-m) - \phi e^{(a-m)t}N(0)\right)N(t) &\leq -\frac{(a-m)e^{(a-m)t}N(0)(\phi N(0) - (a-m))}{\phi N(0) - (a-m)} \\
N(t) &\leq \frac{(a-m)N(0)e^{(a-m)t}}{\phi e^{(a-m)t}N(0) - \phi N(0) + (a-m)} \\
N(t) &\leq \frac{(a-m)N(0)e^{(a-m)t}}{\phi N(0)(e^{(a-m)t} - 1) + (a-m)} \\
N(t) &\leq \frac{(a-m)N(0)e^{(a-m)t}}{\phi N(0)e^{(a-m)t} - \phi N(0) + (a-m)}
\end{aligned}$$

$$N(t) \leq \frac{(a-m)N(0)e^{(a-m)t}}{N(0)e^{(a-m)t}\left(\phi - \phi e^{-(a-m)t} + \frac{(a-m)}{N(0)}e^{-(a-m)t}\right)}$$

$$N(t) \leq \frac{a-m}{\phi - \phi e^{-(a-m)t} + \left(\frac{a-m}{N(0)}\right)e^{-(a-m)t}}.$$

Therefore, we get

$$\limsup_{t\to\infty} N \leq \frac{a-m}{\phi}.$$

Next, we consider $W(t)$,

$$\begin{aligned}\frac{dW}{dt} &= \xi_1 I + \xi_2 A - (d+\phi_2)W \\ &\leq (\xi_1+\xi_2)N - (d+\phi_2)W \\ &\leq \frac{(\xi_1+\xi_2)(a-m)}{\phi} - (d+\phi_2)W,\end{aligned}$$

then

$$\frac{dW}{dt} + (d+\phi_2)W \leq \frac{(\xi_1+\xi_2)(a-m)}{\phi}.$$

By using an integrating factor, we have

$$\frac{d}{dt}\left(W(t)e^{(d+\phi_2)t}\right) \leq \frac{(\xi_1+\xi_2)(a-m)}{\phi}e^{(d+\phi_2)t}.$$

Integrating both sides, we obtain that

$$W(t) \leq \frac{(\xi_1+\xi_2)(a-m)}{(d+\phi_2)\phi} - \left(\frac{(\xi_1+\xi_2)(a-m)}{(d+\phi_2)\phi} - W(0)\right)e^{-(d+\phi_2)t}.$$

Thus, we have

$$\limsup_{t\to\infty} W \leq \frac{(\xi_1+\xi_2)(a-m)}{(d+\phi_2)\phi}.$$

Therefore, the biologically-feasible region for this model is

$$\begin{aligned}\Omega = \Bigg\{(S,I,A,R,W) \in \mathbb{R}^5_+ : S,I,A,R,W \geq 0, S+I+A+R \leq \frac{a-m}{\phi} \\ \text{and } W \leq \frac{(\xi_1+\xi_2)(a-m)}{(d+\phi_2)\phi}\Bigg\}. \qquad (3.3.1)\end{aligned}$$

All solutions of this model enter the region from the boundary of Ω. This means that every solution of this model will enter the region Ω and stay inside Ω. Hence Ω is positively invariant and attracting with respect to model (3.1.1). In this region, the model is mathematically and epidemiologically well-posed.

3.4 Disease-free equilibrium

We find a disease-free equilibrium by setting I, A and W to be equal to zero, i.e. $I = A = W = 0$. First, we set the first equation (3.1.1) to be equal to zero, and we get

$$S = \frac{(a - \phi N + \delta)R}{\phi N + m + \phi_1 - a}. \tag{3.4.1}$$

And, by setting the fourth equation (3.1.1) to zero, we obtain

$$R = \frac{\phi S}{m + \delta}. \tag{3.4.2}$$

Substituting (3.4.2) into equation (3.4.1), we have

$$S = \frac{(a - m)(m + \delta)}{\phi(m + \delta + \phi_1)}. \tag{3.4.3}$$

Substituting (3.4.3) into equation (3.4.2), we have

$$R = \frac{(a - m)\phi_1}{\phi(m + \delta + \phi_1)}. \tag{3.4.4}$$

Therefore, the system (3.1.1) has an evident disease-free equilibrium, which is given by

$$E_0 = (S^0, I^0, A^0, R^0, W^0) = \left(\frac{(a - m)(m + \delta)}{\phi(m + \delta + \phi_1)}, 0, 0, \frac{(a - m)\phi_1}{\phi(m + \delta + \phi_1)}, 0\right)$$

provided $a > m$.

3.5 The basic reproduction number (R_0)

The basic reproduction number, R_0, uses a threshold parameter for the infectious disease, and it is important in determining the spread of the disease. To calculate R_0, we used the next-generation matrix method by van den Driessche et al. [49] and we obtain

$$\mathcal{F} = \begin{bmatrix} \beta_1 \left(\frac{I + \epsilon A}{N}\right) S + \beta_2 SW + e\rho(a - \phi N)(I + A) \\ 0 \\ 0 \end{bmatrix}$$

and

$$\mathcal{V} = \begin{bmatrix} (v+m+\alpha+\gamma)I \\ -pvI + (m+\alpha)A \\ -\xi_1 I - \xi_2 A + (d+\phi_2)W \end{bmatrix}.$$

Let F and V are the 3×3 matrices, defined by

$$F = \left[\frac{\partial \mathcal{F}_i}{\partial x_j}(E_0)\right] \quad \text{and} \quad V = \left[\frac{\partial \mathcal{V}_i}{\partial x_j}(E_0)\right] \quad \text{with} \quad 1 \leq i, j \leq 3,$$

where $x = (I, A, W)$ and E_0 is the disease-free equilibrium of (3.1.1).
Therefore, we have

$$F = \begin{bmatrix} \frac{\beta_1 S^0}{N^0} + e\rho m & \frac{\beta_1 \epsilon S^0}{N^0} + e\rho m & \beta_2 S^0 \\ 0 & 0 & 0 \\ 0 & 0 & 0 \end{bmatrix}$$

and

$$V = \begin{bmatrix} v+m+\alpha+\gamma & 0 & 0 \\ -pv & m+\alpha & 0 \\ -\xi_1 & -\xi_2 & d+\phi_2 \end{bmatrix}.$$

And

$$V^{-1} = \frac{1}{Y_1} \begin{bmatrix} (m+\alpha)(d+\phi_2) & 0 & 0 \\ pv(d+\phi_2) & (v+m+\alpha+\gamma)(d+\phi_2) & 0 \\ pv\xi_2 + \xi_1(m+\alpha) & (v+m+\alpha+\gamma)\xi_2 & (v+m+\alpha+\gamma)(m+\alpha) \end{bmatrix},$$

where $Y_1 = (v+m+\alpha+\gamma)(m+\alpha)(d+\phi_2)$.
The next generation matrix is

$$\begin{aligned} FV^{-1} &= \frac{1}{Y_1} \begin{bmatrix} \frac{\beta_1 S^0}{N^0} + e\rho m & \frac{\beta_1 \epsilon S^0}{N^0} + e\rho m & \beta_2 S^0 \\ 0 & 0 & 0 \\ 0 & 0 & 0 \end{bmatrix} \\ &\quad \times \begin{bmatrix} (m+\alpha)(d+\phi_2) & 0 & 0 \\ pv(d+\phi_2) & (v+m+\alpha+\gamma)(d+\phi_2) & 0 \\ pv\xi_2 + \xi_1(m+\alpha) & (v+m+\alpha+\gamma)\xi_2 & (v+m+\alpha+\gamma)(m+\alpha) \end{bmatrix} \\ &= \frac{1}{Y_1} \begin{bmatrix} Y_2 & Y_3 & Y_4 \\ 0 & 0 & 0 \\ 0 & 0 & 0 \end{bmatrix}, \end{aligned}$$

where

$$Y_2 = \left(\frac{\beta_1 S^0}{N^0} + e\rho m\right)(m+\alpha)(d+\phi_2) + \left(\frac{\beta_1 \epsilon S^0}{N^0} + e\rho m\right)(pv(d+\phi_2)) + \beta_2 S^0(pv\xi_2 + \xi_1(m+\alpha)),$$

$$Y_3 = \left(\frac{\beta_1 \epsilon S^0}{N^0} + e\rho m\right)(v+m+\alpha+\gamma)(d+\phi_2) + \beta_2 S^0(v+m+\alpha+\gamma)\xi_2,$$

$$Y_4 = \beta_2 S^0(v+m+\alpha+\gamma)(m+\alpha).$$

Therefore, the basic reproduction number of system (3.1.1) is given by the sepectal radius of a matrix FV^{-1}, which is

$$\begin{aligned}
R_0 &= \frac{Y_2}{Y_1} \\
&= \frac{\left(\frac{\beta_1 S^0}{N^0} + e\rho m\right)(m+\alpha)(d+\phi_2) + \left(\frac{\beta_1 \epsilon S^0}{N^0} + e\rho m\right)(pv(d+\phi_2)) + \beta_2 S^0(pv\xi_2 + \xi_1(m+\alpha))}{(v+m+\alpha+\gamma)(m+\alpha)(d+\phi_2)} \\
&= \frac{1}{(v+m+\alpha+\gamma)(m+\alpha)(d+\phi_2)}\left[\frac{\beta_1 S^0(m+\alpha)(d+\phi_2)}{N^0} + e\rho m(m+\alpha)(d+\phi_2)\right. \\
&\quad \left. + \frac{\beta_1 \epsilon S^0 pv(d+\phi_2)}{N^0} + e\rho m pv(d+\phi_2) + \beta_2 S^0(pv\xi_2 + \xi_1(m+\alpha))\right] \\
&= \frac{1}{(v+m+\alpha+\gamma)(m+\alpha)(d+\phi_2)}\left[\frac{\beta_1 S^0(d+\phi_2)(m+\alpha+\epsilon_2+\epsilon pv)}{N^0}\right. \\
&\quad \left. + e\rho m(d+\phi_2)(m+\alpha+\epsilon_2+pv) + \beta_2 S^0(pv\xi_2 + \xi_1(m+\alpha))\right].
\end{aligned}$$

Since $S^0 = \frac{(a-m)(m+\delta)}{\phi(m+\delta+\phi_1)}$ and $N^0 = \frac{a-m}{\phi}$, then we obtain that

$$\begin{aligned}
R_0 &= \frac{1}{(v+m+\alpha+\gamma)(m+\alpha)(d+\phi_2)}\left[\beta_1\left(\frac{m+\delta}{m+\delta+\phi_1}\right)(d+\phi_2)(m+\alpha+\epsilon_2+\epsilon pv)\right. \\
&\quad \left. + e\rho m(d+\phi_2)(m+\alpha+\epsilon_2+pv) + \beta_2\left(\frac{(a-m)(m+\delta)}{\phi(m+\delta+\phi_1)}\right)(pv\xi_2 + \xi_1(m+\alpha))\right] \\
&= \frac{1}{k_1 k_2 k_3}\left[\beta_1 k_4 k_3(k_2 + \epsilon pv) + e\rho m k_3(k_2 + pv) + \beta_1\left(\frac{a-m}{\phi}\right)k_4(pv\xi_2 + \xi_1 k_2)\right], \qquad (3.5.1)
\end{aligned}$$

where

$$\begin{aligned}
k_1 &= v+m+\alpha+\gamma \\
k_2 &= m+\alpha \\
k_3 &= d+\phi_2 \\
k_4 &= \frac{m+\delta}{m+\delta+\phi_1}.
\end{aligned}$$

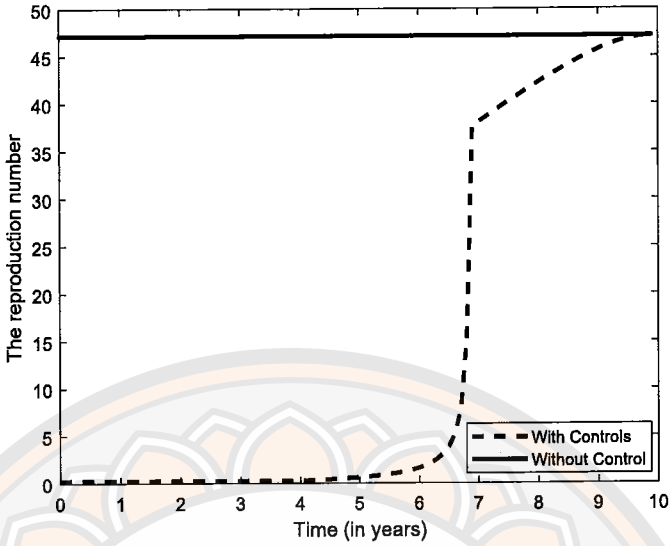

Figure 14 The reproduction numbers of the two models: with controls and without control.

Figure 14 shows the reproduction numbers of the two models. The solid line represents the reproduction number of the model without controls, while the dashed line represents the reproduction number of the model with cooperative controls. Since the reproduction number of no control model is constant and starts at about 47, the disease will spread. However, if controls are implemented at the beginning of the disease onset, the number of infections will not grow since the reproduction number at the beginning of the outbreak is less than 1 (about 0.5, see the zoomed-in version in Figure 15). The reproduction number of the model with optimal control will rise to the original number after a few years (see Figure 14) because of no longer controls needed.

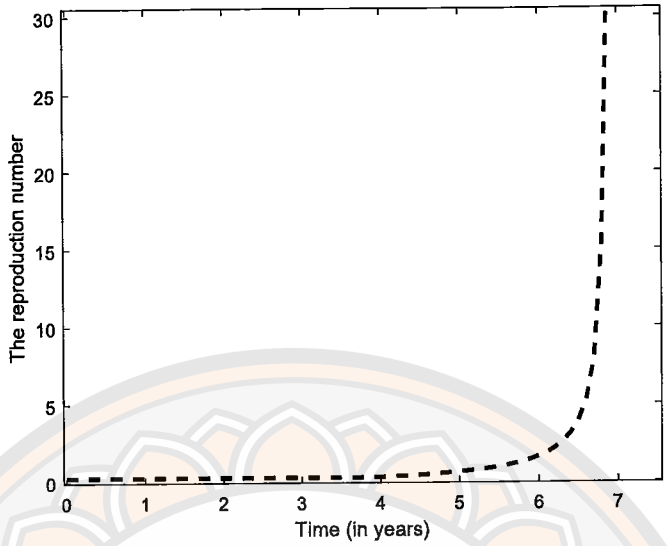

Figure 15 The zoomed-in reproduction number of the model with controls

3.6 The local stability of the disease-free equilibrium point

For the model (3.1.1), it can be established that the disease-free equilibrium is locally asymptotically stable whenever $R_0 < 1$ and unstable $R_0 > 1$. Mathematically, based on the result in Theorem 2.1.1, we have the following theorem.

Theorem 3.6.1. *The disease-free equilibrium, E_0, is locally asymptotically stable when $R_0 < 1$ and unstable when $R_0 > 1$.*

3.7 The global stability of the disease-free equilibrium point

In addition, the global stability of the disease-free equilibrium is analyzed by using the global stability result established in Lemma 2.1.4.

Theorem 3.7.1. *The disease-free equilibrium point, E_0, is globally asymptotically stable provided that $R_0 < 1$.*

Proof. : By following Theorem 2.1.4, we write system (3.1.1) in the form

$$\frac{dX_1}{dt} = F(X_1, X_2)$$

$$\frac{dX_2}{dt} = G(X_1, X_2), \qquad G(X_1, 0) = 0,$$

where $X_1 = (S, R)$ and $X_2 = (I, A, W)$. The disease-free equilibrium is now denoted by $E_0 = (X_1^*, 0)$ where $X_1^* = \left(\frac{(a-m)(m+\delta)}{\phi(m+\delta+\phi_1)}, \frac{(a-m)\phi_1}{\phi(m+\delta+\phi_1)}\right)$. We note that the system is linear and its solution can be easily found as

$$\begin{aligned}\frac{dX_1}{dt} &= F(X_1, X_2) \\ &= \begin{bmatrix} (a-\phi N)(S+R) + (1-e)\rho(a-\phi N)(I+A) + \delta R - \left(\beta_1\left(\frac{I+\epsilon A}{N}\right)S + \beta_2 SW\right) - (m+\phi_1)S \\ (1-p)vI + \phi_1 S - (m+\delta)R \end{bmatrix}.\end{aligned}$$

Therefore, we have

$$\frac{dX_1}{dt} = F(X_1, 0) = \begin{bmatrix} (a-\phi N)(S+R) + \delta R - (m+\phi_1)S \\ \phi_1 S - (m+\delta)R \end{bmatrix}, \tag{3.7.1}$$

is linear and its solution can be easily found. As for R, we can deduce from the equation above that

$$\frac{dR}{dt} = \phi_1 S - (m+\delta)R.$$

Since $S + R \leq \frac{a-m}{\phi}$, it follows that

$$\begin{aligned}\frac{dR}{dt} &\leq \phi_1\left(\frac{a-m}{\phi} - R\right) - (m+\delta)R \\ \frac{dR}{dt} &\leq \phi_1\left(\frac{a-m}{\phi}\right) - (m+\delta+\phi_1)R \\ \frac{dR}{dt} + (m+\delta+\phi_1)R &\leq \phi_1\left(\frac{a-m}{\phi}\right).\end{aligned}$$

By using an integrating factor, we have

$$\frac{d}{dt}\left(e^{(m+\delta+\phi_1)t}R\right) = e^{(m+\delta+\phi_1)t}\phi_1\left(\frac{a-m}{\phi}\right).$$

Integrate both sides of the above equation, we have

$$e^{(m+\delta+\phi_1)t}R = \frac{e^{(m+\delta+\phi_1)t}(a-m)\phi_1}{\phi(m+\delta+\phi_1)} + C_0,$$

for arbitrary constant value of C_0. Thus, we have

$$R = \frac{(a-m)\phi_1}{\phi(m+\delta+\phi_1)} + C_0 e^{-(m+\delta+\phi_1)t}.$$

Since $R \leq \frac{a-m}{\phi} - S$ and we assume that $N = \frac{a-m}{\phi}$, then we get

$$\begin{aligned}\frac{dS}{dt} &= (a-\phi N)(S+R) + \delta R - (m+\phi_1)S \\ &\leq (m+\delta)\left(\frac{a-m}{\phi}\right) - (m+\phi_1+\delta)S.\end{aligned}$$

And by using the same technique, we obtain that

$$S = \frac{(a-m)(m+\delta)}{\phi(m+\delta+\phi_1)} + C_1 e^{-(m+\delta+\phi_1)t},$$

where C_1 arbitrary constant value.

It followed that, $S(t) \to S^0$ and $R(t) \to R^0$, as $t \to \infty$. Therefore $X_1^* = (S^0, R^0)$ is globally asymptotically stable.

Next consider that

$$G(X_1, X_2) = \begin{bmatrix} \beta_1\left(\frac{I+\epsilon A}{N}\right)S + \beta_2 SW + e\rho(a-\phi N)(I+A) - k_1 I \\ pvI - k_2 A \\ \xi_1 I + \xi_2 A - k_3 W \end{bmatrix}.$$

Then

$$\frac{\partial G}{\partial X_2}(X_1, X_2)$$

$$= \begin{bmatrix} \frac{N\beta_1 S - \beta_1(I+\epsilon A)S}{N^2} + e\rho(a-\phi N) + (I+A)(-e\rho\phi) - k_1 & \frac{N\beta_1 S - \beta_1(I+\epsilon A)S}{N^2} + e\rho(a-\phi N) + (I+A)(-e\rho\phi) & \beta_2 S \\ pv & -k_2 & 0 \\ \xi_1 & \xi_2 & -k_3 \end{bmatrix}.$$

Hence, we have

$$\frac{\partial G}{\partial X_2}(X_1^*, 0) = A_M = \begin{bmatrix} \frac{\beta_1 S^0}{N} + e\rho(a-\phi N) - k_1 & \frac{\beta_1 \epsilon S^0}{N} + e\rho(a-\phi N) & \beta_2 S^0 \\ pv & -k_2 & 0 \\ \xi_1 & \xi_2 & -k_3 \end{bmatrix}.$$

This matrix is an M-matrix, meaning it has non-negative in its off-diagonal elements.

Therefore, we have

$$\begin{aligned} G(X_1, X_2) &= A_M X_2 - \hat{G}(X_1, X_2) \\ \hat{G}(X_1, X_2) &= A_M X_2 - G(X_1, X_2) \\ &= \begin{bmatrix} \frac{\beta_1 S^0}{N} + e\rho(a-\phi N) - k_1 & \frac{\beta_1 \epsilon S^0}{N} + e\rho(a-\phi N) & \beta_2 S^0 \\ pv & -k_2 & 0 \\ \xi_1 & \xi_2 & -k_3 \end{bmatrix} \begin{bmatrix} I \\ A \\ W \end{bmatrix} \end{aligned}$$

$$
\begin{aligned}
&- \begin{bmatrix} \beta_1 \left(\frac{I+\epsilon A}{N}\right) S + \beta_2 SW + e\rho(a-\phi N)(I+A) - k_1 I \\ pvI - k_2 A \\ \xi_1 I + \xi_2 A - k_3 W \end{bmatrix} \\
&= \begin{bmatrix} \frac{\beta_1 S^0}{N} I + e\rho(a-\phi N)I - k_1 I + \frac{\beta_1 \epsilon S^0}{N} A + e\rho(a-\phi N)A + \beta_2 S^0 W \\ pvI - k_2 A \\ \xi_1 I + \xi_2 A - k_3 W \end{bmatrix} \\
&- \begin{bmatrix} \beta_1 \left(\frac{I+\epsilon A}{N}\right) S + \beta_2 SW + e\rho(a-\phi N)(I+A) - k_1 I \\ pvI - k_2 A \\ \xi_1 I + \xi_2 A - k_3 W \end{bmatrix} \\
&= \begin{bmatrix} \frac{\beta(I+\epsilon A)}{N}(S^0 - S) + \beta_2 W(S^0 - S) \\ 0 \\ 0 \end{bmatrix}
\end{aligned}
$$

Meanwhile, we consider the first equation of system (3.1.1) and since $S+I+A+R \leq \frac{a-m}{\phi}$, it follows that

$$
\begin{aligned}
\frac{dS}{dt} &\leq (a-\phi N)(S+R) + \rho(a-\phi N)(I+A) + \delta R - (m+\phi_1)S \\
&\leq (a-\phi N)\left(\frac{a-m}{\phi} - (I+A)\right) + \rho(a-\phi N)(I+A) \\
&\quad + \delta\left(\frac{a-m}{\phi} - S\right) - (m+\phi_1)S \\
&= (m+\delta)\left(\frac{a-m}{\phi}\right) - (m+\phi_1+\delta)S - (1-\rho)(a-\phi N)(I+A) \\
&\leq (m+\delta)\left(\frac{a-m}{\phi}\right) - (m+\phi_1+\delta)S.
\end{aligned}
$$

Clearly, $S(t) \to \frac{(a-m)(m+\delta)}{\phi(m+\delta+\phi_1)} = S^0$, as $t \to \infty$. Therefore, we get $S(t) \leq S^0$. This implies that $\hat{G}(X_1, X_2) \geq 0$. By Lemma 2.1.4, we can conclude that the disease-free equilibrium, denoted as E_0, is globally asymptotically stable. $\square$

3.8 The endemic equilibrium point

The endemic equilibrium $E^* = (S^*, I^*, A^*, R^*, W^*)$ is determined by equations:

$$\begin{aligned}
0 &= (a-\phi N)(S^*+R^*) + (1-e)\rho(a-\phi N)(I^*+A^*) + \delta R^* \\
&\quad - \left(\beta_1\left(\frac{I^*+\epsilon A^*}{N}\right)S^* + \beta_2 S^* W^*\right) - (m+\phi_1)S^* \\
0 &= \beta_1\left(\frac{I^*+\epsilon A^*}{N}\right)S^* + \beta_2 S^* W^* + e\rho(a-\phi N)(I^*+A^*) \\
&\quad - (v+m+\alpha+\gamma)I^* \\
0 &= pvI^* - (m+\alpha)A^* \\
0 &= (1-p)vI^* + \phi_1 S^* - (m+\delta)R^* \\
0 &= \xi_1 I^* + \xi_2 A^* - (d+\phi_2)W^*.
\end{aligned} \tag{3.8.1}$$

From the third equation and the last equation in (3.8.1), we get

$$I^* = \frac{(m+\alpha)A^*}{pv}$$

and

$$\begin{aligned}
W^* &= \frac{\xi_1 I^* + \xi_2 A^*}{d+\phi_2} \\
&= \frac{1}{(d+\phi_2)(pv)}\left[(\xi_1(m+\alpha)+\xi_2 pv)A^*\right],
\end{aligned}$$

respectively.

Substitute I^* into the fourth equation in (3.8.1), we obtain that

$$R^* = \frac{1}{(m+\delta)(pv)}\left((1-p)v(m+\alpha)A^* + \phi_1 pvS^*\right).$$

Theorem 3.8.1. *When $R_0 > 1$, there exists a unique endemic equilibrium point of system* (3.1.1).

Proof. : First, we can reduce the dimension of the system into four by setting

$R = N - S - I - A$ to get

$$\begin{aligned}
\frac{dS}{dt} &= (a - \phi N)[N + (\rho(1-e) - 1)(I + A)] + \delta(N - S - I - A), \\
&\quad - \left(\beta_1 \left(\frac{I + \epsilon A}{N}\right) S + \beta_2 SW\right) - (m + \phi_1)S, \\
\frac{dI}{dt} &= \beta_1 \left(\frac{I + \epsilon A}{N}\right) S + \beta_2 SW + e\rho(a - \phi N)(I + A), \\
&\quad - (m + \alpha + \gamma + v)I, \\
\frac{dA}{dt} &= pvI - (m + \alpha)A, \\
\frac{dW}{dt} &= \xi_1 I + \xi_2 A - (d + \phi_2)W.
\end{aligned} \tag{3.8.2}$$

The endemic equilibrium of system (3.8.2) is determined by equations

$$\begin{aligned}
0 =& (a - \phi N)[N + (\rho(1-e) - 1)(I^* + A^*)] - (m + \phi_1)S^* \\
&+ \delta(N - S^* - I^* - A^*) - \left(\beta_1 \left(\frac{I^* + \epsilon A^*}{N}\right) + \beta_2 \left(\frac{\xi_1 I^* + \xi_2 A^*}{d + \phi_2}\right)\right),
\end{aligned} \tag{3.8.3}$$

$$\begin{aligned}
0 =& \beta_1 \left(\frac{I^* + \epsilon A^*}{N}\right) S^* + \beta_2 S^* \left(\frac{\xi_1 I^* + \xi_2 A^*}{d + \phi_2}\right) + e\rho(a - \phi N)(I^* + A^*) \\
&- (m + \alpha + \gamma + v)I^*
\end{aligned} \tag{3.8.4}$$

$$0 = pvI^* - (m + \alpha)A^*. \tag{3.8.5}$$

From (3.8.5), we have

$$I^* = \frac{(m + \alpha)A^*}{pv} = \frac{k_2 A^*}{pv} \tag{3.8.6}$$

$$I^* + A^* = M_1 A^*, \tag{3.8.7}$$

$$I^* + \epsilon A = M_2 A^* \tag{3.8.8}$$

and

$$\xi_1 I^* + \xi_2 A^* = M_3 A^*, \tag{3.8.9}$$

with

$$M_1 = \frac{k_2 + pv}{pv},$$

$$M_2 = \frac{k_2 + \epsilon pv}{pv},$$

and

$$M_3 = \frac{\xi_1 k_2 + \xi_2 pv}{pv}.$$

It follows from equation (3.8.3) that

$$\begin{aligned} 0 =& (a-\phi N)[N + (\rho(1-e)-1)(M_1 A^*)] - (m+\phi_1)S^* \\ &+ \delta(N - S^* - I^* - A^*) - \left(\frac{\beta_1 M_2 A^*}{N} + \frac{\beta_2 M_3 A^*}{d+\phi_2}\right) S^*. \end{aligned}$$

Then, we get

$$(a-\phi N)[N + (\rho(1-e)-1)(M_1 A^*)] + \delta(N - M_1 A^*) = \left(m + \delta + \phi_1 + \frac{\beta_1}{N} M_2 A^* + \frac{\beta_2 M_3}{d+\phi}\right) S^*$$

$$S^* = \frac{(a-\phi N)N + (a-\phi N)\rho M_1 A^* - (a-\phi N)\rho e M_1 A^* - (a-\phi N)M_1 A^* + \delta N - \delta M_1 A^*}{m + \delta + \phi_1 + \frac{\beta_1}{N} M_2 A^* + \frac{\beta_2 M_3}{d+\phi}}, \tag{3.8.10}$$

for $A^* \neq 0$, substituting (3.8.6)-(3.8.9) into (3.8.4), we get

$$0 = \frac{\beta_1 M_2 A^* S^*}{N} + \frac{\beta_2 S^* M_3 A^*}{d+\phi_2} + e\rho(a-\phi N)(M_1 A^*) - k_1 I^*$$

$$A^* S^* \left(\frac{\beta_1 k_3 M_2 + \beta_2 N M_3}{N k_3}\right) = \frac{k_1 k_2 A^*}{pv} - e\rho(a-\phi N) M_1 A^*.$$

As a result, we achieve

$$S^* = \frac{k_1 k_2 k_3 N - e\rho(a-\phi N) pv k_3 N M_1}{pv(\beta_1 k_3 M_2 + \beta_2 N M_3)}. \tag{3.8.11}$$

Substituting (3.8.10) into (3.8.11) for $A = A^*$, we get

$$F_1(A) = F_2(A)$$

where

$$\begin{aligned} F_1(A) =& \frac{(a-\phi N)N + (a-\phi N)\rho M_1 A - (a-\phi N)\rho e M_1 A}{m + \delta + \phi_1 + \frac{\beta_1 M_2 A}{N} + \frac{\beta_2 M_3 A}{d+\phi_2}} \\ &+ \frac{-(a-\phi N)M_1 A + \delta N - \delta M_1 A}{m + \delta + \phi_1 + \frac{\beta_1 M_2 A}{N^*} + \frac{\beta_2 M_3 A}{d+\phi_2}} \\ &+ \frac{e\rho(a-\phi N) pv k_3 N M_1}{pv(\beta_1 k_3 M_2 + \beta_2 N M_3)} - \frac{k_1 k_2 k_3 N}{pv(\beta_1 k_3 M_2 + \beta_2 N M_3)}, \end{aligned} \tag{3.8.12}$$

$$F_2(A) = 0. \tag{3.8.13}$$

Clearly, F_1 and F_2 are differentiable functions for all $A \geq 0$. Direct calculation for $A \geq 0$ shows

$$F_2'(A) = 0,$$

$$F_1'(A) = \frac{(m+\delta+\phi_1+\frac{\beta_1 M_2 A}{N}+\frac{\beta_2 M_3 A}{d+\phi_2})\left[(a-\phi N)\rho M_1-(a-\phi N)\rho e M_1-(a-\phi N)M_1-\delta M_1\right]}{(m+\delta+\phi_1+\frac{\beta_1 M_2 A}{N}+\frac{\beta_2 M_3 A}{d+\phi_2})^2}$$

$$- \frac{\left[(a-\phi N)N+(a-\phi N)(\rho M_1 A)-(a-\phi N)\rho e M_1 A-(a-\phi N)(M_1 A)+\delta N-\delta M_1 A\right](\frac{\beta M_2}{N}+\frac{\beta_1 M_3}{d+\phi_2})}{(m+\delta+\phi_1+\frac{\beta M_2 A}{N}+\frac{\beta_1 M_3 A}{d+\phi_2})^2}$$

$$= \frac{-(m+\delta+\phi_1)\left[(a-\phi N)M_1(1-\rho)+(a-\phi N)\rho e M_1 \delta M_1+(a-\phi N)NX_1+\delta N X_1\right]}{X_2^2},$$

where

$$X_1 = \frac{\beta_1 M_2}{N^*}+\frac{\beta_2 M_3}{k_3} \quad \text{and} \quad X_2 = m+\delta+\phi_1+X_1 A^*.$$

Since $\rho \in [0,1]$, it implies that $F_1'(A) < 0$. Thus the function $F_1(A)$ is monotonic decreasing function for $A > 0$, and it follows that

$$F_1(0) = \frac{(a-\phi N^*)N^*}{m+\delta+\phi_1}+\frac{e\rho(a-\phi N^*)pvk_3 N M_1}{pv(\beta_1 k_3 M_2+\beta_2 N M_3)}-\frac{k_1k_2k_3N}{pv(\beta_1 k_3 M_2+\beta_2 N M_3)}.$$

Since $N = \frac{a-m}{\phi}$, then

$$\begin{aligned}
F_1(0) &= \frac{(m+\delta)N^*}{m+\delta+\phi_1}+\frac{e\rho(a-\phi N^*)pvk_3 N M_1}{pv(\beta_1 k_3 M_2+\beta_2 N M_3)}-\frac{k_1k_2k_3N}{pv(\beta_1 k_3 M_2+\beta_2 N M_3)} \\
&= \frac{k_1k_2k_3N}{pv(\beta_1 k_3 M_2+\beta_2 N M_3)}\left[\frac{(m+\delta)(\beta_1 k_3 M_2+\beta_2 N M_3)}{(m+\delta+\phi_1)(k_1k_2k_3)}+\frac{e\rho m pv M_1}{k_1k_2}-1\right] \\
&= \frac{k_1k_2k_3N}{pv(\beta_1 k_3 M_2+\beta_2 N M_3)}\left[\frac{1}{k_1k_2k_3}\left(\frac{m+\delta}{m+\delta+\phi_1}\right)(\beta_1 k_3 M_2 pv+\beta_2 N M_3 pv)\right. \\
&\quad \left.+\frac{1}{k_1k_2k_3}(e\rho m pv M_1 k_3)-1\right] \\
&= \frac{k_1k_2k_3N}{pv(\beta_1 k_3 M_2+\beta_2 N M_3)}\left[\frac{1}{k_1k_2k_3}\left(\frac{m+\delta}{m+\delta+\phi_1}\right)(\beta_1 k_3(k_2+\epsilon pv)\right. \\
&\quad \left.+\beta_2\left(\frac{a-m}{\phi}\right)(\xi_1 k_2+\xi_2 pv)+\frac{1}{k_1k_2k_3}(e\rho m k_3(k_2+pv))-1\right] \\
&= \frac{k_1k_2k_3N(R_0-1)}{pv(\beta_1 k_3 M_2+\beta_2 N M_3)}.
\end{aligned}$$

Therefore, we obtain that $F_1(0) > 0 = F_2(0)$ when $R_0 > 1$. Since the function $F_1(A)$ is a monotonically decreasing function and $F_2(A) = 0$, we can conclude that the function F_1 intersects the constant function F_2. This implies that there exists a unique positive root in the interval $\left[0, \frac{a-m}{\phi}\right]$ when $R_0 > 1$ and there is no positive root in the interval $\left[0, \frac{a-m}{\phi}\right]$ when $R_0 < 1$. Thus model (3.1.1) has a unique endemic equilibrium $E^* = (S^*, I^*, A^*, W^*)$. □

3.9 Global stability of the endemic equilibrium point

We now discuss the global stability of the endemic equilibrium point. To do that, we analyze the point by using the geometric approach proposed by Li and Muldowney [52] as follows:

Theorem 3.9.1. *The endemic equilibrium point, E^*, is globally asymptotically stable in Ω when $R_0 > 1$ and $\bar{b} > 0$, such that*

$$\begin{aligned}
\bar{b} = \min\Bigg\{ & -(M_{11}+M_{22}) - \inf\left\{-\beta_2 S, -\frac{\beta_2 SA}{I}, -B_1 - \frac{\beta_1 \epsilon S}{N}\right\} + \frac{I'}{I}, \\
& -pv - \xi_1 - M_{11} + k_2 - \inf\left\{-B_1 - \frac{\beta_1 S}{N}, \frac{-\beta_2 SA}{I}\right\} + \frac{I'}{I}, \\
& -pv - \xi_1 + (m+\phi_1+\delta+d+\phi_2) - \left(B_1 + \frac{\beta_1 S}{N}\right)\frac{A}{I} + \frac{I'}{I} \\
& -pv - \xi_1 - \xi_2 - \left(\beta_1\left(\frac{I+\epsilon A}{N}\right) + \beta_2 W\right)\left(1+\frac{I}{A}\right) - \left(\beta_2 A - \frac{\beta_1 \epsilon A}{N} - \beta_2 W\right)\frac{S}{I} \\
& + e\rho(a-\phi N)\left(\frac{A}{I}\right) + (m+\alpha), \\
& -pv - \xi_1 - \xi_2 - \left(\beta_1\left(\frac{I+\epsilon A}{N}\right) + \beta_2 W\right)\left(1+\frac{I}{A}\right) - (\xi_1+\xi_2 - pv)\frac{I}{A} \\
& -e\rho(a-\phi N) + (d+\phi_2) - \inf\left\{-\frac{\beta_1 S}{N} + (v+\alpha) - pv, \frac{-\beta_1 \epsilon S}{N}\right\}\Bigg\}.
\end{aligned}$$

Proof. : The Jacobian matrix of system (3.1.1) is

$$J(S,I,A,W) = \begin{bmatrix} M_{11} & M_{12} & M_{13} & -\beta_2 S \\ \left(\frac{I+\epsilon A}{N}\right) + \beta_2 W & M_{22} & \frac{\beta_1 \epsilon S}{N} + e\rho(a-\phi N) & \beta_2 S \\ 0 & pv & -(m+\alpha) & 0 \\ 0 & \xi_1 & \xi_2 & -(d+\phi_2) \end{bmatrix}, \tag{3.9.1}$$

where

$$\begin{aligned}
M_{11} &= -\delta - \left(\beta_1\left(\frac{I+\epsilon A}{N}\right) + \beta_2 W\right) - (m+\phi_1), \\
M_{12} &= (a-\phi N)(\rho(1-e)-1) - \frac{\beta_1 S}{N} - \delta, \\
M_{13} &= (a-\phi N)(\rho(1-e)-1) - \delta - \frac{\beta_1 \epsilon S}{N}, \\
M_{22} &= \frac{\beta_1 S}{N} + e\rho(a-\phi N) - (v+m+\alpha+\gamma).
\end{aligned}$$

Its corresponding second additive compound matrix $J^{[2]}$ is given by,

$$J^{[2]} = \begin{bmatrix} M_{11}+M_{22} & \frac{\beta_1 \epsilon S}{N} + e\rho(a-\phi N) & \beta_2 S & B_1 + \frac{\beta_1 \epsilon S}{N} & \beta_2 S & 0 \\ pv & M_{11}-k_2 & 0 & -B_1 - \frac{\beta_1 S}{N} & 0 & \beta_2 S \\ \xi_1 & \xi_2 & M_{11}-k_3 & 0 & -B_1 - \frac{\beta_1 S}{N} & -B_1 - \frac{\beta_1 \epsilon S}{N} \\ 0 & \beta_1\left(\frac{I+\epsilon A}{N}\right) + \beta_2 W & 0 & M_{22}-k_2 & 0 & -\beta_2 S \\ 0 & 0 & \beta_1\left(\frac{I+\epsilon A}{N}\right) + \beta_2 W & \xi_2 & M_{22}-k_3 & \frac{\beta_1 \epsilon S}{N} + e\rho(a-\phi N) \\ 0 & 0 & 0 & -\xi_1 & pv & -k_2-k_3 \end{bmatrix}, \tag{3.9.2}$$

where $B_1 = (a-\phi N)\rho e + (a-\phi N)(1-\rho) + \delta$.

We take the function $Q = Q(S, I, A, W) = \operatorname{diag}\left(1, 1, 1, 1, \frac{I}{A}, \frac{I}{A}\right)$. Then we get

$$Q_f Q^{-1} = \operatorname{diag}\left(0, 0, 0, 0, \frac{I'}{I} - \frac{A'}{A}, \frac{I'}{I} - \frac{A'}{A}\right).$$

Next, since $C = Q_f Q^{-1} + Q J^{[2]} Q^{-1}$, therefore

$$C = \begin{bmatrix} 0 & 0 & 0 & 0 & 0 & 0 \\ 0 & 0 & 0 & 0 & 0 & 0 \\ 0 & 0 & 0 & 0 & 0 & 0 \\ 0 & 0 & 0 & 0 & 0 & 0 \\ 0 & 0 & 0 & 0 & \frac{I'}{I} - \frac{A'}{A} & 0 \\ 0 & 0 & 0 & 0 & 0 & \frac{I'}{I} - \frac{A'}{A} \end{bmatrix}$$

$$+ \begin{bmatrix} M_{11}+M_{22} & \frac{\beta_1 \epsilon S}{N} + e\rho(a-\phi N) & \beta_2 S & B_1 + \frac{\beta_1 \epsilon S}{N} & \frac{\beta_2 SA}{I} & 0 \\ pv & M_{11}-k_2 & 0 & -B_1 - \frac{\beta_1 S}{N} & 0 & \frac{\beta_2 SA}{I} \\ \xi_1 & \xi_2 & M_{11}-k_3 & 0 & \left(-B_1 - \frac{\beta_1 S}{N}\right)\frac{A}{I} & \left(-B_1 - \frac{\beta_1 \epsilon S}{N}\right)\frac{A}{I} \\ 0 & \beta_1\left(\frac{I+\epsilon A}{N}\right) + \beta_2 W & 0 & M_{22}-k_2 & 0 & -\frac{\beta_2 SA}{I} \\ 0 & 0 & \left(\beta_1\left(\frac{I+\epsilon A}{N}\right) + \beta_2 W\right)\frac{I}{A} & \frac{\xi_2 I}{A} & M_{22}-k_3 & \frac{\beta_1 \epsilon S}{N} + e\rho(a-\phi N) \\ 0 & 0 & 0 & \frac{-\xi_1 I}{A} & pv & -(k_2+k_3) \end{bmatrix}$$

$$= \begin{bmatrix} M_{11}+M_{22} & \frac{\beta_1 \epsilon S}{N} + e\rho(a-\phi N) & \beta_2 S & B_1 + \frac{\beta_1 \epsilon S}{N} & \frac{\beta_2 SA}{I} & 0 \\ pv & M_{11}-k_2 & 0 & -B_1 - \frac{\beta_1 S}{N} & 0 & \frac{\beta_2 SA}{I} \\ \xi_1 & \xi_2 & M_{11}-k_3 & 0 & \left(-B_1 - \frac{\beta_1 S}{N}\right)\frac{A}{I} & \left(-B_1 - \frac{\beta_1 \epsilon S}{N}\right)\frac{A}{I} \\ 0 & \beta_1\left(\frac{I+\epsilon A}{N}\right) + \beta_2 W & 0 & M_{22}-k_2 & 0 & -\frac{\beta_2 SA}{I} \\ 0 & 0 & \left(\beta_1\left(\frac{I+\epsilon A}{N}\right) + \beta_2 W\right)\frac{I}{A} & \frac{\xi_2 I}{A} & M_{22}-k_3+\frac{I'}{I}-\frac{A'}{A} & \frac{\beta_1 \epsilon S}{N} + e\rho(a-\phi N) \\ 0 & 0 & 0 & \frac{-\xi_1 I}{A} & pv & -(k_2+k_3)+\frac{I'}{I}-\frac{A'}{A} \end{bmatrix}$$

$$= \begin{bmatrix} C_{11} & C_{12} \\ C_{21} & C_{22} \end{bmatrix},$$

where

$$C_{11} = M_{11} + M_{22},$$

$$C_{12} = \begin{bmatrix} \frac{\beta_1 \epsilon S}{N} + e\rho(a-\phi N) & \beta_2 S & B_1 + \frac{\beta_1 \epsilon S}{N} & \frac{\beta_2 SA}{I} & 0 \end{bmatrix},$$

$$C_{21} = \begin{bmatrix} pv \\ \xi_1 \\ 0 \\ 0 \\ 0 \end{bmatrix},$$

$$C_{22} = \begin{bmatrix} M_{11}-k_2 & 0 & -B_1 - \frac{\beta_1 S}{N} & 0 & \left(-B_1 - \frac{\beta_1 \epsilon S}{N}\right)\frac{A}{I} \\ \xi_2 & M_{11}-k_3 & 0 & \left(-B_1 - \frac{\beta_1 S}{N}\right)\frac{A}{I} & -\frac{\beta_2 SA}{I} \\ \beta_1\left(\frac{I+\epsilon A}{N}\right) + \beta_2 W & 0 & M_{22}-k_2 & 0 & \frac{\beta_1 \epsilon S}{N} + e\rho(a-\phi N) \\ 0 & \left(\beta_1\left(\frac{I+\epsilon A}{N}\right) + \beta_2 W\right)\frac{I}{A} & \frac{\xi_2 I}{A} & M_{22}-k_3+\frac{I'}{I}-\frac{A'}{A} & -(k_2+k_3)+\frac{I'}{I}-\frac{A'}{A} \\ 0 & 0 & \frac{-\xi_1 I}{A} & pv & \end{bmatrix}.$$

The *Lozinskiĭ* measure of matrix C is defined as follows:

$$\mu(C) \leq \max\{g_1, g_2\}, \tag{3.9.3}$$

where $g_1 = \mu(C_{11}) + \|C_{12}\|$ and $g_2 = \|C_{21}\| + \mu(C_{22})$.

Thus we have

$$\begin{aligned}
\mu(C_{11}) &= M_{11} + M_{22}, \\
\|C_{12}\| &= \max\left\{\beta_2 S, \frac{\beta_2 SA}{I}, B_1 + \frac{\beta_1 \epsilon S}{N}\right\}, \\
\|C_{21}\| &= pv + \xi_1.
\end{aligned}$$

Therefore, we have

$$\begin{aligned}
g_1 &= \mu(C_{11}) + \|C_{12}\| \\
&= M_{11} + M_{22} + \max\left\{\beta_2 S, \frac{\beta_2 SA}{I}, B_1 + \frac{\beta_1 \epsilon S}{N}\right\}, \qquad (3.9.4) \\
g_2 &= \|C_{21}\| + \mu(C_{22}) \\
&= pv + \xi_1 + \mu(C_{22}). \qquad (3.9.5)
\end{aligned}$$

The matrix C_{22} is now partitioned as,

$$C_{22} = D = \begin{bmatrix} D_{11} & D_{12} \\ D_{21} & D_{22} \end{bmatrix},$$

where

$$D_{11} = M_{11} - k_2,$$

$$D_{12} = \begin{bmatrix} 0 & -B_1 - \frac{\beta_1 S}{N} & 0 & \frac{\beta_2 SA}{I} \end{bmatrix},$$

$$D_{21} = \begin{bmatrix} \xi_2 \\ \beta_1\left(\frac{I+\epsilon A}{N}\right) + \beta_2 W \\ 0 \\ 0 \end{bmatrix},$$

$$D_{22} = \begin{bmatrix} M_{11} - k_3 & 0 & \left(-B_1 - \frac{\beta_1 S}{N}\right)\frac{A}{I} & \left(-B_1 - \frac{\beta_1 \epsilon S}{N}\right)\frac{A}{I} \\ 0 & M_{22} - k_2 & 0 & -\frac{\beta_2 SA}{I} \\ \left(\beta_1\left(\frac{I+\epsilon A}{N}\right) + \beta_2 W\right)\frac{I}{A} & \frac{\xi_2 I}{A} & M_{22} - k_3 + \frac{I'}{I} - \frac{A'}{A} & \frac{\beta_1 \epsilon S}{N} + e\rho(a - \phi N) \\ 0 & \frac{-\xi_1 I}{A} & pv & -(k_2 + k_3) + \frac{I'}{I} - \frac{A'}{A} \end{bmatrix}.$$

We define the *Lozinskiĭ* measure of matrix D as follows:

$$\mu(D) \leq \max\{g_3, g_4\}, \qquad (3.9.6)$$

where $g_3 = \mu(D_{11}) + \|D_{12}\|$ and $g_4 = \|D_{21}\| + \mu(D_{22})$.

Thus, we have

$$\begin{aligned}
\mu(D_{11}) &= M_{11} - k_2, \\
\|D_{12}\| &= \max\left\{B_1 + \frac{\beta_1 S}{N}, \frac{\beta_2 SA}{I}\right\}, \\
\|D_{21}\| &= \xi_2 + \beta_1\left(\frac{I+\epsilon A}{N}\right) + \beta_2 W.
\end{aligned}$$

Hence, we have

$$\begin{aligned}
g_3 &= \mu(D_{11}) + \|D_{12}\| \\
&= M_{11} - k_2 + \max\left\{B_1 + \frac{\beta_1 S}{N}, \frac{\beta_2 SA}{I}\right\}, \qquad (3.9.7) \\
g_4 &= \|D_{21}\| + \mu(D_{22}) \\
&= \xi_2 + \beta_1\left(\frac{I+\epsilon A}{N}\right) + \beta_2 W + \mu(D_{22}). \qquad (3.9.8)
\end{aligned}$$

Again, the matrix D_{22} is partitioned as,

$$D_{22} = E = \begin{bmatrix} E_{11} & E_{12} \\ E_{21} & E_{22} \end{bmatrix},$$

where

$$\begin{aligned}
E_{11} &= M_{11} - k_3, \\
E_{12} &= \begin{bmatrix} 0 & \left(-B_1 - \frac{\beta_1 S}{N}\right)\frac{A}{I} & \left(-B_1 - \frac{\beta_1 \epsilon S}{N}\right)\frac{A}{I} \end{bmatrix}, \\
E_{21} &= \begin{bmatrix} 0 \\ \left(\beta_1\left(\frac{I+\epsilon A}{N}\right) + \beta_2 W\right)\frac{I}{A} \\ 0 \end{bmatrix}, \\
E_{22} &= \begin{bmatrix} M_{22} - k_2 & 0 & -\frac{\beta_2 SA}{I} \\ \frac{\xi_2 I}{A} & M_{22} - k_3 + \frac{I'}{I} - \frac{A'}{A} & \frac{\beta_1 \epsilon S}{N} + e\rho(a - \phi N) \\ \frac{-\xi_1 I}{A} & pv & -(k_2 + k_3) + \frac{I'}{I} - \frac{A'}{A} \end{bmatrix}.
\end{aligned}$$

Now, we define the *Lozinskiĭ* measure of matrix E as follows:

$$\mu(E) \leq \max\{g_5, g_6\}, \qquad (3.9.9)$$

where $g_5 = \mu(E_{11}) + \|E_{12}\|$ and $g_6 = \|E_{21}\| + \mu(E_{22})$.

Thus, we have

$$\mu(E_{11}) = M_{11} - k_3,$$

$$\begin{aligned}\|E_{12}\| &= \max\left\{\left|\left(-B_1 - \frac{\beta_1 S}{N}\right)\frac{A}{I}\right|, \left|\left(-B_1 - \frac{\beta_1 \epsilon S}{N}\right)\frac{A}{I}\right|\right\} \\ &= \max\left\{\left(B_1 + \frac{\beta_1 S}{N}\right)\frac{A}{I}, \left(B_1 + \frac{\beta_1 \epsilon S}{N}\right)\frac{A}{I}\right\}.\end{aligned}$$

Since $\epsilon < 1$, then we get

$$\|E_{12}\| = \left(B_1 + \frac{\beta_1 S}{N}\right)\frac{A}{I}.$$

In addition, we obtain that

$$\|E_{21}\| = \left(\beta_1\left(\frac{I + \epsilon A}{N}\right) + \beta_2 W\right)\frac{I}{A}.$$

Therefore, we have

$$\begin{aligned} g_5 &= \mu(E_{11}) + \|E_{12}\| \\ &= M_{11} - k_3 + \left(B_1 + \frac{\beta_1 S}{N}\right)\frac{A}{I}, \end{aligned} \tag{3.9.10}$$

$$\begin{aligned} g_6 &= \|E_{21}\| + \mu(E_{22}) \\ &= \left(\beta_1\left(\frac{I + \epsilon A}{N}\right) + \beta_2 W\right)\frac{I}{A} + \mu(E_{22}). \end{aligned} \tag{3.9.11}$$

We need to determine $\mu(E_{22})$, therefore the matrix E_{22} is again partitioned as,

$$E_{22} = F = \begin{bmatrix} F_{11} & F_{12} \\ F_{21} & F_{22} \end{bmatrix},$$

where

$$\begin{aligned} F_{11} &= M_{22} - k_2, \\ F_{12} &= \begin{bmatrix} 0 & -\frac{\beta_2 S A}{I} \end{bmatrix}, \\ F_{21} &= \begin{bmatrix} \frac{\xi_2 I}{A} \\ \frac{-\xi_1 I}{A} \end{bmatrix}, \\ F_{22} &= \begin{bmatrix} M_{22} - k_3 + \frac{I'}{I} - \frac{A'}{A} & \frac{\beta_1 \epsilon S}{N} + e\rho(a - \phi N) \\ pv & -(k_2 + k_3) + \frac{I'}{I} - \frac{A'}{A} \end{bmatrix}. \end{aligned}$$

Next, we again define the *Lozinskiĭ* measure of matrix F as follows:

$$\mu(F) \leq \max\{g_7, g_8\}, \tag{3.9.12}$$

where $g_7 = \mu(F_{11}) + \|F_{12}\|$ and $g_8 = \|F_{21}\| + \mu(F_{22})$.

Thus, we have

$$\begin{aligned}\mu(F_{11}) &= M_{22} - k_2,\\ \|F_{12}\| &= \frac{\beta_2 SA}{I},\\ \|F_{21}\| &= \frac{\xi_2 I}{A} + \frac{\xi_1 I}{A}.\end{aligned}$$

And,

$$\begin{aligned}\mu(F_{22}) &= \max\left\{M_{22} - k_3 + \frac{I'}{I} - \frac{A'}{A} + pv, -(k_2+k_3) + \frac{I'}{I} - \frac{A'}{A} + \frac{\beta_1 \epsilon S}{N} + e\rho(a-\phi N)\right\}\\ &= \max\left\{\frac{\beta_1 S}{N} + e\rho(a-\phi N) - (v+m+\alpha+\gamma) - (d+\phi_2) + \frac{I'}{I} - \frac{A'}{A} + pv,\right.\\ &\qquad \left. -(m+\alpha+d+\phi_2) + \frac{I'}{I} - \frac{A'}{A} + \frac{\beta_1\epsilon S}{N} + e\rho(a-\phi N)\right\}\\ &= e\rho(a-\phi N) + \frac{I'}{I} - \frac{A'}{A} - (m+\alpha+d+\phi_2) + \sup\left\{\frac{\beta_1 S}{N} - (v+\alpha) + pv, \frac{\beta_1\epsilon S}{N}\right\}\end{aligned}$$

Therefore, we have

$$\begin{aligned}g_7 &= \mu(F_{11}) + \|F_{12}\|\\ &= M_{22} - k_2 + \frac{\beta_2 SA}{I}\\ &= \frac{\beta_1 S}{N} + e\rho(a-\phi N) - (v+m+\alpha+\gamma) - k_2 + \frac{\beta_2 SA}{I}, \qquad (3.9.13)\\ g_8 &= \|F_{21}\| + \mu(F_{22})\\ &= \frac{\xi_2 I}{A} + \frac{\xi_1 I}{A} + e\rho(a-\phi N) + \frac{I'}{I} - \frac{A'}{A} - (m+\alpha+d+\phi_2)\\ &\quad + \sup\left\{\frac{\beta_1 S}{N} - (v+\alpha) + pv, \frac{\beta_1\epsilon S}{N}\right\}. \qquad (3.9.14)\end{aligned}$$

Next, considering the second equation of system (3.1.1), we get

$$\begin{aligned}I' &= \beta_1\left(\frac{I+\epsilon A}{N}\right)S + \beta_2 SW + e\rho(a-\phi N)(I+A) - (v+m+\alpha+\gamma)I,\\ \frac{I'}{I} &= \frac{\beta_1 S}{I}\left(\frac{I+\epsilon A}{N}\right) + \frac{\beta_2 SW}{I} + \frac{e\rho(a-\phi N)(I+A)}{I} - (v+m+\alpha+\gamma).\end{aligned}$$

Thus, we have

$$\frac{I'}{I} - \frac{\beta_1 S}{I}\left(\frac{I+\epsilon A}{N}\right) - \frac{\beta_2 SW}{I} - \frac{e\rho(a-\phi N)(I+A)}{I} = -(v+m+\alpha+\gamma). \quad (3.9.15)$$

Substituting (3.9.15) into (3.9.13), we have

$$g_7 = \frac{\beta_1 S}{N} + e\rho(a-\phi N) + \frac{I'}{I} - \frac{\beta_1 S}{I}\left(\frac{I+\epsilon A}{N}\right) - \frac{\beta_2 SW}{I}$$

$$- \frac{e\rho(a-\phi N)(I+A)}{I} - k_2 + \frac{\beta_2 SA}{I} \tag{3.9.16}$$

$$= \frac{I'}{I} - \left(\frac{\beta_1 \epsilon A}{N} + \beta_2 W - \beta_2 A\right)\frac{S}{I} - e\rho(a-\phi N)\left(\frac{A}{I}\right) - k_2. \tag{3.9.17}$$

Next, from the third equation of system (3.1.1), we have

$$A' = pvI - (m+\alpha)A$$

$$\frac{A'}{A} = \frac{pvI}{A} - (m+\alpha). \tag{3.9.18}$$

Again, substituting (3.9.18) into (3.9.14), we have

$$\begin{aligned} g_8 &= \frac{\xi_2 I}{A} + \frac{\xi_1 I}{A} + e\rho(a-\phi N) + \frac{I'}{I} - \frac{pvI}{A} + (m+\alpha) \\ &\quad - (m+\alpha+d+\phi_2) + \sup\left\{\frac{\beta_1 S}{N} - (v+\alpha) + pv, \frac{\beta_1 \epsilon S}{N}\right\} \\ &= \frac{I'}{I} + (\xi_1 + \xi_2 - pv)\frac{I}{A} + e\rho(a-\phi N) - (d+\phi_2) \\ &\quad + \sup\left\{\frac{\beta_1 S}{N} - (v+\alpha) + pv, \frac{\beta_1 \epsilon S}{N}\right\}. \end{aligned} \tag{3.9.19}$$

Thus,

$$\begin{aligned} \mu(F) &\leq \max\{g_7, g_8\} \\ &= \frac{I'}{I} + \max\left\{\left(\beta_2 A - \frac{\beta_1 \epsilon A}{N} - \beta_2 W\right)\frac{S}{I} - e\rho(a-\phi N)\left(\frac{A}{I}\right) - k_2,\right. \\ &\quad (\xi_1 + \xi_2 - pv)\frac{I}{A} + e\rho(a-\phi N) - (d+\phi_2) \\ &\quad \left. + \sup\left\{\frac{\beta_1 S}{N} - (v+\alpha) + pv, \frac{\beta_1 \epsilon S}{N}\right\}\right\}. \end{aligned} \tag{3.9.20}$$

Now from (3.9.9),

$$\mu(E) \leq \max\{g_5, g_6\},$$

where

$$g_5 = M_{11} - k_3 + \left(B_1 + \frac{\beta_1 S}{N}\right)\frac{A}{I} \quad \text{and} \quad g_6 = \left(\beta_1\left(\frac{I+\epsilon A}{N}\right) + \beta_2 W\right)\frac{I}{A} + \mu(E_{22}),$$

and we consider

$$\begin{aligned} g_5 &= M_{11} - k_3 + \left(B_1 + \frac{\beta_1 S}{N}\right)\frac{A}{I} + 0 \\ &= M_{11} - k_3 + \left(B_1 + \frac{\beta_1 S}{N}\right)\frac{A}{I} + \frac{I'}{I} - \frac{I'}{I} \end{aligned}$$

$$= \frac{I'}{I} + M_{11} - k_3 + \left(B_1 + \frac{\beta_1 S}{N}\right)\frac{A}{I} - \frac{I'}{I}.$$

Therefore, we have

$$\begin{aligned}\mu(E) \leq \frac{I'}{I} + \max\Bigg\{ & M_{11} - k_3 + \left(B_1 + \frac{\beta_1 S}{N}\right)\frac{A}{I} - \frac{I'}{I}, \\ & \left(\beta_1\left(\frac{I+\epsilon A}{N}\right) + \beta_2 W\right)\frac{I}{A} + \left(\beta_2 A - \frac{\beta_1 \epsilon A}{N} - \beta_2 W\right)\frac{S}{I} - e\rho(a-\phi N)\left(\frac{A}{I}\right) - k_2, \\ & \left(\beta_1\left(\frac{I+\epsilon A}{N}\right) + \beta_2 W\right)\frac{I}{A} + (\xi_1 + \xi_2 - pv)\frac{I}{A} + e\rho(a-\phi N) - (d+\phi_2) \\ & + \sup\left\{\frac{\beta_1 S}{N} - (v+\alpha) + pv, \frac{\beta_1 \epsilon S}{N}\right\}\Bigg\}.\end{aligned}$$

Now from (3.9.6),

$$\mu(D) \leq \max\{g_3, g_4\},$$

where

$$g_3 = M_{11} - k_2 + \max\left\{B_1 + \frac{\beta_1 S}{N}, \frac{\beta_2 SA}{I}\right\} \text{ and } g_4 = \xi_2 + \beta_1\left(\frac{I+\epsilon A}{N}\right) + \beta_2 W + \mu(D_{22}),$$

and we consider

$$\begin{aligned} g_3 &= M_{11} - k_2 + \max\left\{B_1 + \frac{\beta_1 S}{N}, \frac{\beta_2 SA}{I}\right\} + 0 \\ &= \frac{I'}{I} + M_{11} - k_2 + \max\left\{B_1 + \frac{\beta_1 S}{N}, \frac{\beta_2 SA}{I}\right\} - \frac{I'}{I}. \end{aligned}$$

Therefore, again we have

$$\begin{aligned}\mu(D) \leq \frac{I'}{I} + \max\Bigg\{ & M_{11} - k_2 + \sup\left\{B_1 + \frac{\beta_1 S}{N}, \frac{\beta_2 SA}{I}\right\} - \frac{I'}{I}, \\ & \xi_2 - (m + \phi_1 + \delta + d + \phi_2) + \left(B_1 + \frac{\beta_1 S}{N}\right)\frac{A}{I} - \frac{I'}{I}, \\ & \xi_2 + \left(\beta_1\left(\frac{I+\epsilon A}{N}\right) + \beta_2 W\right)\left(1 + \frac{I}{A}\right) + \left(\beta_2 A - \frac{\beta_1 \epsilon A}{N} - \beta_2 W\right)\frac{S}{I} \\ & \qquad - e\rho(a-\phi N)\left(\frac{A}{I}\right) - (m+\alpha), \\ & \left(\beta_1\left(\frac{I+\epsilon A}{N}\right) + \beta_2 W\right)\left(1 + \frac{I}{A}\right) + (\xi_1 + \xi_2 - pv)\frac{I}{A} + e\rho(a-\phi N) \\ & \qquad \xi_2 - (d+\phi_2) + \sup\left\{\frac{\beta_1 S}{N} - (v+\alpha) + pv, \frac{\beta_1 \epsilon S}{N}\right\}\Bigg\}.\end{aligned}$$

Now from (3.9.3),

$$\mu(C) \leq \max\{g_1, g_2\},$$

where

$$g_1 = M_{11} + M_{22} + \max\left\{\beta_2 S, \frac{\beta_2 SA}{I}, B_1 + \frac{\beta_1 \epsilon S}{N}\right\} \quad \text{and} \quad g_2 = pv + \xi_1 + \mu(C_{22}),$$

and we consider

$$\begin{aligned} g_1 &= M_{11} + M_{22} + \max\left\{\beta_2 S, \frac{\beta_2 SA}{I}, B_1 + \frac{\beta_1 \epsilon S}{N}\right\} + 0 \\ &= \frac{I'}{I} + M_{11} + M_{22} + \max\left\{\beta_2 S, \frac{\beta_2 SA}{I}, B_1 + \frac{\beta_1 \epsilon S}{N}\right\} - \frac{I'}{I}. \end{aligned}$$

Therefore, we get

$$\begin{aligned} \mu(C) \leq \frac{I'}{I} + \max\Bigg\{ & M_{11} + M_{22} + \sup\left\{\beta_2 S, \frac{\beta_2 SA}{I}, B_1 + \frac{\beta_1 \epsilon S}{N}\right\} - \frac{I'}{I}, \\ & pv + \xi_1 + M_{11} - k_2 + \sup\left\{B_1 + \frac{\beta_1 S}{N}, \frac{\beta_2 SA}{I}\right\} - \frac{I'}{I}, \\ & pv + \xi_1 - (m + \phi_1 + \delta + d + \phi_2) + \left(B_1 + \frac{\beta_1 S}{N}\right)\frac{A}{I} - \frac{I'}{I}, \\ & pv + \xi_1 + \xi_2 + \left(\beta_1\left(\frac{I + \epsilon A}{N}\right) + \beta_2 W\right)\left(1 + \frac{I}{A}\right) + \left(\beta_2 A - \frac{\beta_1 \epsilon A}{N} - \beta_2 W\right)\frac{S}{I} \\ & \quad - e\rho(a - \phi N)\left(\frac{A}{I}\right) - (m + \alpha), \\ & pv + \xi_1 + \xi_2 + \left(\beta_1\left(\frac{I + \epsilon A}{N}\right) + \beta_2 W\right)\left(1 + \frac{I}{A}\right) + (\xi_1 + \xi_2 - pv)\frac{I}{A} \\ & \quad + e\rho(a - \phi N) - (d + \phi_2) + \sup\left\{\frac{\beta_1 S}{N} - (v + \alpha) + pv, \frac{\beta_1 \epsilon S}{N}\right\}\Bigg\} \end{aligned}$$

$$\begin{aligned} = \frac{I'}{I} - \min\Bigg\{ & -(M_{11} + M_{22}) - \inf\left\{-\beta_2 S, -\frac{\beta_2 SA}{I}, -B_1 - \frac{\beta_1 \epsilon S}{N}\right\} + \frac{I'}{I}, \\ & - pv - \xi_1 - M_{11} + k_2 - \inf\left\{-B_1 - \frac{\beta_1 S}{N}, \frac{-\beta_2 SA}{I}\right\} + \frac{I'}{I}, \\ & - pv - \xi_1 + (m + \phi_1 + \delta + d + \phi_2) - \left(B_1 + \frac{\beta_1 S}{N}\right)\frac{A}{I} + \frac{I'}{I}, \\ & - pv - \xi_1 - \xi_2 - \left(\beta_1\left(\frac{I + \epsilon A}{N}\right) + \beta_2 W\right)\left(1 + \frac{I}{A}\right) - \left(\beta_2 A - \frac{\beta_1 \epsilon A}{N} - \beta_2 W\right)\frac{S}{I} \\ & \quad + e\rho(a - \phi N)\left(\frac{A}{I}\right) + (m + \alpha), \\ & - pv - \xi_1 - \xi_2 - \left(\beta_1\left(\frac{I + \epsilon A}{N}\right) + \beta_2 W\right)\left(1 + \frac{I}{A}\right) - (\xi_1 + \xi_2 - pv)\frac{I}{A} \\ & \quad - e\rho(a - \phi N) + (d + \phi_2) - \inf\left\{-\frac{\beta_1 S}{N} + (v + \alpha) - pv, \frac{-\beta_1 \epsilon S}{N}\right\}\Bigg\}. \end{aligned}$$

Hence, we obtain that $\mu(C) \leq \frac{I'}{I} - \bar{b}$, where

$$\bar{b} = \min\left\{-(M_{11} + M_{22}) - \inf\left\{-\beta_2 S, -\frac{\beta_2 SA}{I}, -B_1 - \frac{\beta_1 \epsilon S}{N}\right\} + \frac{I'}{I},\right.$$

$$
\begin{aligned}
&-pv-\xi_1-M_{11}+k_2-\inf\left\{-B_1-\frac{\beta_1 S}{N},\frac{-\beta_2 SA}{I}\right\}+\frac{I'}{I},\\
&-pv-\xi_1+(m+\phi_1+\delta+d+\phi_2)-\left(B_1+\frac{\beta_1 S}{N}\right)\frac{A}{I}+\frac{I'}{I}\\
&-pv-\xi_1-\xi_2-\left(\beta_1\left(\frac{I+\epsilon A}{N}\right)+\beta_2 W\right)\left(1+\frac{I}{A}\right)-\left(\beta_2 A-\frac{\beta_1\epsilon A}{N}-\beta_2 W\right)\frac{S}{I}\\
&\quad+e\rho(a-\phi N)\left(\frac{A}{I}\right)+(m+\alpha),\\
&-pv-\xi_1-\xi_2-\left(\beta_1\left(\frac{I+\epsilon A}{N}\right)+\beta_2 W\right)\left(1+\frac{I}{A}\right)-(\xi_1+\xi_2-pv)\frac{I}{A}\\
&\quad-e\rho(a-\phi N)+(d+\phi_2)-\inf\left\{-\frac{\beta_1 S}{N}+(v+\alpha)-pv,\frac{-\beta_1\epsilon S}{N}\right\}\Bigg\}.
\end{aligned}
$$

Finally, let us consider any solution $S(t), I(t), A(t), W(t)$ emanating from the compact absorbing set $\Gamma \subset \Omega$. Let $\bar{t}$ be large enough such that the system is persistent and $(S(t), I(t), A(t), W(t)) \subset \Gamma$ for all $t \geq \bar{t}$. The along each solution $S(t), I(t), A(t), W(t)$ such that $(S(0), I(0), A(0), W(0)) \in \Gamma$, for $t > \bar{t}$, $\frac{1}{t}[\ln I(t) - \ln I(0)] < \frac{\bar{b}}{2}$. As a result

$$
\begin{aligned}
\frac{1}{t}\int_0^t \mu(C)ds &\leq \frac{1}{t}\int_0^t \left(\frac{I'}{I}-\bar{b}\right)ds\\
&= \frac{1}{t}\left(\ln I(t)-\ln I(0)-\bar{b}t\right)\\
&= \frac{\ln I(t)-\ln I(0)}{t}-\bar{b}\\
&< -\frac{\bar{b}}{2}
\end{aligned}
$$

which implies that $\bar{q_2} \leq -\frac{\bar{b}}{2} < 0$. This completes the proof. □

Figure 16 shows that all eigenvalues of the Jacobian matrix approach negative numbers. This numerical result confirms that the endemic equilibrium points are stable. Besides, as shown in Figure 17, for each initial conditions (by assuming that $I(0) = 1, I(0) = 200$, and $I(0) = 450$), all the curves converge to an equilibrium point. Consequently, this numerical simulation confirms our analysis that the endemic equilibrium point is globally stable.

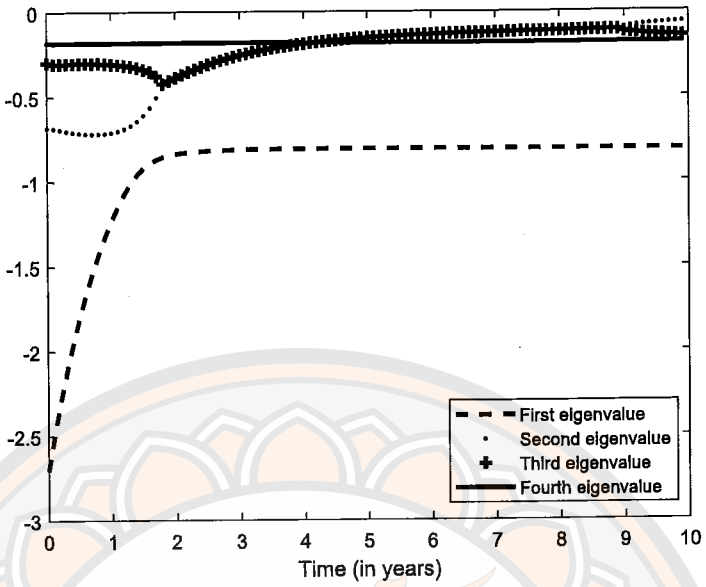

Figure 16 The eigenvalue approximation of the Jacobian matrix in our model

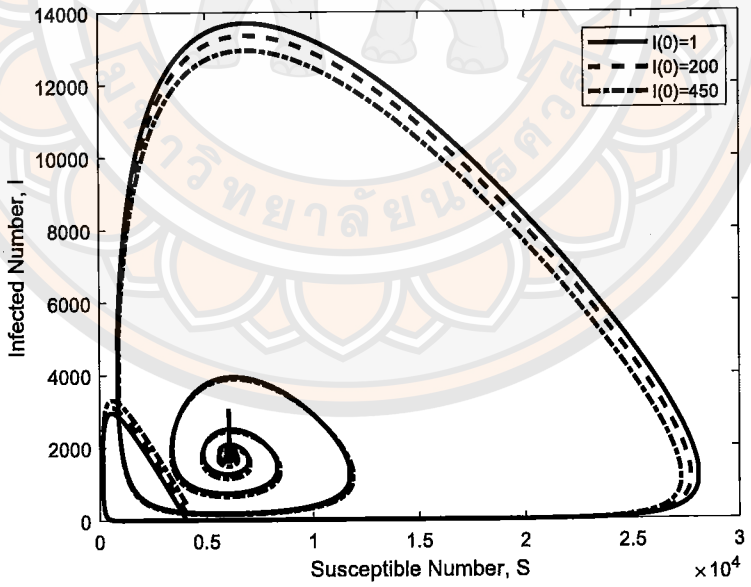

Figure 17 Phase plot for each number of initial infected individuals. It is clearly seen that all the curves converge to an endemic equilibrium point. This simulation ran for 4,000 months. We have conducted running longer than this period, and it gave a similar result.

3.10 Sensitivity Analysis

Sensitivity analysis informs us about the importance of each parameter in disease transmission. This is accomplished by calculating sensitivity indices of the basic reproduction number with respect to the model's parameters (see Section 2.1.8).

Table 1 Parameter values of the Brucellosis in bison model

Symbol	Value	Unit	Reference
N	4500	animals	[17]
a	0.0517	month^{-1}	[15]
ϕ	3.3×10^{-6}	month^{-1}	[17]
m	0.0058	month^{-1}	[17]
α	0.0042	month^{-1}	[17]
δ	0.0017	month^{-1}	[17]
v	0.0417	month^{-1}	[17]
β_1	0.0062	month^{-1}	[17]
β_2	2.9167×10^{-4}	month^{-1}	Assumed
e	0.0750	month^{-1}	[17]
ρ	0.0417	unitless	[17]
p	0.0417	unitless	[17]
ϵ	0.0067	unitless	[17]
γ	0.0333	month^{-1}	[17]
ξ_1	0.12	month^{-1}	Assumed
ξ_2	0.1	month^{-1}	Assumed
d	0.00005	month^{-1}	Assumed
ϕ_1	0.0263	month^{-1}	[12]
ϕ_2	0.004	month^{-1}	Assumed

Table 2 Numerical values of sensitivity indices of R_0

Parameter	Sensitivity index	Parameter	Sensitivity index
a	$+1.1272$	ρ	$+6.9381 \times 10^{-7}$
ϕ	-0.9999	p	$+0.0130$
m	$+0.4490$	ϵ	$+5.4621 \times 10^{-9}$
α	-0.0208	γ	-0.1626
δ	$+0.1730$	ξ_1	$+0.4016$
v	-0.1903	ξ_2	$+0.0012$
β_1	$+5.1917 \times 10^{-5}$	d	-0.0123
β_2	$+0.9999$	ϕ_1	-0.7783
e	$+6.9381 \times 10^{-7}$	ϕ_2	-0.9876

Table 2 shows the sensitivity index of each parameter. The values are calculated using the parameters given in Table 1. As presented in the table, a, m, δ, β_1, β_2, e, ρ, p, ϵ, ξ_1, and ξ_2 have a positive sensitivity index showing that when these parameters are increased, the value of R_0 increases as well. Therefore, to reduce the value of R_0, we should consider reducing the value of these parameters. Meanwhile, $\phi_1, \phi_2, \phi, \alpha, v, \gamma$, and d have a negative sensitivity index. The most negative sensitive parameter is the density-dependent reduction in births, ϕ. Other interesting two parameters that give a negative sensitivity index are ϕ_1 and ϕ_2. These two parameters are initially considered as constant controls that we have included in our model. Since the parameter ϕ depends on other factors that we may not be able to control the value, hence we will study the control parameters instead. If ϕ_1 and ϕ_2 are increased by 10%, then the basic reproduction number decreases approximately by 8% and 10%, respectively. Hence, under this situation, the infected population decreases as well.

3.11 Optimal control

Our goal in this section is to determine the implementation optimal control strategies of vaccination ($u_1(t)$), the elimination of Brucella in the environment ($u_2(t)$), and culling infected animals ($u_3(t)$) that will result in minimizing the disease transmission. Now, the system of differential equations describing our model with time-dependent controls is

$$\begin{aligned}
\frac{dS}{dt} &= (a-\phi N)(S+R)+(1-e)\rho(a-\phi N)(I+A)+\delta R \\
&\quad -\left(\beta_1\left(\frac{I+\epsilon A}{N}\right)S+\beta_2 SW\right)-mS-u_1(t)S \\
\frac{dI}{dt} &= \beta_1\left(\frac{I+\epsilon A}{N}\right)S+\beta_2 SW+e\rho(a-\phi N)(I+A) \\
&\quad -(v+m+\alpha)I-u_3(t)I \\
\frac{dA}{dt} &= pvI-(m+\alpha)A \\
\frac{dR}{dt} &= (1-p)vI+u_1(t)S-(m+\delta)R \\
\frac{dW}{dt} &= \xi_1 I+\xi_2 A-dW-u_2(t)W.
\end{aligned} \tag{3.11.1}$$

We consider the system on a time interval $[0,T]$. The functions $u_1(t), u_2(t)$, and $u_3(t)$ are assumed to be at least Lebesgue measurable on $[0,T]$. The control set is defined as

$$\begin{aligned}
\Omega = \{u_1(t), u_2(t), u_3(t) | 0 \le u_1(t) \le u_{1max}, \\
0 \le u_2(t) \le u_{2max}, \\
0 \le u_3(t) \le u_{3max}\},
\end{aligned} \tag{3.11.2}$$

where u_{1max}, u_{2max}, and u_{3max} denotes the upper bound for the effort of vaccination, elimination of Brucella in the environment, and culling, respectively. The bound reflects a practical limitation on the maximum rate of control in a given period. Our goal here is to minimize the total number of infectious bison and the costs of control over the time interval $[0,T]$. We consider the following objective functional

$$J(u_1^*, u_2^*, u_3^*) = \min \int_0^T (I + c_1 u_1(t) S + c_2 u_2(t) W + c_3 u_3(t) I + \frac{1}{2}\left(c_4 u_1^2(t) + c_5 u_2^2(t) + c_6 u_3^2(t)\right))dt, \tag{3.11.3}$$

where c_i $(i = 1, 2, 3)$ represents the appropriate positive balancing constants, and terms $c_4 u_1^2(t), c_5 u_2^2(t)$, and $c_6 u_3^2(t)$ represent the cost associated with vaccination control, elimination control of Brucella in the environment, and culling control of infected bison, respectively. By utilizing the Prontryagin's minimum Principle (section 2.1.9), we have the following Hamiltonian function H:

$$\begin{aligned}
H = & \left[I + c_1 u_1(t) S + c_2 u_2(t) W + c_3 u_3(t) I + \frac{1}{2}\left(c_4 u_1^2(t) + c_5 u_2^2(t) + c_6 u_3^2(t)\right)\right] \\
& + \lambda_S \Bigg[(a - \phi N)(S + R) + (1 - e)\rho(a - \phi N)(I + A) + \delta R \\
& \quad - \left(\beta_1 \left(\frac{I + \epsilon A}{N}\right) S + \beta_2 S W\right) - mS - u_1(t) S\Bigg] \\
& + \lambda_I \left[\beta_1 \left(\frac{I + \epsilon A}{N}\right) S + \beta_2 S W + e\rho(a - \phi N)(I + A)\right. \\
& \quad \left. - (v + m + \alpha) I - u_3(t) I\right] \\
& + \lambda_A \left[pvI - (m + \alpha) A\right] \\
& + \lambda_R \left[(1 - p) vI + u_1(t) S - (m + \delta) R\right] \\
& + \lambda_W \left[\xi_1 I + \xi_2 A - dW - u_2(t) W\right]
\end{aligned}$$

Given an optimal control $u_1^*(t), u_2^*(t)$, and $u_3^*(t)$, there exist adjoint functions, $\lambda_S, \lambda_I, \lambda_A, \lambda_R$, and λ_W, corresponding to the state S, I, A, R and W, respectively satisfying

$$\begin{aligned}
\frac{d\lambda_S}{dt} &= -\frac{\partial H}{\partial S} \\
&= -\Bigg[c_1 u_1(t) + \lambda_S \left((a - \phi N) - \beta_1 \left(\frac{I + \epsilon A}{N}\right) - \beta_2 - m - u_1(t)\right) \\
&\quad + \lambda_I \left(\beta_1 \left(\frac{I + \epsilon A}{N}\right) + \beta_2 W\right) + \lambda_R u_1(t)\Bigg] \qquad (3.11.4) \\
\frac{d\lambda_I}{dt} &= -\frac{\partial H}{\partial I} \\
&= -\Bigg[1 + c_3 u_3(t) + \lambda_S \left((1 - e)\rho(a - \phi N) + \frac{\beta_1 S}{N}\right)
\end{aligned}$$

$$+\lambda_I\left(\frac{\beta_1 S}{N}+e\rho(a-\phi N)-(m+\alpha+v)-u_3(t)\right)$$
$$+\lambda_A pv+\lambda_R(1-p)v+\lambda_W\xi_1\Big] \tag{3.11.5}$$

$$\frac{d\lambda_A}{dt}=-\frac{\partial H}{\partial A}$$
$$=-\Big[\lambda_S\left((1-e)\rho(a-\phi N)-\frac{\beta_1\epsilon S}{N}\right)+\lambda_I\left(\frac{\beta_1\epsilon S}{N}+e\rho(a-\phi N)\right)$$
$$-\lambda_A(m+\alpha)+\lambda_W\xi_2\Big] \tag{3.11.6}$$

$$\frac{d\lambda_R}{dt}=-\frac{\partial H}{\partial R}$$
$$=-\Big[\lambda_S\big((a-\phi N)+\delta\big)-\lambda_R(m+\delta)\Big] \tag{3.11.7}$$

$$\frac{d\lambda_W}{dt}=-\frac{\partial H}{\partial W}$$
$$=-\Big[c_2u_2(t)-\lambda_S\beta_2 S+\lambda_I\beta_2 S-\lambda_W(d+u_2(t))\Big]. \tag{3.11.8}$$

With transversality conditions,

$$\lambda_S(T)=0,\ \lambda_I(T)=0,\ \lambda_A(T)=0,\ \lambda_R(T)=0,\ \text{and}\ \lambda_W(T)=0.$$

The characterizations of the optimal controls $u_1(t), u_2(t)$, and $u_3(t)$ are then based on the conditions

$$\frac{\partial H}{\partial u_1}=0,\ \frac{\partial H}{\partial u_2}=0,\ \text{and}\ \frac{\partial H}{\partial u_3}=0,$$

subject to the constraints $0\le u_1(t)\le u_{1max},\quad 0\le u_2(t)\le u_{2max}$, and $0\le u_3(t)\le u_{3max}$. Furthermore, the optimal controls are characterized by the optimality conditions:

$$u_1^*(t)=\max\left\{0,\min\left\{u_1(t),u_{1max}\right\}\right\},$$
$$u_2^*(t)=\max\left\{0,\min\left\{u_2(t),u_{2max}\right\}\right\},$$
$$u_3^*(t)=\max\left\{0,\min\left\{u_3(t),u_{3max}\right\}\right\},$$

where

$$u_1(t)=\frac{\lambda_S S-\lambda_R S-c_1 S}{c_4}, \tag{3.11.9}$$
$$u_2(t)=\frac{\lambda_W W-c_2 W}{c_5}, \tag{3.11.10}$$
$$u_3(t)=\frac{\lambda_I I-c_3 I}{c_6}. \tag{3.11.11}$$

3.12 Numerical simulations

In this section, the forward-backward sweep method is used to solve the optimality system numerically. Table 1 contains the model parameters, sources, and the values used in our numerical simulations. For simplicity, in our numerical simulation we set $S(0) = 4050, I(0) = 450, A(0) = 0, R(0) = 0$ and $W(0) = 10000$. Furthermore, we set $u_{1\max} = u_{2\max} = u_{3\max} = 0.7, c_4 = 1, c_5 = 1, c_6 = 1$ and the entire period of time $T = 100$ months.

Figure 18(a) shows the infection curves for the model without control (solid line) and with the optimal control (dashed line) in which the cost parameters are $c_1 = 0.01$, $c_2 = 0.001$, and $c_3 = 0.01$. The basic reproduction number with this set of parameter values is about 45. We can see that the infection level is reduced in the control condition and approaches zero about seven months after the disease onset. Besides, as presented in Figure 18(b), we observe that applying controls can reduce the number of chronically infected animals (carriers). The solid curve in Figure 18(a) represents that the number of infectious animals reaches its peak of approximately 3,500 cases after the disease onset in just a few months. On the other hand, the dashed-line curve shows that we can reduce the highest number of infected cases down to just about 2,500 cases, and the number of infections sharply reduces to zero only in a few months after the disease outbreak. Figure 18(c) confirms that if the controls are applied, the number of Brucella in the environment is significantly reduced to almost zero within 20 months after the disease outbreak. Consequently, the number of infectious cases and carriers or chronic state is small.

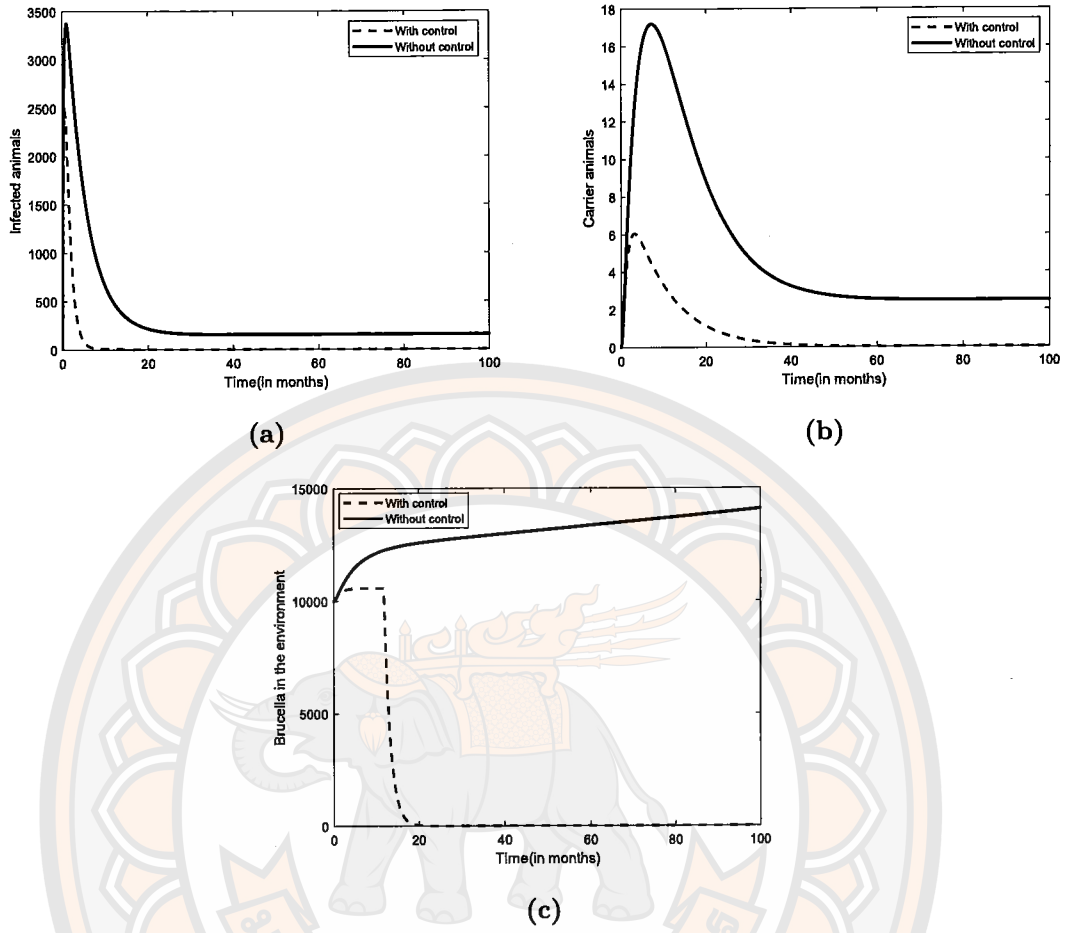

Figure 18 Simulation results: (a) infected animals (b) chronically infected animals (c) Brucella in the environment. Note that the basic reproduction number value for this set of parameters is about 45 with other cost values $c_1 = 0.01, c_2 = 0.001$ and $c_3 = 0.01$.

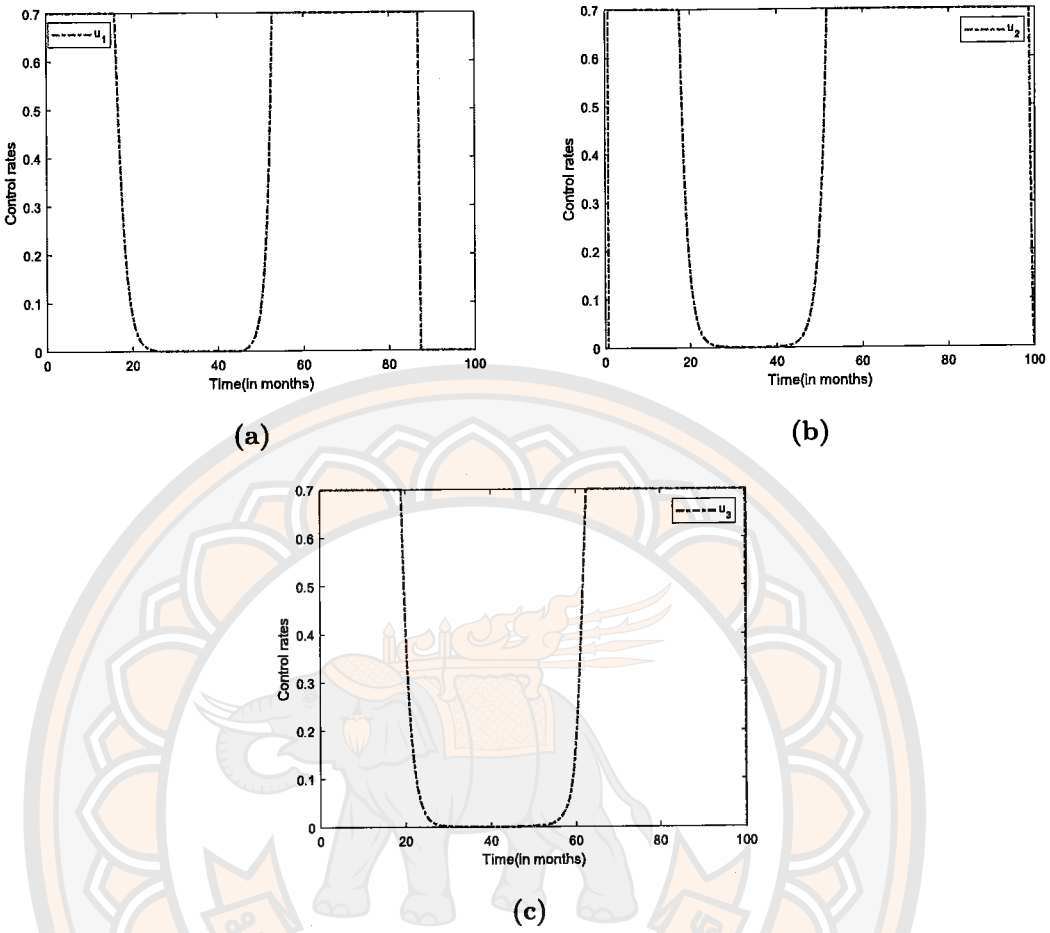

Figure 19 Dynamics of controls (a) vaccination ($u_1(t)$), (b) elimination of Brucella in the environment ($u_2(t)$) and (c) culling of infected bison ($u_3(t)$).

Figure 19 (a) says that the vaccination rate should be implemented in the first 20 months with a rate of about 0.7 after the disease onset. Then, the rate is sharply reduced to zero, and it stays at that level for about 30 months before taking off another round of implementation. Meanwhile, the eliminating and culling rates are also distributed in similar patterns, which you can see in Figures 19 (b) and (c).

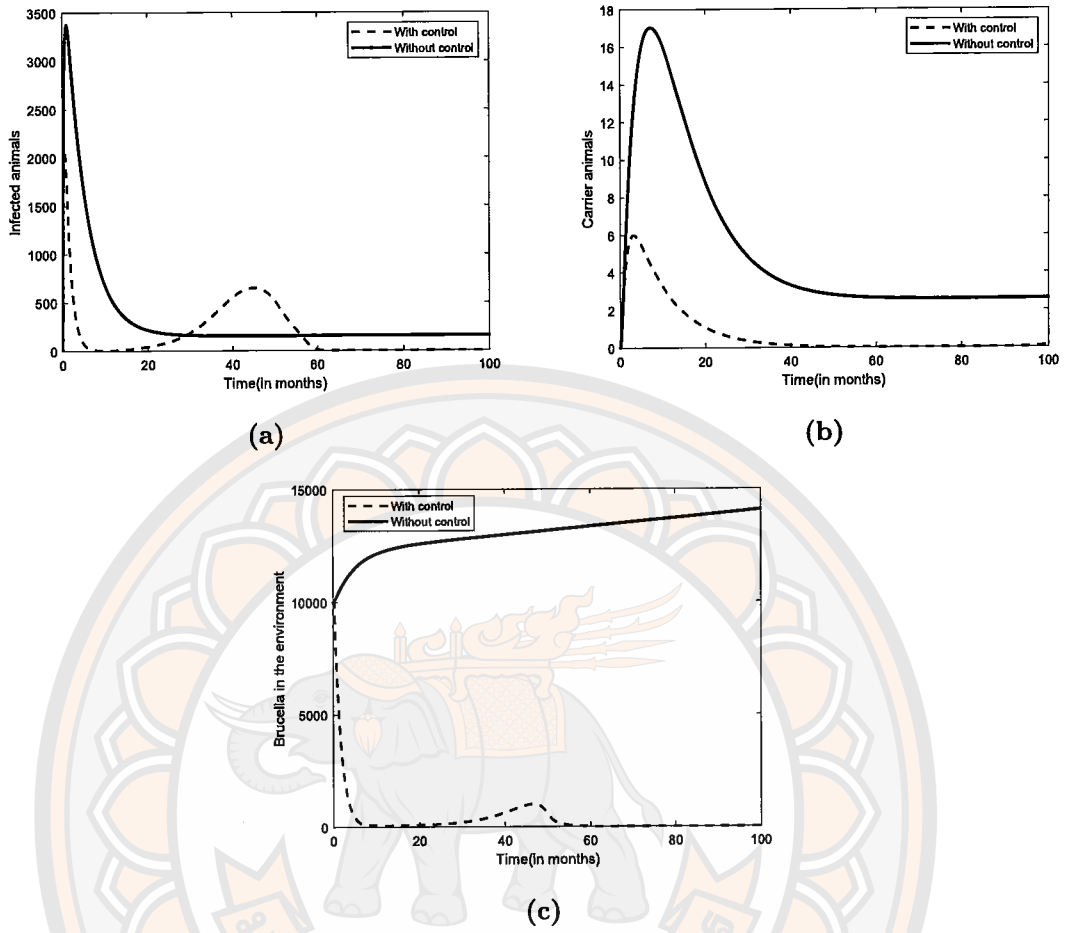

Figure 20 Simulation results: (a) infected animals (b) chronically infected animals (c) Brucella in the environment. Note that the basic reproduction number value for this set of parameters is about 45 with other cost values $c_1 = 0.00001, c_2 = 0.001$ and $c_3 = 0.01$.

Next, we investigate another set of cost parameters. Now, we reduce the vaccination cost (c_1) lower than that of the other costs say $c_1 = 0.00001$, $c_2 = 0.001$, and $c_3 = 0.01$. Figure 20 demonstrates that only the numbers of infected animals and Brucella in the environment are affected by this strategy. Besides, due to a lower vaccination cost, the peak of the infection curve is not as high as the previous case. The control measures are presented in Figure 21.

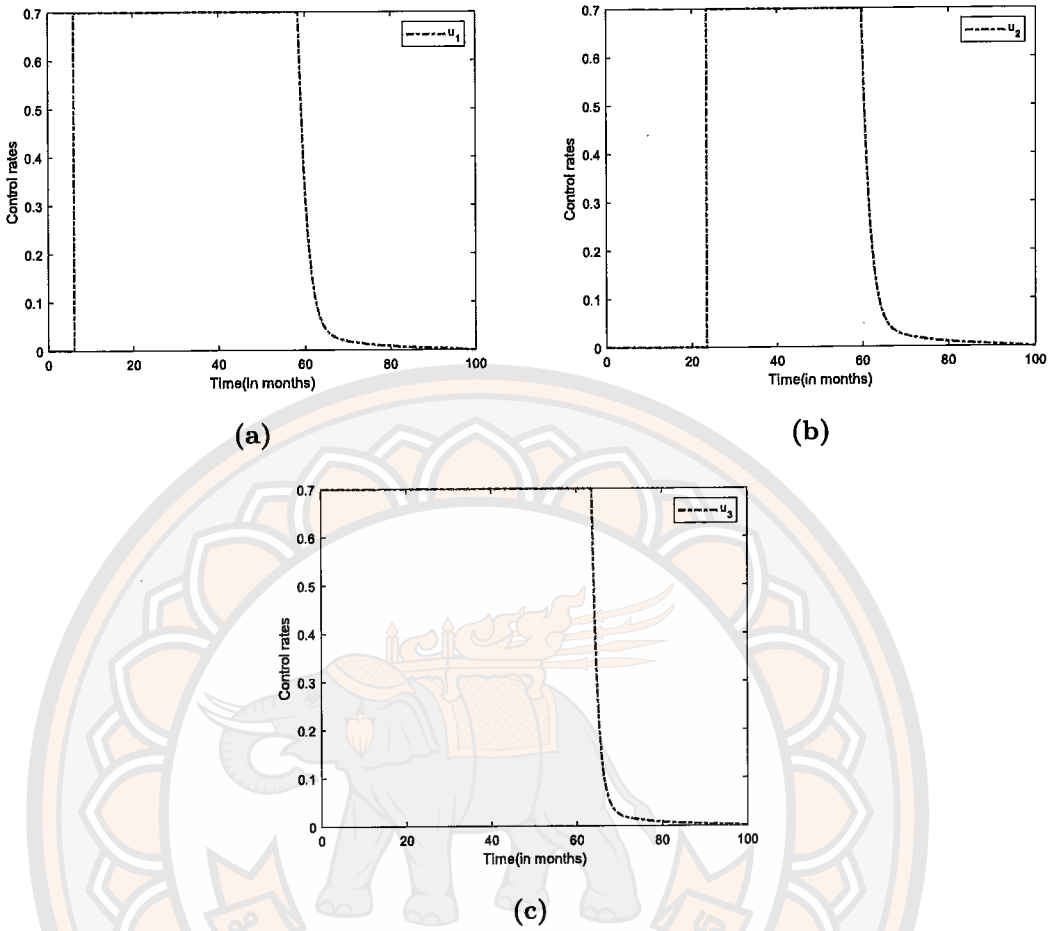

Figure 21 Dynamics of controls (a) vaccination ($u_1(t)$), (b) elimination of Brucella in the environment ($u_2(t)$) and (c) culling of infected bison ($u_3(t)$).

The last case of our simulations is when all control costs are the same. In this simulation, we let $c_1 = c_2 = c_3 = 0.001$, and the results are shown in Figure 22 and Figure 23. In this case, only eliminating bacteria and culling animal controls are implemented, so the second round of the disease outbreak can occur, which you can see in Figure 22 (a) and Figure 22 (b). However, the total number of cases is still not that much as without the control model.

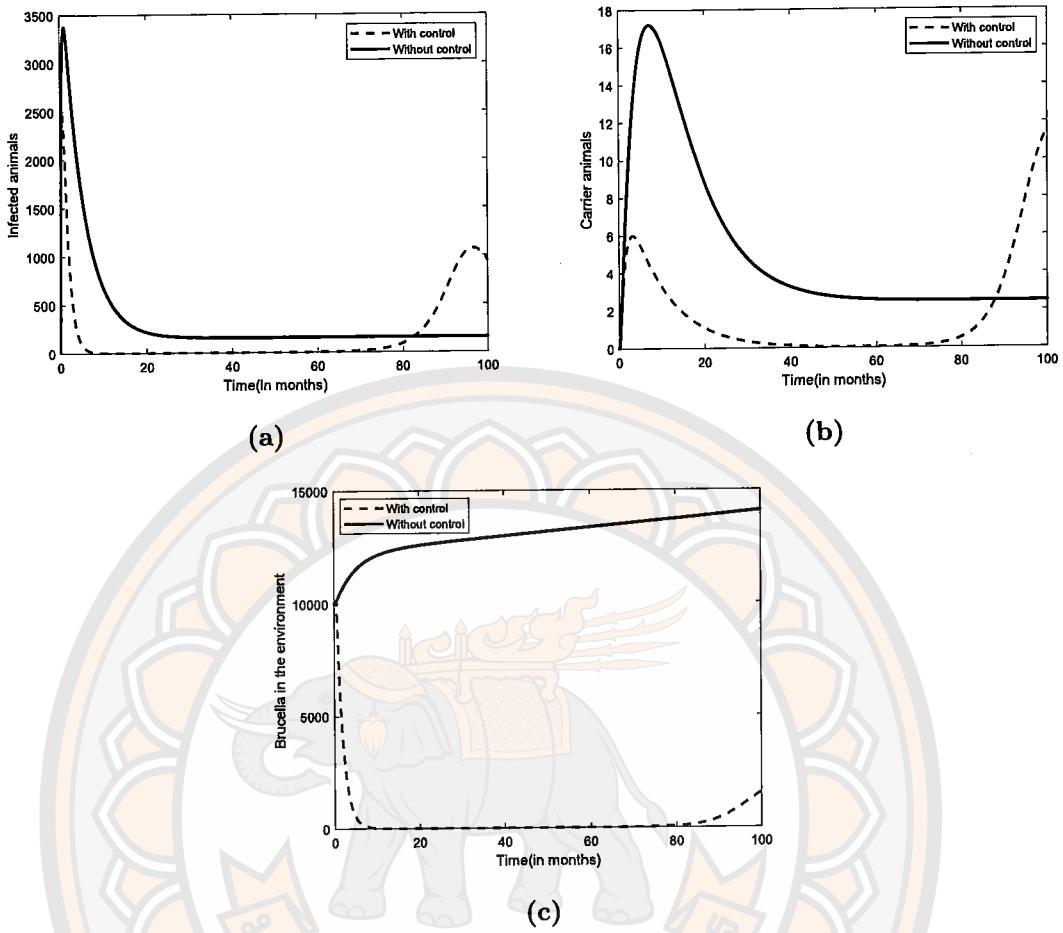

Figure 22 Simulation results: (a) infected animals (b) chronically infected animals (c) Brucella in the environment. Note that the basic reproduction number value for this set of parameters is about 45 with other cost values $c_1 = 0.001, c_2 = 0.001$ and $c_3 = 0.001$.

Our model is formulated based on bison population data, and there are just a few research to compare with our results. However, we have looked closely at the research proposed by Lolika et al. [17] that focused on investigating the dynamics of brucellosis infection in the bison population. They also formulated an optimal control problem that included culling measures to eradicate the disease. We see that our results with more controls show flexible public interventions to stop the disease outbreaks.

From our observation, when the environmental rate increases, the number

of infections increases as well. We also have simulated with no environmental factors and found that the number of infections among bison increased slower than that with the transmission pathway from the environment. It indicates that environmental factors are one of the most important keys to be considered.

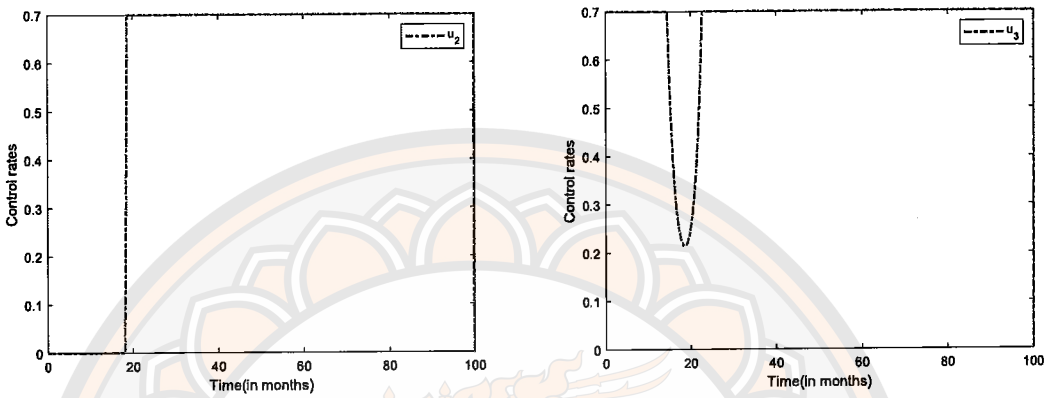

Figure 23 Dynamics of controls: vaccination $u_1(t) = 0$, (a) elimination of Brucella in the environment $(u_2(t))$ and (b) culling of infected bison $(u_3(t))$.

CHAPTER IV

MATHEMATICAL MODEL OF BRUCELLOSIS AND BOVINE TUBERCULOSIS CO-INFECTION

4.1 Model formulation

This section introduces a classification of the total animal population at time t, denoted as $N(t)$, into four distinct compartments: susceptible animals $(S(t))$, animals infected with brucellosis $(I_1(t))$, animals infected with bovine tuberculosis $(I_2(t))$, and animals infected with both brucellosis and bovine tuberculosis $(I_{12}(t))$. Consequently, the overall animal population is represented as $N(t) = S(t) + I_1(t) + I_2(t) + I_{12}(t)$. We make the assumption that animals tend to group together within their habitats. Consequently, the spread of a disease within one group can lead to contamination of the surrounding environment. In this context, we define $W_1(t)$ and $W_2(t)$ as the concentrations of *Brucella* and *Mycobacterium bovis* in the environment, respectively.

Further, we assume that susceptible animals cannot simultaneously contract both brucellosis and bovine tuberculosis infections. The population of susceptible animals increases through recruitment from births and immigration, occurring at a constant rate Λ, while experiencing a natural mortality rate of μ. When susceptible animals have close contact with brucellosis-infected animals, they can contract *Brucella* at a rate of β_{11}. Similarly, they can contract *Mycobacterium bovis* from infectious bovine tuberculosis animals at a rate of β_{22}. Additionally, animals with bovine tuberculosis can become co-infected by *Brucella* at the same rate β_{11}. Interestingly, we find that the transmission rates for these two scenarios are not distinct, thus allowing us to employ a unified value for the sake of simplicity. Similarly, animals infected with *Brucella* have the potential to contract bovine tuberculosis at the rate of β_{22} and become co-infected individuals.

Likewise, when encountering the co-infection state, a susceptible individual can undergo various outcomes. They may remain uninfected, contract

brucellosis at a rate of β_{01}, or contract bovine tuberculosis at a rate of β_{02}. For simplicity, we assume that an individual infected with brucellosis can also become co-infected by acquiring bovine tuberculosis at the rate β_{02}. Similarly, an individual with bovine tuberculosis can contract brucellosis and become co-infected at a rate of β_{01}.

Regarding environmental factors, we consider that animals inhabit specific habitats. If one group becomes infected with brucellosis, the surrounding environment may become contaminated with *Brucella* (denoted as W_1). Additionally, another infectious group with bovine tuberculosis (*Mycobacterium bovis*) might release the pathogen into the environment in that area (denoted as W_2). In the absence of controlled animal movement, animals can move between different locations, facilitating the exchange of different disease agents. In simpler terms, susceptible individuals can ingest contaminated food from W_1 at a rate of α_1 and from W_2 at a rate of α_2.

Furthermore, δ_{11}, δ_{22}, and δ_{12} represent the disease-related death rates for individuals infected solely with brucellosis, individuals infected solely with bovine tuberculosis, and co-infected individuals, respectively. The culling rate for infected animals is denoted as γ. Brucellosis-infected and co-infected animals can shed *Brucella* into the environment at a rate of ξ_1 due to factors such as abortion, animal secretions, and related factors. Similarly, the shedding rate of *Mycobacterium bovis* from bovine tuberculosis-infected and co-infected individuals is ξ_2, resulting from activities like urination, fecal excretion, and related factors.

It is also assumed that the natural death rates of *Brucella* and *Mycobacterium bovis* in the environment are represented by d_1 and d_2, respectively. Furthermore, ϕ_1 and ϕ_2 denote the rates of elimination for *Brucella* and *Mycobacterium bovis* in the environment, respectively. A schematic representation of the transmission diagram used to derive our model is displayed in Fig. 24.

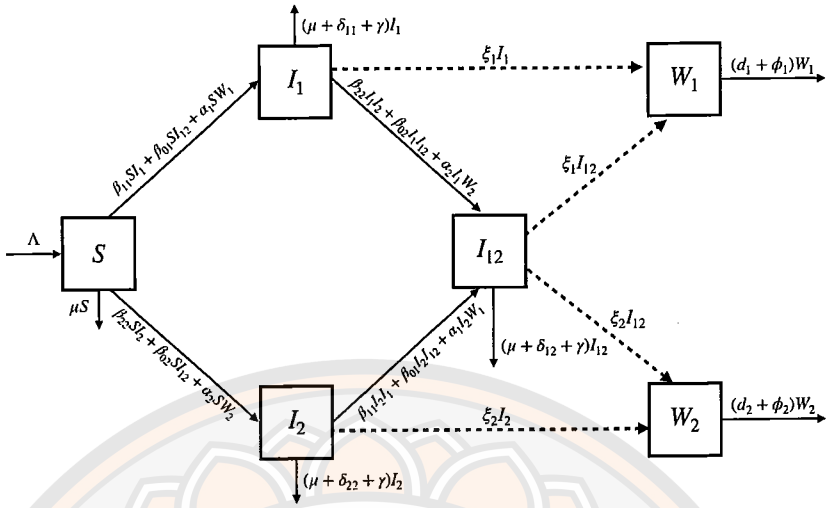

Figure 24 The diagram illustrates the model for brucellosis and bovine tuberculosis.

The system of differential equations below corresponds to the flowchart diagram of the brucellosis-bovine tuberculosis co-infection model depicted in Figure 24:

$$\begin{aligned}
\frac{dS}{dt} &= \Lambda - (\beta_{11}SI_1 + \beta_{01}SI_{12} + \alpha_1SW_1) - (\beta_{22}SI_2 + \beta_{02}SI_{12} + \alpha_2SW_2) - \mu S,\\
\frac{dI_1}{dt} &= (\beta_{11}SI_1 + \beta_{01}SI_{12} + \alpha_1SW_1) - (\beta_{22}I_1I_2 + \beta_{02}I_1I_{12} + \alpha_2I_1W_2)\\
&\quad - (\mu + \delta_{11} + \gamma)I_1,\\
\frac{dI_2}{dt} &= (\beta_{22}SI_2 + \beta_{02}SI_{12} + \alpha_2SW_2) - (\beta_{11}I_2I_1 + \beta_{01}I_2I_{12} + \alpha_1I_2W_1)\\
&\quad - (\mu + \delta_{22} + \gamma)I_2,\\
\frac{dI_{12}}{dt} &= (\beta_{22}I_1I_2 + \beta_{02}I_1I_{12} + \alpha_2I_1W_2) + (\beta_{11}I_2I_1 + \beta_{01}I_2I_{12} + \alpha_1I_2W_1)\\
&\quad - (\mu + \delta_{12} + \gamma)I_{12},\\
\frac{dW_1}{dt} &= (I_1 + I_{12})\xi_1 - (d_1 + \phi_1)W_1,\\
\frac{dW_2}{dt} &= (I_2 + I_{12})\xi_2 - (d_2 + \phi_2)W_2.
\end{aligned} \tag{4.1.1}$$

The model is initialized with the following initial conditions:

$$S(0) \geq 0, I_1(0) \geq 0, I_2(0) \geq 0, I_{12}(0) \geq 0, W_1(0) \geq 0, W_2(0) \geq 0.$$

4.2 Positivity and boundedness of solutions

The model system (4.1.1) delineates the dynamics of the total population. It is crucial to establish the non-negativity of all variables, including $S(t)$, $I_1(t)$, $I_2(t)$, $I_{12}(t)$, $W_1(t)$, and $W_2(t)$, for all time instances. Consequently, solutions of the model system (4.1.1) with positive initial data will maintain positivity over all time intervals $t \geq 0$ and will remain bounded within the domain Ω.

Theorem 4.2.1. *The solutions $S(t), I_1(t), I_2(t), I_{12}(t), W_1(t)$ and $W_2(t)$ of the model system (4.1.1) with initial condition are positive and bounded for $t \geq 0$.*

Proof. : Let the initial conditions $S(0) \geq 0, I_1(0) \geq 0, I_2(0) \geq 0, I_{12}(0) \geq 0, W_1(0) \geq 0$ and $W_2(0) \geq 0$. We will prove that $S(t)$ is positive, we assume a contradiction: that there exists a first time t_1: $S(t_1) = 0, S'(t_1) < 0$ and $S(t) > 0, I_1(t) > 0, I_2(t) > 0, I_{12}(t) > 0, W_1(t) > 0$ and $W_2(t) > 0$ for $0 < t < t_1$. By the first equation of (4.1.1), we have

$$\begin{aligned}\frac{dS(t_1)}{dt} &= \Lambda - (\beta_{11}S(t_1)I_1(t_1) + \beta_{01}S(t_1)I_{12}(t_1) + \alpha_1 S(t_1)W_1(t_1)) \\ &\quad - (\beta_{22}S(t_1)I_2(t_1) + \beta_{02}S(t_1)I_{12}(t_1) + \alpha_2 S(t_1)W_2(t_1)) - \mu S(t_1) \\ &= \Lambda > 0,\end{aligned}$$

which leads to a contradiction, implying that $S(t)$ remains positive.

Similarly, we prove that $I_1(t)$ is positive. Assume that there exists a first time $t_2 : I_1(t_2) = 0, I_1'(t_2) < 0$ and $S(t) > 0, I_2(t) > 0, I_{12} > 0, W_1(t) > 0, W_2(t) > 0$ for $0 < t < t_2$. Using the second equation from (4.1.1), we obtain that

$$\begin{aligned}\frac{dI_1(t_2)}{dt} &= (\beta_{11}S(t_2)I_1(t_2) + \beta_{01}S(t_2)I_{12}(t_2) + \alpha_1 S(t_2)W_1(t_2)) \\ &\quad - (\beta_{22}I_1(t_2)I_2(t_2) + \beta_{02}I_1(t_2)I_{12}(t_2) + \alpha_2 I_1(t_2)W_2(t_2)) \\ &= \beta_{01}S(t_2)I_{12}(t_2) + \alpha_1 S(t_2)W_1(t_2) > 0,\end{aligned}$$

which constitutes a contradiction, implying that $I_1(t)$ remains positive.

Next, we will demonstrate the positivity of $I_2(t)$. Let's assume the existence of a first time $t_3 : I_2(t_3) = 0, I_2'(t_3) < 0$ and $S(t) > 0, I_1(t) > 0, I_{12} > 0, W_1(t) > 0, W_2(t) > 0$ for $0 < t < t_3$. Utilizing the third equation in (4.1.1), we

find that

$$\begin{aligned}\frac{dI_2(t_3)}{dt} &= (\beta_{22}S(t_3)I_2(t_3) + \beta_{02}S(t_3)I_{12}(t_3) + \alpha_2 S(t_3)W_2(t_3)) \\ &\quad - (\beta_{11}I_2(t_3)I_1(t_3) + \beta_{01}I_2(t_3)I_{12}(t_3) + \alpha_1 I_2(t_3)W_1(t_3)) \\ &= \beta_{02}S(t_3)I_{12}(t_3) + \alpha_2 S(t_3)W_2(t_3) > 0,\end{aligned}$$

which leads to a contradiction, implying that $I_2(t)$ remains positive.

Next, we will show that $I_{12}(t)$ is positive. Assume that there exists a first time $t_4 : I_{12}(t_4) = 0, I'_{12}(t_4) < 0$ and $S(t) > 0, I_1(t) > 0, I_2 > 0, W_1(t) > 0, W_2(t) > 0$ for $0 < t < t_4$. From the fourth equation in (4.1.1), it follows that

$$\begin{aligned}\frac{dI_{12}(t_4)}{dt} &= (\beta_{22}I_1(t_4)I_2(t_4) + \beta_{02}I_1(t_4)I_{12}(t_4) + \alpha_2 I_1(t_4)W_2(t_4)) \\ &\quad + (\beta_{11}I_2(t_4)I_1(t_4) + \beta_{01}I_2(t_4)I_{12}(t_4) + \alpha_1 I_2(t_4)W_1(t_4)) \\ &= \beta_{22}I_1(t_4)I_2(t_4) + \alpha_2 I_1(t_4)W_2(t_4) + \beta_{11}I_2(t_4)I_1(t_4) + \alpha_1 I_2(t_4)W_1(t_4) > 0,\end{aligned}$$

leading to a contradiction, implying that I_{12} remains positive.

Following this, we seek to establish the positivity of $W_1(t)$. Assuming the existence of a first time $t_5 : W_1(t_5) = 0, W'_1(t_5) < 0$ and $S(t) > 0, I_1(t) > 0, I_2 > 0, I_{12}(t) > 0, W_2(t) > 0$ for $0 < t < t_5$. By the fifth equation of (4.1.1), we obtain that

$$\begin{aligned}\frac{dW_1(t_5)}{dt} &= (I_1(t_5) + I_{12}(t_5))\xi_1 - (d_1 + \phi_1)W_1(t_5) \\ &= (I_1(t_5) + I_{12}(t_5))\xi_1 > 0,\end{aligned}$$

which is a contradiction meaning that W_1 remains positive.

Finally, we will show that $W_2(t)$ is positive. Assume that there exists a first time $t_4 : W_2(t_6) = 0, W'_2(t_6) < 0$ and $S(t) > 0, I_1(t) > 0, I_2 > 0, I_{12}(t) > 0, W_1(t) > 0$ for $0 < t < t_6$. From the sixth equation in (4.1.1), it follows that

$$\begin{aligned}\frac{dW_2(t_6)}{dt} &= (I_2(t_6) + I_{12}(t_6))\xi_2 - (d_2 + \phi_2)W_2(t_6) \\ &= (I_2(t_6) + I_{12}(t_6))\xi_2 > 0,\end{aligned}$$

which leads to a contradiction, implying that $W_2(t)$ remains positive. Therefore, all solutions of model (4.1.1) are positive whenever $t \geq 0$.

We consider the boundary of solutions of the system of (4.1.1). Since the total animal population of the model is $N = S + I_1 + I_2 + I_{12}$, then

$$\begin{aligned}\frac{dN}{dt} &= \frac{dS}{dt} + \frac{dI_1}{dt} + \frac{dI_2}{dt} + \frac{dI_{12}}{dt} \\ &= \Lambda - \mu(S + I_1 + I_2 + I_{12}) - (\delta_{11} + \gamma)I_1 - (\delta_{22} + \gamma)I_2 - (\delta_{12} + \gamma)I_{12} \\ &\leq \Lambda - \mu N.\end{aligned}$$

Then, we obtain that

$$\frac{dN}{dt} + \mu N \leq \Lambda.$$

Next, by using an interating factor, we get

$$\frac{d}{dt}\left(Ne^{\mu t}\right) \leq \Lambda e^{\mu t}.$$

Integrating both sides, we have

$$\begin{aligned}\int_0^t \frac{d}{dt}\left(Ne^{\mu t}\right) dt &\leq \int_0^t \Lambda e^{\mu t} dt \\ e^{\mu t}N(t) - N(0) &\leq \frac{\Lambda}{\mu}(e^{\mu t}) - \frac{\Lambda}{\mu} \\ e^{\mu t}N(t) &\leq \frac{\Lambda}{\mu}(e^{\mu t}) - \left(\frac{\Lambda}{\mu} - N(0)\right) \\ N(t) &\leq \frac{\Lambda}{\mu} - \left(\frac{\Lambda}{\mu} - N(0)\right)(e^{-\mu t}).\end{aligned}$$

Therefore, we have

$$\limsup_{t\to\infty} N(t) \leq \frac{\Lambda}{\mu}.$$

Next, we consider $W_1(t)$. From the fifth equation in (4.1.1), we have

$$\begin{aligned}\frac{dW_1}{dt} &= (I_1 + I_{12})\xi_1 - (d_1 + \phi_1)W_1 \\ &\leq \xi_1 N - (d_1 + \phi_1)W_1 \\ &\leq \frac{\xi_1\Lambda}{\mu} - (d_1 + \phi_1)W_1.\end{aligned}$$

Thus, we have

$$\frac{dW_1}{dt} + (d_1 + \phi_1)W_1 \leq \frac{\xi_1\Lambda}{\mu}$$

Furthermore, by utilizing the second equation from (4.1.1), we obtain that

$$\frac{dW_2}{dt} = (I_2 + I_{12})\xi_2 - (d_2 + \phi_2)W_2$$

$$\leq \xi_2 N - (d_2 + \phi_2)W_1$$
$$\leq \frac{\xi_2 \Lambda}{\mu} - (d_2 + \phi_2)W_2.$$

Therefore, we have

$$\frac{dW_2}{dt} + (d_2 + \phi_2)W_2 \leq \frac{\xi_2 \Lambda}{\mu}$$

In the same way of solving the inequation by using the integrating factor, we have

$$\limsup_{t\to\infty} W_1 \leq \frac{\Lambda\xi_1}{\mu(d_1+\phi_1)} \quad \text{and} \quad \limsup_{t\to\infty} W_2 \leq \frac{\Lambda\xi_2}{\mu(d_2+\phi_2)}.$$

Therefore, we can conclude that the set

$$\Omega = \left\{(S, I_1, I_2, I_{12}, W_1, W_2) \in \mathbb{R}^6_+ | S, I_1, I_2, I_{12}, W_1, W_2 \geq 0, \right.$$
$$\left. 0 \leq S + I_1 + I_2 + I_{12} \leq \frac{\Lambda}{\mu}, W_1 \leq \frac{\Lambda\xi_1}{\mu(d_1+\phi_1)}, W_2 \leq \frac{\Lambda\xi_2}{\mu(d_2+\phi_2)}\right\} \quad (4.2.1)$$

is positively invariant with respect to system (4.1.1). This means that every solution of this model will enter the region Ω and stay inside Ω and it is sufficient to consider the dynamics of the model (4.1.1) in Ω. In this region, the model is mathematically and epidemiologically well-posed. □

4.3 Brucellosis submodel

We have the brucellosis submodel when $I_2 = I_{12} = W_2 = 0$, which is given by,

$$\begin{aligned}
\frac{dS}{dt} &= \Lambda - (\beta_{11} S I_1 + \alpha_1 S W_1) - \mu S, \\
\frac{dI_1}{dt} &= \beta_{11} S I_1 + \alpha_1 S W_1 - (\mu + \delta_{11} + \gamma) I_1, \\
\frac{dW_1}{dt} &= \xi_1 I_1 - (d_1 + \phi_1) W_1,
\end{aligned} \quad (4.3.1)$$

with $S(0) \geq 0, I_1(0) \geq 0, W_1(0) \geq 0$ as the initial conditions, and the total population is given by

$$N_B(t) = S(t) + I_1(t).$$

Therefore, the biologically-feasible region for this model is

$$\Omega_1 = \left\{(S, I_1, W_1) \in \mathbb{R}^3_+ | S, I_1, W_1 \geq 0, 0 \leq S + I_1 \leq \frac{\Lambda}{\mu}, W_1 \leq \frac{\Lambda\xi_1}{\mu(d_1+\phi_1)}\right\} \quad (4.3.2)$$

It can be shown that the solutions S, I_1, W_1 of the submodel system (4.3.1) are positive for $t \geq 0$. Hence Ω_1 is positively invariant and attracting with respect to model (4.3.1).

4.3.1 The disease-free equilibrium point and the basic reproduction number

The brucellosis-only model (4.3.1) has the disease-free equilibrium, obtained by setting the right-hand sides of the equations in the model to zero, given by

$$E_B^0 = (S^0, I_1^0, W_1^0) = \left(\frac{\Lambda}{\mu}, 0, 0\right). \tag{4.3.3}$$

The stablility of this equilibrium is determine by its basic reproduction number R_B, which is computed using the next generation operator method in the work of van den Driessche and Watmough [49] on system (4.3.1). The matrix F and V, for the new infection terms and the remaining transfer terms are, respectively, given by

$$F = \begin{bmatrix} \beta_{11}\frac{\Lambda}{\mu} & \alpha_1\frac{\Lambda}{\mu} \\ 0 & 0 \end{bmatrix} \quad \text{and} \quad V = \begin{bmatrix} \mu + \delta_{11} + \gamma & 0 \\ -\xi_1 & d_1 + \phi_1 \end{bmatrix}$$

The next generation matrix is

$$FV^{-1} = \frac{1}{(\mu + \delta_{11} + \gamma)(d_1 + \phi_1)} \begin{bmatrix} \frac{\beta_{11}\Lambda(d_1+\phi_1)}{\mu} + \frac{\alpha_1\Lambda\xi_1}{\mu} & \frac{\alpha_1\Lambda(\mu+\delta_{11}+\gamma)}{\mu} \\ 0 & 0 \end{bmatrix}.$$

It follows that the basic reproduction number for brucellosis submodel system is given by the sepectal radius of a matrix FV^{-1}, which is

$$R_B = \frac{\Lambda(\beta_{11}(d_1 + \phi_1) + \alpha_1\xi_1)}{\mu(\mu + \delta_{11} + \gamma)(d_1 + \phi_1)} \tag{4.3.4}$$

4.3.2 The local stability of disease-free equilibrium point

Using Theorem 2.1.1, the following result is established.

Theorem 4.3.1. *The disease-free equilibrium, E_B^0 is locally asymptotically stable when $R_B < 1$ and unstable when $R_B > 1$.*

Theorem 4.3.1 can also be proven using the Jacobian matrix as follows:

$$J = \begin{bmatrix} -\beta_{11}I_1 - \alpha_1 W_1 - \mu & -\beta_{11}S & -\alpha_1 S \\ \beta_{11}I_1 + \alpha_1 W_1 & \beta_{11}S - (\mu + \delta_{11} + \gamma) & \alpha_1 S \\ 0 & \xi_1 & -(d_1 + \phi_1) \end{bmatrix}.$$

The Jacobian matrix at that the disease-free equilibrium, E_B^0 of the submodel system (4.3.1) is

$$J(E_B^0) = \begin{bmatrix} -\mu & \frac{-\beta_{11}\Lambda}{\mu} & \frac{-\alpha_1\Lambda}{\mu} \\ 0 & \frac{\beta_{11}\Lambda}{\mu} - (\mu + \delta_{11} + \gamma) & \frac{\alpha_1\Lambda}{\mu} \\ 0 & \xi_1 & -(d_1 + \phi_1) \end{bmatrix}.$$

The eigenvalues of $J(E_B^0)$ are calculated using $\det(J(E_B^0) - \lambda I) = 0$, then we obtain that

$$(-\mu - \lambda)\left(\lambda^2 + \left(\mu + \delta_{11} + \gamma + d_1 + \phi_1 - \frac{\beta_{11}\Lambda}{\mu}\right)\lambda + (\mu + \delta_{11} + \gamma)(d_1 + \phi_1) - \frac{\xi_1\alpha_1\Lambda}{\mu}\right) = 0$$

Therefore, $\lambda_1 = -\mu < 0$.

Next, we consider $\lambda^2 + a_1\lambda + a_2 = 0$, where

$$a_1 = \mu + \delta_{11} + \gamma + d_1 + \phi_1 - \frac{\beta_{11}\Lambda}{\mu},$$
$$a_2 = (\mu + \delta_{11} + \gamma)(d_1 + \phi_1) - \frac{\xi_1\alpha_1\Lambda}{\mu}.$$

Since $R_B < 1$, we obtain that

$$\beta_{11}\Lambda(d_1 + \phi_1) + \alpha_1\Lambda\xi_1 < \mu(\mu + \delta_{11} + \gamma)(d_1 + \phi_1).$$

Since $\beta_{11}\Lambda(d_1 + \phi_1) < \beta_{11}\Lambda(d_1 + \phi_1) + \alpha_1\Lambda\xi_1$, then

$$\beta_{11}\Lambda(d_1 + \phi_1) < \mu(\mu + \delta_{11} + \gamma)(d_1 + \phi_1)$$
$$\beta_{11}\Lambda < \mu(\mu + \delta_{11} + \gamma)$$
$$\frac{\beta_{11}\Lambda}{\mu} < \mu + \delta_{11} + \gamma.$$

As $\mu + \delta_{11} + \gamma < \mu + \delta_{11} + \gamma + d_1 + \phi_1$, we get

$$\frac{\beta_{11}\Lambda}{\mu} < \mu + \delta_{11} + \gamma + d_1 + \phi_1.$$

Therefore, this implies that $a_1 > 0$.

Furthermore, as $R_B < 1$ and $\alpha_1\Lambda\xi_1 < \beta_{11}\Lambda(d_1+\phi_1) + \alpha_1\Lambda\xi_1$, we deduce that

$$\alpha_1\Lambda\xi_1 < \mu(\mu+\delta_{11}+\gamma)(d_1+\phi_1)$$
$$\frac{\alpha_1\Lambda\xi_1}{\mu} < (\mu+\delta_{11}+\gamma)(d_1+\phi_1).$$

This deduction leads to the conclusion that $a_2 > 0$. Therefore, by the criteria of Routh–Hurwitz, E_B^0 is locally asymptotically stable when $R_B < 1$ and unstable when $R_B > 1$.

4.3.3 The global stability of the disease-free equilibrium point

To invesitgate the global stability of the disease-free equilibrium, we will utilize the method outlined in Lemma 2.1.4.

Theorem 4.3.2. *The disease-free equilibrium point, E_B^0, is globally asymptotically stable provided that $R_B < 1$ and conditions (H1) and (H2) are satisfied.*

Proof. In Theorem 4.3.1 we have E_B^0 is locally asymptotically stable when $R_B < 1$. Rewrite the brucellosis submodel system (4.3.1) as:

$$\frac{dX_1}{dt} = F(X_1, X_2) = \left[\Lambda - (\beta_{11}SI_1 + \alpha_1 SW_1)\mu S\right],$$
$$\frac{dX_2}{dt} = G(X_1, X_2) = \begin{bmatrix} \beta_{11}SI_1 + \alpha_1 SW_1 - (\mu+\delta_{11}+\gamma)I_1 \\ \xi_1 I_1 - (d_1+\phi_1)W_1 \end{bmatrix}, \quad G(X_1, 0) = 0,$$

where $X_1 \in \mathbb{R}$ denotes the number of uninfected individuals, that is $X_1 = (S)$. Moreover $X_2 \in \mathbb{R}^n$ denotes the number of infected individuals including latent, infectious, that is $X_2 = (I_1, W_1)$.

The disease-free equilibrium is denoted by

$$E_B^0 = (X_1^*, 0), \qquad \text{where } X_1^* = \left(\frac{\Lambda}{\mu}\right). \tag{4.3.5}$$

Consider

$$F(X_1, 0) = \left[\Lambda - \mu S\right].$$

As for S, we can deduce from the equation above that

$$\frac{dS}{dt} = \Lambda - \mu S$$
$$\frac{dS}{dt} + \mu S = \Lambda$$

We solve this equation using the integrating factor, which results in $S(t) \to \frac{\Lambda}{\mu}$ as $t \to \infty$. Therefore X_1^* is globally asymptotically stable.

Next, let's consider

$$\frac{\partial G}{\partial X_2}(X_1, X_2) = \begin{bmatrix} \beta_{11}S - (\mu + \delta_{11} + \gamma) & \alpha_1 S \\ \xi_1 & -(d_1 + \phi_1) \end{bmatrix}.$$

Thus, we have

$$A = \frac{\partial G}{\partial X_2}(X_1^*, 0) = \begin{bmatrix} \frac{\beta_{11}\Lambda}{\mu} - (\mu + \delta_{11} + \gamma) & \frac{\alpha_1 \Lambda}{\mu} \\ \xi_1 & -(d_1 + \phi_1) \end{bmatrix}$$

This matrix is an M-matrix, meaning it has non-negative in its off-diagonal elements. Furthermore, based on $(H2)$ we will show that $\hat{G}(X_1, X_2)$ must be greater than or equal to zero. Thus, we consider

$$\begin{aligned} \hat{G}(X_1, X_2) &= AX_2 - G(X_1, X_2) \\ &= \begin{bmatrix} \frac{\beta_{11}\Lambda}{\mu} - (\mu + \delta_{11} + \gamma) & \frac{\alpha_1 \Lambda}{\mu} \\ \xi_1 & -(d_1 + \phi_1) \end{bmatrix} \begin{bmatrix} I_1 \\ W_1 \end{bmatrix} \\ &\quad - \begin{bmatrix} \beta_{11}SI_1 + \alpha_1 SW_1 - (\mu + \delta_{11} + \gamma)I_1 \\ \xi_1 I_1 - (d_1 + \phi_1)W_1 \end{bmatrix} \\ &= \begin{bmatrix} \beta_{11}I_1\left(\frac{\Lambda}{\mu} - S\right) + \frac{\alpha_1}{\mu}W_1\left(\frac{\Lambda}{\mu} - S\right) \\ 0 \end{bmatrix}. \end{aligned}$$

Meanwhile, we consider the first equation of system (4.3.1), then we get

$$\begin{aligned} \frac{dS}{dt} &= \Lambda - (\beta_{11}SI_1 + \alpha_1 SW_1) - \mu S \\ &\leq \Lambda - \mu S. \end{aligned}$$

Thus,

$$\limsup_{t \to \infty} S \leq \frac{\Lambda}{\mu} = S^0.$$

Hence, we have $S(t) \leq S^0$, which leads to $\widehat{G}(X_1, X_2) \geq 0$. Therefore E_B^0, is globally asymptotically stable when $R_B < 1$. □

4.3.4 The endemic equilibrium point

The endemic equilibrium point is denoted by $E_B^* = (S^*, I_1^*, W_1^*)$ and it occurs when there is a persistence of the disease. It can be obtained by equating the model equations (4.3.1) to zero. Therefore, we have

$$\begin{aligned} 0 &= \Lambda - (\beta_{11} S^* I_1^* + \alpha_1 S^* W_1^*) - \mu S^*, \\ 0 &= \beta_{11} S^* I_1^* + \alpha_1 S^* W_1^* - (\mu + \delta_{11} + \gamma) I_1^*, \\ 0 &= \xi_1 I_1^* - (d_1 + \phi_1) W_1^*, \end{aligned} \tag{4.3.6}$$

From the third equation in (4.3.6), we have

$$W^* = \frac{\xi_1 I_1^*}{d_1 + \phi_1}. \tag{4.3.7}$$

According to the second equation in (4.3.6), we obtain

$$S^* = \frac{(\mu + \delta_{11} + \gamma)(d_1 + \phi_1)}{\beta_{11}(d_1 + \phi_1) + \alpha_1 \xi_1}. \tag{4.3.8}$$

Furthermore, based on the first equation in (4.3.6), we find that

$$I_1^* = \frac{\left(\frac{\Lambda}{S^*} - \mu\right)(d_1 + \phi_1)}{\beta_{11}(d_1 + \phi_1) + \alpha_1 \xi_1}. \tag{4.3.9}$$

Substituting (4.3.8) into equation (4.3.9), we can deduce that

$$\begin{aligned} I_1^* &= \frac{\left(\frac{\Lambda(\beta_{11}(d_1+\phi_1)+\alpha_1\xi_1)}{(\mu+\delta_{11}+\gamma)(d_1+\phi_1)} - \mu\right)(d_1 + \phi_1)}{\beta_{11}(d_1 + \phi_1) + \alpha_1 \xi_1} \\ &= \frac{(\mu R_B - \mu)(d_1 + \phi_1)}{\beta_{11}(d_1 + \phi_1) + \alpha_1 \xi_1} \\ &= \frac{\mu(R_B - 1)(d_1 + \phi_1)}{\beta_{11}(d_1 + \phi_1) + \alpha_1 \xi_1}. \end{aligned} \tag{4.3.10}$$

Substituting (4.3.10) into equation (4.3.7), we obtain that

$$W_1^* = \frac{\xi_1 \mu (R_B - 1)}{\beta_{11}(d_1 + \phi_1) + \alpha_1 \xi_1}. \tag{4.3.11}$$

Therefore, we have is $E_B^* = (S^*, I_1^*, W_1^*)$, where

$$\begin{aligned} S^* &= \frac{(\mu + \delta_{11} + \gamma)(d_1 + \phi_1)}{\beta_{11}(d_1 + \phi_1) + \alpha_1 \xi_1}, \\ I_1^* &= \frac{\mu(d_1 + \phi_1)(R_B - 1)}{\beta_{11}(d_1 + \phi_1) + \alpha_1 \xi_1}, \\ W_1^* &= \frac{\xi_1 \mu (R_B - 1)}{\beta_{11}(d_1 + \phi_1) + \alpha_1 \xi_1}. \end{aligned}$$

Furthermore, we see that for the endemic equilibrium to exist, when $R_B > 1$.

4.3.5 Local stability of the endemic equilibrium point

We use the Centre Manifold theory [61] as described in Theorem 4.1 by Castillo-Chavez and Song [50], to establish the local asymptotic stability of the endemic equilibrium (see the Theorem 2.1.2 in Chapter 2). To apply this theory, the following simplification and change of variables are made first. Let $S = x_1, I_1 = x_2$ and $W_1 = x_3$, so that $N = x_1 + x_2$. We now use the notation $X = (x_1, x_2, x_3)^T$. Thus, the brucellosis-only model (4.3.1) can be written in the form $\frac{dX}{dt} = F(X)$, with $F = (f_1, f_2, f_3)^T$, as follows:

$$\begin{aligned}
\frac{dx_1}{dt} &= f_1 = \Lambda - (\beta_{11}x_1x_2 + \alpha_1x_1x_3) - \mu x_1,\\
\frac{dx_2}{dt} &= f_2 = \beta_{11}x_1x_2 + \alpha_1x_1x_3 - (\mu + \delta_{11} + \gamma)x_2,\\
\frac{dx_3}{dt} &= f_3 = \xi_1x_2 - (d_1 + \phi_1)x_3.
\end{aligned} \tag{4.3.12}$$

The Jacobian of the system (4.3.12) at E_B^0 is given by

$$J(E_B^0) = \begin{bmatrix} -\mu & \frac{-\beta_{11}\Lambda}{\mu} & \frac{-\alpha_1\Lambda}{\mu} \\ 0 & \frac{\beta_{11}\Lambda}{\mu} - (\mu + \delta_{11} + \gamma) & \frac{\alpha_1\Lambda}{\mu} \\ 0 & \xi_1 & -(d_1 + \phi_1) \end{bmatrix}.$$

Choose β_{11} as the bifurcation parameter, then setting $R_B = 1$ gives

$$\beta_{11} = \beta_{11}^* = \frac{\mu(\mu + \delta_{11} + \gamma)}{\Lambda} - \frac{\alpha_1\xi_1}{d_1 + \phi_1}.$$

The eigenvalues of $J(E_B^0)$ are calculated using $\det(J(E_B^0) - \lambda I) = 0$, then we obtain that

$$(-\mu - \lambda)\left(\left(\frac{\beta_{11}\Lambda}{\mu} - (\mu + \delta_{11} + \gamma) - \lambda\right)(-(d_1 + \phi_1) - \lambda) - \frac{\xi_1\alpha_1\Lambda}{\mu}\right) = 0.$$

Since $\beta_{11} = \frac{\mu(\mu+\delta_{11}+\gamma)}{\Lambda} - \frac{\alpha_1\xi_1}{d_1+\phi_1}$, then we can deduce that

$$0 = (-\mu - \lambda)\left(\left(-\frac{\alpha_1\xi_1\Lambda}{\mu(d_1 + \phi_1)} - \lambda\right)(-(d_1 + \phi_1) - \lambda) - \frac{\xi_1\alpha_1\Lambda}{\mu}\right).$$

Thus, we get $\lambda_1 = -\mu$. Next, we consider

$$\begin{aligned}
0 &= \left(-\frac{\alpha_1\xi_1\Lambda}{\mu(d_1 + \phi_1)} - \lambda\right)(-(d_1 + \phi_1) - \lambda) - \frac{\xi_1\alpha_1\Lambda}{\mu}\\
&= \frac{\alpha_1\xi_1\Lambda}{\mu} + \frac{\alpha_1\xi_1\Lambda\lambda}{\mu(d_1 + \phi_1)} + (d_1 + \phi_1)\lambda + \lambda^2 - \frac{\xi_1\alpha_1\Lambda}{\mu}
\end{aligned}$$

$$= \lambda^2 + \left(\frac{\alpha_1\xi_1\Lambda}{\mu(d_1+\phi_1)} + (d_1+\phi_1)\right)\lambda$$
$$= \lambda\left(\lambda + \frac{\alpha_1\xi_1\Lambda}{\mu(d_1+\phi_1)} + (d_1+\phi_1)\right).$$

Therefore, we have $\lambda_2 = 0$ and $\lambda_3 = -\left(\frac{\alpha_1\xi_1\Lambda}{\mu(d_1+\phi_1)} + (d_1+\phi_1)\right)$.

Note that the linearised system (4.3.12) at E_B^0 evaluated for $\beta_{11} = \beta_{11}^*$ has a simple zero eigenvalue, and all other eigenvalues have negative real part. Hence, the Centre Manifold theory can be used to analyze the dynamics of (4.3.12) near $\beta_{11} = \beta_{11}^*$.

It can be shown that the Jacobian of (4.3.12) at $\beta_{11} = \beta_{11}^*$ (denoted by $J_{\beta_{11}^*}$) has a right eigenvector (corresponding to the zero eigenvalue) given by $w = [w_1, w_2, w_3]^T$, such that

$$-\mu w_1 - \frac{\beta_{11}\Lambda}{\mu}w_2 - \frac{\alpha_1\Lambda}{\mu}w_3 = 0 \tag{4.3.13}$$
$$\left(\frac{\beta_{11}\Lambda}{\mu} - (\mu+\delta_{11}+\gamma)\right)w_2 + \frac{\alpha_1\Lambda}{\mu}w_3 = 0 \tag{4.3.14}$$
$$\xi_1 w_2 - (d_1+\phi_1)w_3 = 0. \tag{4.3.15}$$

Considering equation (4.3.15), we can observe that

$$w_3 = \frac{\xi_1 w_2}{d_1+\phi_1}. \tag{4.3.16}$$

Substituting equation (4.3.16) into equation (4.3.14), we obtain that

$$\left(\frac{\beta_{11}\Lambda}{\mu} - (\mu+\delta_{11}+\gamma) + \frac{\alpha_1\Lambda\xi_1}{\mu(d_1+\phi_1)}\right)w_2 = 0$$

Since $\beta_{11} = \frac{\mu(\mu+\delta_{11}+\gamma)}{\Lambda} - \frac{\alpha_1\xi_1}{d_1+\phi_1}$, then we can deduce that

$$\left((\mu+\delta_{11}+\gamma) - \frac{\alpha_1\xi_1\Lambda}{\mu(d_1+\phi_1)} - (\mu+\delta_{11}+\gamma) + \frac{\alpha_1\Lambda\xi_1}{\mu(d_1+\phi_1)}\right)w_2 = 0$$
$$(0)w_2 = 0.$$

As a result, w_2 can assume any value. Thus, we choose $w_2 > 0$.

Next, substituting equation w_3 into equation (4.3.13) yields

$$0 = -\mu w_1 - \frac{\beta_{11}\Lambda}{\mu}w_2 - \frac{\alpha_1\Lambda}{\mu}\left(\frac{\xi_1 w_2}{d_1+\phi_1}\right)$$

$$w_1 = \frac{1}{\mu}\left(-\frac{\beta_{11}\Lambda}{\mu} - \frac{\alpha_1\xi_1\Lambda}{\mu(d_1+\phi_1)}\right)w_2$$

Since $\beta_{11} = \frac{\mu(\mu+\delta_{11}+\gamma)}{\Lambda} - \frac{\alpha_1\xi_1}{d_1+\phi_1}$, then we get that

$$\begin{aligned} w_1 &= \frac{1}{\mu}\left(-(\mu+\delta_{11}+\gamma) + \frac{\alpha_1\xi_1\Lambda}{\mu(d_1+\phi_1)} - \frac{\alpha_1\xi_1\Lambda}{\mu(d_1+\phi_1)}\right)w_2 \\ &= \frac{-(\mu+\delta_{11}+\gamma)w_2}{\mu}. \end{aligned}$$

Further, $J_{\beta_{11}^*}$ has a left eigenvector associated with the zero eigenvalue at $\beta_{11} = \beta_{11}^*$ is given by $v = [v_1, v_2, v_3]$, where

$$-\mu v_1 = 0 \tag{4.3.17}$$

$$\frac{-\beta_{11}\Lambda}{\mu}v_1 + \left(\frac{\beta_{11}\Lambda}{\mu} - (\mu+\delta_{11}+\gamma)\right)v_2 + \xi_1 v_3 = 0 \tag{4.3.18}$$

$$-\frac{\alpha_1\Lambda}{\mu}v_1 + \frac{\alpha_1\Lambda}{\mu}v_2 - (d_1+\phi_1)v_3 = 0. \tag{4.3.19}$$

Considering equation (4.3.17), we find that $v_1 = 0$.

When substituting equation $v_1 = 0$ into equation (4.3.18), we find that

$$\left(\frac{\beta_{11}\Lambda}{\mu} - (\mu+\delta_{11}+\gamma)\right)v_2 + \xi_1 v_3 = 0$$

Since $\beta_{11} = \frac{\mu(\mu+\delta_{11}+\gamma)}{\Lambda} - \frac{\alpha_1\xi_1}{d_1+\phi_1}$, then we get that

$$-\frac{\alpha_1\xi_1\Lambda}{\mu(d_1+\phi_1)}v_2 + \xi_1 v_3 = 0$$

$$v_2 = \frac{\mu(d_1+\phi_1)v_3}{\alpha_1\Lambda}. \tag{4.3.20}$$

By substituting the equation $v_1 = 0$ and (4.3.20) into equation (4.3.19), we obtain that

$$\begin{aligned} \frac{\alpha_1\Lambda}{\mu}v_2 - (d_1+\phi_1)v_3 &= 0 \\ \frac{\alpha_1\Lambda}{\mu}\left(\frac{\mu(d_1+\phi_1)v_3}{\alpha_1\Lambda}\right) - (d_1+\phi_1)v_3 &= 0 \\ (0)v_3 &= 0. \end{aligned}$$

As a consequence, we have v_3 can take any value. Therefore, we choose $v_3 > 0$.

Computation of a and b:

For the system (4.3.12), the associated non-zero partial derivatives of $F = (f_1, f_2, f_3)^T$ (at the disease-free equilibrium) are given by

$$\frac{\partial^2 f_1}{\partial x_1 \partial x_2} = -\beta_{11}, \quad \frac{\partial^2 f_1}{\partial x_1 \partial x_3} = -\alpha_1, \quad \frac{\partial^2 f_2}{\partial x_1 \partial x_2} = \beta_{11}, \quad \frac{\partial^2 f_2}{\partial x_1 \partial x_3} = -\alpha_1.$$

It follows from the above expression that

$$\begin{aligned}
a &= \sum_{k,i,j=1}^{n} v_k w_i w_j \frac{\partial^2 f_k}{\partial x_i \partial x_j}(0,0) \\
&= 2v_1 w_1 w_2(-\beta_{11}) + 2v_1 w_1 w_3(-\alpha_1) + 2v_2 w_1 w_2(\beta_{11}) + 2v_2 w_1 w_3(-\alpha_1) \\
&= 2v_2 w_1(\beta_{11} w_2 + \alpha_1 w_3) \\
&= 2\left(\frac{\mu(d_1+\phi_1)v_3}{\alpha_1 \Lambda}\right)\left(\frac{-(\mu+\delta_{11}+\gamma)w_2}{\mu}\right)\left(\beta_{11} w_2 + \alpha\left(\frac{\xi_1 w_2}{d_1+\phi_1}\right)\right) \\
&= -2\left(\frac{(d_1+\phi_1)(\mu+\delta_{11}+\gamma)}{\alpha_1 \Lambda}\right)\left(\beta_{11} + \frac{\alpha\xi_1}{d_1+\phi_1}\right) v_3 w_2^2 < 0.
\end{aligned}$$

For the sign of b, it is associated with the following non-vanishing partial derivatives of $F = (f_1, f_2, f_3)^T$,

$$\frac{\partial^2 f_1}{\partial x_2 \beta_{11}^*} = -\frac{\Lambda}{\mu}, \quad \frac{\partial^2 f_2}{\partial x_2 \beta_{11}^*} = \frac{\Lambda}{\mu}.$$

So, we get

$$\begin{aligned}
b &= \sum_{k,i=1}^{n} v_k w_i \frac{\partial^2 f_k}{\partial x_i \partial \phi}(0,0) \\
&= v_1 w_2\left(-\frac{\Lambda}{\mu}\right) + v_2 w_2\left(\frac{\Lambda}{\mu}\right) \\
&= \frac{\Lambda(d_1+\phi_1)}{\alpha_1 \Lambda} v_3 w_2 > 0.
\end{aligned}$$

Since $a < 0$ and $b > 0$ at $\beta_{11} = \beta_{11}^*$, and Theorem 2.1.2 item (iv), therefore a forward or transcritical bifurcation occurs at $R_B = 1$ as depicted in Fig. 2. Hence the following result is established.

Theorem 4.3.3. *The endemic equilibrium E_B^* of the brucellosis submodel is locally asymptotically stable for $R_B > 1$, but close to unity.*

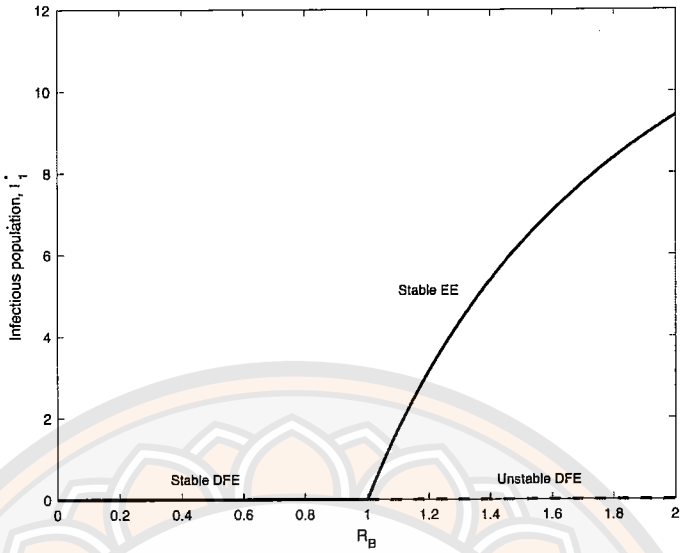

Figure 25 Forward bifurcation for the infectious population (I_1^*) of the model (4.3.1). Using the parameter values: $\Lambda = 16.6667, \mu = 0.0058, \delta_{11} = 0.0125, \gamma = 0.0333, \xi_1 = 0.8333, d_1 = 0.00005, \phi_1 = 8.333 \times 10^{-5}, \alpha_1 = 2.9167 \times 10^{-5}$.

4.3.6 Global stability of the endemic equilibrium point

We analyze the global stability of the endemic equilibrium of system (4.3.1) by using a Lyapunov function. It is important for us to understand the extinction and persistence of the disease.

Theorem 4.3.4. *The endemic equilibrium E_B^* of the brucellosis submodel system* (4.3.1) *is globally asymptotically stable if $R_B > 1$.*

Proof. Consider the first equation (4.3.1), we have

$$\begin{aligned}\frac{dS}{dt} &= \Lambda - (\beta_{11} S I_1 + \alpha_1 S W_1) - \mu S \\ &= S\left(\frac{\Lambda}{S} - (\beta_{11} I_1 + \alpha_1 W_1) - \mu\right).\end{aligned}$$

Substituting endemic equilibrium $E_B^* = (S^*, I_1^*, W_1^*)$ to the first equation (4.3.1), we obtain that

$$0 = \Lambda - (\beta_{11} S^* I_1^* + \alpha_1 S^* W_1^*) - \mu S^*$$

When we multiply every term by $\frac{1}{S^*}$, we obtain

$$0 = \frac{\Lambda}{S^*} - (\beta_{11} I_1^* + \alpha_1 W_1^*) - \mu.$$

Thus, we get

$$\begin{aligned}
\frac{dS}{dt} &= S\left(\frac{\Lambda}{S} - (\beta_{11} I_1 + \alpha_1 W_1) - \mu - 0\right) \\
&= S\left(\frac{\Lambda}{S} - (\beta_{11} I_1 + \alpha_1 W_1) - \mu - \left(\frac{\Lambda}{S^*} - (\beta_{11} I_1^* + \alpha_1 W_1^*) - \mu\right)\right) \\
&= S\left(\frac{\Lambda}{S} - \frac{\Lambda}{S^*} - \beta_{11} I_1 + \beta_{11} I_1^* - \alpha_1 W_1 + \alpha_1 W_1^*\right) \\
&= S\left(\frac{\Lambda}{S^*}\left(\frac{S^*}{S} - 1\right) - \beta_{11} I_1^*\left(\frac{I_1}{I_1^*} - 1\right) - \alpha_1 W_1^*\left(\frac{W_1}{W_1^*} - 1\right)\right).
\end{aligned}$$

Next, we consider the second equation in (4.3.1), we have

$$\frac{dI_1}{dt} = \beta_{11} S I_1 + \alpha_1 S W_1 - (\mu + \delta_{11} + \gamma) I_1.$$

Substituting endemic equilibrium $E_B^* = (S^*, I_1^*, W_1^*)$ to the second equation (4.3.1), we obtain that

$$0 = \beta_{11} S^* I_1^* + \alpha_1 S^* W_1^* - (\mu + \delta_{11} + \gamma) I_1^*$$

When we multiply every term by $\frac{1}{I_1^*}$ and subsequently by I_1, we obtain

$$0 = \beta_{11} S^* I_1 + \frac{\alpha_1 S^* W_1^* I_1}{I_1^*} - (\mu + \delta_{11} + \gamma) I_1^*.$$

Hence, we get

$$\begin{aligned}
\frac{dI_1}{dt} &= \beta_{11} S I_1 + \alpha_1 S W_1 - (\mu + \delta_{11} + \gamma) I_1 - 0 \\
&= \beta_{11} S I_1 + \alpha_1 S W_1 - (\mu + \delta_{11} + \gamma) I_1 - \left(\beta_{11} S^* I_1 + \frac{\alpha_1 S^* W_1^* I_1}{I_1^*} - (\mu + \delta_{11} + \gamma) I_1^*\right) \\
&= \beta_{11} S I_1 - \beta_{11} I_1 S^* + \alpha_1 S W_1 - \frac{\alpha_1 S^* W_1^* I_1}{I_1^*} \\
&= \beta_{11} I_1 S^*\left(\frac{S}{S^*} - 1\right) + \frac{\alpha_1 S^* W_1^* I_1}{I_1^*}\left(\frac{S W_1 I_1^*}{S^* W_1^* I_1} - 1\right) \\
&= \frac{I_1 S^*}{I_1^*}\left(\beta_{11} I_1^*\left(\frac{S}{S^*} - 1\right) + \alpha_1 W_1^*\left(\frac{S W_1 I_1^*}{S^* W_1^* I_1} - 1\right)\right).
\end{aligned}$$

Next, we consider the third equation (4.3.1), we have

$$\frac{dW_1}{dt} = \xi_1 I_1 - (d_1 + \phi_1) W_1.$$

Substituting endemic equilibrium $E_B^* = (S^*, I_1^*, W_1^*)$ to the third equation (4.3.1), we obtain that

$$0 = \xi_1 I_1 - (d_1 + \phi_1) W_1$$

When we multiply every term by $\frac{1}{W_1^*}$ and subsequently by W_1, we obtain

$$0 = \frac{\xi_1 I_1^* W_1}{W_1^*} - (d_1 + \phi_1) W_1.$$

Thus, we have

$$\begin{aligned}
\frac{dW_1}{dt} &= \xi_1 I_1 - (d_1 + \phi_1) W_1 - 0 \\
&= \xi_1 I_1 - (d_1 + \phi_1) W_1 - \left(\frac{\xi_1 I_1^* W_1}{W_1^*} - (d_1 + \phi_1) W_1 \right) \\
&= \xi_1 I_1 - \frac{\xi_1 I_1^* W_1}{W_1^*} \\
&= \frac{\xi_1 I_1^* W_1}{W_1^*} \left(\frac{I_1 W_1^*}{I_1^* W_1} - 1 \right).
\end{aligned}$$

Therefore, the system given by (4.3.1) can be transformed into the following form

$$\begin{aligned}
\frac{dS}{dt} &= S \left(\frac{\Lambda}{S^*} \left(\frac{S^*}{S} - 1 \right) - \beta_{11} I_1^* \left(\frac{I_1}{I_1^*} - 1 \right) - \alpha_1 W_1^* \left(\frac{W_1}{W_1^*} - 1 \right) \right), \\
\frac{dI_1}{dt} &= \frac{I_1 S^*}{I_1^*} \left(\beta_{11} I_1^* \left(\frac{S}{S^*} - 1 \right) + \alpha_1 W_1^* \left(\frac{S W_1 I_1^*}{S^* W_1^* I_1} - 1 \right) \right), \\
\frac{dW_1}{dt} &= \frac{\xi_1 I_1^* W_1}{W_1^*} \left(\frac{I_1 W_1^*}{I_1^* W_1} - 1 \right).
\end{aligned} \tag{4.3.21}$$

We construct the Lyapunov function as:

$$L = \left(S - S^* - S^* \ln \frac{S}{S^*} \right) + \left(I_! - I_1^* - I_1^* \ln \frac{I_1}{I_1^*} \right) + \frac{\alpha_1 S^* W_1^*}{\xi_1 I_1^*} \left(W_1 - W_1^* - W_1^* \ln \frac{W_1}{W_1^*} \right).$$

Therefore, the derivative of L along solutions of system (4.3.21) is

$$\begin{aligned}
\frac{dL}{dt} &= \left(1 - \frac{S^*}{S} \right) \frac{dS}{dt} + \left(1 - \frac{I_1^*}{I_1} \right) \frac{dI_1}{dt} + \frac{\alpha_1 S^* W_1^*}{\xi_1 I_1^*} \left(1 - \frac{W_1^*}{W_1} \right) \frac{dW_1}{dt} \\
&= (S - S^*) \left(\frac{\Lambda}{S^*} \left(\frac{S^*}{S} - 1 \right) - \beta_{11} I_1^* \left(\frac{I_1}{I_1^*} - 1 \right) - \alpha_1 W_1^* \left(\frac{W_1}{W_1^*} - 1 \right) \right) \\
&\quad + (I_1 - I_1^*) \left(\frac{S^*}{I_1^*} \right) \left(\beta_{11} I_1^* \left(\frac{S}{S^*} - 1 \right) + \alpha_1 W_1^* \left(\frac{S W_1 I_1^*}{S^* W_1^* I_1} - 1 \right) \right) \\
&\quad + \frac{\xi_1 I_1^* W_1}{W_1^*} (W_1 - W_1^*) \left(\frac{\xi_1 I_1^*}{W_1^*} \right) \left(\frac{I_1 W_1^*}{I_1^* W_1} - 1 \right)
\end{aligned}$$

$$
\begin{aligned}
&= \Lambda(S-S^*)\left(\frac{1}{S}-\frac{1}{S^*}\right) - \beta_{11}(S-S^*)(I_1-I_1^*) - \alpha_1(S-S^*)(W_1-W_1^*) \\
&\quad + \beta_{11}(I_1-I_1^*)(S-S^*) + \alpha_1 S^* W_1^*(I_1-I_1^*)\left(\frac{SW_1}{S^*W_1^*I_1}-\frac{1}{I_1^*}\right) \\
&\quad + \alpha_1 S^*(W_1-W_1^*)\left(\frac{I_1W_1^*}{I_1^*W_1}-1\right) \\
&= \Lambda\left(2-\frac{S}{S^*}-\frac{S^*}{S}\right) + \alpha_1 SW_1^* - \frac{\alpha_1 SW_1I_1^*}{I_1} - \frac{\alpha_1 S^*I_1W_1^{*2}}{I_1^*W_1} + \alpha_1 S^*W_1^* \\
&= \Lambda\left(2-\frac{S}{S^*}-\frac{S^*}{S}\right) + \alpha_1 S^*W_1^*\left(1+\frac{S}{S^*}-\frac{SW_1I_1^*}{S^*W_1^*I_1}-\frac{I_1W_1^*}{I_1^*W_1}\right) \\
&= \Lambda\left(2-\frac{S}{S^*}-\frac{S^*}{S}\right) + \alpha_1 S^*W_1^*\left((3-2)+\frac{S}{S^*}-\frac{S^*}{S}+\frac{S^*}{S}-\frac{SW_1I_1^*}{S^*W_1^*I_1}-\frac{I_1W_1^*}{I_1^*W_1}\right) \\
&= \Lambda\left(2-\frac{S}{S^*}-\frac{S^*}{S}\right) + \alpha_1 S^*W_1^*\left(3-\frac{S^*}{S}-\frac{SW_1I_1^*}{S^*W_1^*I_1}-\frac{I_1W_1^*}{I_1^*W_1}\right) \\
&\quad - \alpha_1 S^*W_1^*\left(2-\frac{S}{S^*}-\frac{S^*}{S}\right).
\end{aligned}
$$

Substituting endemic equilibrium $E_B^* = (S^*, I_1^*, W_1^*)$ to the first equation in (4.3.1), we have

$$\Lambda = \beta_{11}S^*I_1^* + \alpha_1 S^*W_1^* + \mu S^*$$

Therefore, we get

$$\frac{dL}{dt} = (\beta_{11}S^*I_1^* + \mu S^*)\left(2-\frac{S}{S^*}-\frac{S^*}{S}\right) + \alpha_1 S^*W_1^*\left(3-\frac{S^*}{S}-\frac{SW_1I_1^*}{S^*W_1^*I_1}-\frac{I_1W_1^*}{I_1^*W_1}\right).$$

Thus, by the arithmetic-geometric mean inequality, we get $\frac{dL}{dt} \leq 0$. The equality $\frac{dL}{dt} = 0$ holds, if and only if $S = S^*, I_1 = I_1^*, W_1 = W_1^*$. Therefore, by LaSalle's invariance principle, the endemic equilibrium E_B^* is globally asymptotically stable when $R_B < 1$. This completes the proof. □

4.4 Bovine Tuberculosis (BTB) submodel

The model with bovine tuberculosis only (obtained by setting $I_1 = 0, I_{12} = 0, W_2 = 0$ in (4.1.1)) is given by

$$
\begin{aligned}
\frac{dS}{dt} &= \Lambda - (\beta_{22}SI_1 + \alpha_2 SW_2) - \mu S, \\
\frac{dI_2}{dt} &= \beta_{22}SI_2 + \alpha_2 SW_2 - (\mu + \delta_{22} + \gamma)I_2, \\
\frac{dW_2}{dt} &= \xi_2 I_2 - (d_2 + \phi_2)W_2,
\end{aligned}
\tag{4.4.1}
$$

with $S(0) \geq 0, I_2(0) \geq 0, W_2(0) \geq 0$ as the initial conditions, and the total population is given by

$$N_T(t) = S(t) + I_2(t).$$

Therefore, it can be shown that the region,

$$\Omega_2 = \left\{ (S, I_2, W_2) \in \mathbb{R}^3_+ | S, I_2, W_2 \geq 0, 0 \leq S + I_2 \leq \frac{\Lambda}{\mu}, W_2 \leq \frac{\Lambda \xi_2}{\mu(d_2 + \phi_2)} \right\}, \tag{4.4.2}$$

is positively-invariant and attracting. Therefore, the dynamics of the bovine tuberculosis submodel will be considered in Ω_2.

4.4.1 The equilibrium point and stability analysis

The bovine tuberculosis submodel (4.4.1) has the disease-free equilibrium given by

$$E_T^0 = (S^0, I_2^0, W_2^0) = \left(\frac{\Lambda}{\mu}, 0, 0 \right). \tag{4.4.3}$$

Moreover, the F and V matrices are given, respectively, by

$$F = \begin{bmatrix} \beta_{22}\frac{\Lambda}{\mu} & \alpha_2 \frac{\Lambda}{\mu} \\ 0 & 0 \end{bmatrix} \quad \text{and} \quad V = \begin{bmatrix} \mu + \delta_{22} + \gamma & 0 \\ -\xi_2 & d_2 + \phi_2 \end{bmatrix}.$$

It follows that

$$R_T = \frac{\Lambda(\beta_{22}(d_2 + \phi_2) + \alpha_2 \xi_2)}{\mu(\mu + \delta_{22} + \gamma)(d_2 + \phi_2)}. \tag{4.4.4}$$

Similar results about existence and stability of brucellosis submodel can be obtain for bovine tuberculosis submodel, such that the endemic equilibrium point of bovine tuberculosis submodel $E_T^* = (S, I_2, W_2)$ upon the change of variables: $\beta_{11} \to \beta_{22}, \delta_{11} \to \delta_{22}, \xi_1 \to \xi_2, d_1 \to d_2, \phi_1 \to \phi_2$ and $R_B \to R_T$. Therefore, we have established the following result.

Theorem 4.4.1. *The disease-free equilibrium of the bovine tuberculosis submodel, E_T^0 is locally asymptotically stable if $R_T < 1$ and unstable if $R_T > 1$.*

Theorem 4.4.2. *The disease-free equilibrium point, E_T^0, is globally asymptotically stable provided that $R_T < 1$ and conditions (H1) and (H2) are satisfied.*

Theorem 4.4.3. *The endemic equilibrium E_T^* of the bovine tuberculosis submodel is locally asymptotically stable for $R_T > 1$, but close to unity.*

Theorem 4.4.4. *The endemic equilibrium E_T^* of the bovine tuberculosis system (4.4.1) is globally asymptotically stable if $R_T > 1$.*

4.5 Analysis of the Brucellosis-Bovine Tuberculosis model

In this section, we delve into the dynamics of two sub-models within the context of the complete model (4.1.1).

4.5.1 The disease-free equilibrium point and its stability

The disease-free equilibrium point is given by

$$\begin{aligned} E_{BT}^0 &= (S^0, I_1^0, I_2^0, I_{12}^0, W_1^0, W_2^0) \\ &= \left(\frac{\Lambda}{\mu}, 0, 0, 0, 0, 0\right). \end{aligned} \tag{4.5.1}$$

Using the next generation method in [49], we obtain F and V in the following:

$$F = \begin{bmatrix} \beta_{11}\frac{\Lambda}{\mu} & 0 & \beta_{01}\frac{\Lambda}{\mu} & \alpha_1\frac{\Lambda}{\mu} & 0 \\ 0 & \beta_{22}\frac{\Lambda}{\mu} & \beta_{02}\frac{\Lambda}{\mu} & 0 & \alpha_2\frac{\Lambda}{\mu} \\ 0 & 0 & 0 & 0 & 0 \\ 0 & 0 & 0 & 0 & 0 \end{bmatrix}, \quad \text{and}$$

$$V = \begin{bmatrix} \mu+\delta_{11}+\gamma & 0 & 0 & 0 & 0 \\ 0 & \mu+\delta_{22}+\gamma & 0 & 0 & 0 \\ 0 & 0 & \mu+\delta_{12}+\gamma & 0 & 0 \\ -\xi_1 & 0 & -\xi_1 & d_1+\phi_1 & 0 \\ 0 & -\xi_2 & -\xi_2 & 0 & d_2+\phi_2 \end{bmatrix}.$$

It follows that

$$V^{-1} = \begin{bmatrix} \frac{1}{\mu+\delta_{11}+\gamma} & 0 & 0 & 0 & 0 \\ 0 & \frac{1}{\mu+\delta_{22}+\gamma} & 0 & 0 & 0 \\ 0 & 0 & \frac{1}{\mu+\delta_{12}+\gamma} & 0 & 0 \\ \frac{\xi_1}{(mu+\delta_{11}+\gamma)(d_1+\phi_1)} & 0 & \frac{\xi_1}{(\mu+\delta_{12}+\gamma)(d_1+\phi_1)} & \frac{1}{d_1+\phi_1} & 0 \\ 0 & \frac{\xi_2}{(\mu+\delta_{22}+\gamma)(d_2+\phi_2)} & \frac{\xi_2}{(\mu+\delta_{12}+\gamma)(d_2+\phi_2)} & 0 & \frac{1}{d_2+\phi_2} \end{bmatrix}.$$

Therefore, we have

$$FV^{-1} = \begin{bmatrix} \frac{\Lambda(\beta_{11}(d_1+\phi_1)+\alpha_1\xi_1)}{\mu(\mu+\delta_{11}+\gamma)(d_1+\phi_1)} & 0 & \frac{\Lambda(\beta_{01}(d_1+\phi_1)+\alpha_1\xi_1)}{\mu(\mu+\delta_{12}+\gamma)(d_1+\phi_1)} & \frac{\Lambda\alpha_1}{\mu(d_1+\phi_1)} & 0 \\ 0 & \frac{\Lambda(\beta_{22}(d_2+\phi_2)+\alpha_2\xi_2)}{\mu(\mu+\delta_{22}+\gamma)(d_2+\phi_2)} & \frac{\Lambda(\beta_{02}(d_2+\phi_2)+\alpha_2\xi_2)}{\mu(\mu+\delta_{12}+\gamma)(d_2+\phi_2)} & 0 & \frac{\Lambda\alpha_2}{\mu(d_2+\phi_2)} \\ 0 & 0 & 0 & 0 & 0 \\ 0 & 0 & 0 & 0 & 0 \\ 0 & 0 & 0 & 0 & 0 \end{bmatrix}$$

Therefore, the basic reproduction number for the brucellosis-bovine tuberculosis model (4.1.1) (denoted by R_{BT}) is given by

$$\begin{aligned} R_{BT} &= \max\left\{\frac{\Lambda(\beta_{11}(d_1+\phi_1)+\alpha_1\xi_1)}{\mu(\mu+\delta_{11}+\gamma)(d_1+\phi_1)}, \frac{\Lambda(\beta_{22}(d_2+\phi_2)+\alpha_2\xi_2)}{\mu(\mu+\delta_{22}+\gamma)(d_2+\phi_2)}\right\} \\ &= \max\{R_B, R_T\}, \end{aligned}$$

where R_B and R_T are the basic reproduction numbers of brucellosis submodel and bovine tuberculosis submodel, respectively. So that the following results follows from Theorem 2.1.1.

Theorem 4.5.1. *The disease-free equilibrium, E^0_{BT} is locally asymptotically stable if $R_{BT} < 1$ and unstable if $R_{BT} > 1$.*

The local asymptotic stability of the disease-free equilibrium in the brucellosis-bovine tuberculosis model is demonstrated in Theorem 4.5.1 when $R_{BT} < 1$. To explore the global stability of this equilibrium, we employ the approach of Castillo-Chaves et al. [51] (See Lemma 2.1.4 in Chapter 2). The equation governing the co-infection model for brucellosis and bovine tuberculosis (4.1.1) is reformulated as follows:

$$\begin{aligned} \frac{dX_1}{dt} &= F(X_1, X_2) \\ \frac{dX_2}{dt} &= G(X_1, X_2), \qquad G(X_1, 0) = 0, \end{aligned}$$

where $X_1 = (S)$ and $X_2 = (I_1, I_2, I_{12}, W_1, W_2)^T$. The disease-free equilibrium is now denoted by $E^0_{BT} = (S^0, I^0_1, I^0_2, I^0_{12}, W^0_1, W^0_2)$ where $X^* = \left(\frac{\Lambda}{\mu}\right)$. We note that the system is linear and its solution can be easily found as

$$\frac{dX_1}{dt} = F(X_1, X_2)$$
$$= \Big[\Lambda - (\beta_{11}SI_1 + \beta_{01}SI_{12} + \alpha_1 SW_1) - (\beta_{22}SI_2 + \beta_{02}SI_{12} + \alpha_2 SW_2) - \mu S\Big].$$

So, we have

$$F(X_1, 0) = \Big[\Lambda - \mu S\Big].$$

As for S, we can deduce from the equation above that

$$\frac{dS}{dt} = \Lambda - \mu S$$
$$\frac{dS}{dt} + \mu S = \Lambda$$

We solve this equation using the integrating factor, which results in $S(t) \to \frac{\Lambda}{\mu}$ as $t \to \infty$. Therefore X^* is globally asymptotically stable.
Next, we consider

$$G(X_1, X_2) = \begin{bmatrix} (\beta_{11}SI_1 + \beta_{01}SI_{12} + \alpha_1 SW_1) - (\beta_{22}I_1I_2 + \beta_{02}I_1I_{12} + \alpha_2 I_1W_2) - (\mu + \delta_{11} + \gamma)I_1 \\ (\beta_{22}SI_2 + \beta_{02}SI_{12} + \alpha_2 SW_2) - (\beta_{11}I_2I_1 + \beta_{01}I_2I_{12} + \alpha_1 I_2W_1) - (\mu + \delta_{22} + \gamma)I_2 \\ (\beta_{22}I_1I_2 + \beta_{02}I_1I_{12} + \alpha_2 I_1W_2) + (\beta_{11}I_2I_1 + \beta_{01}I_2I_{12} + \alpha_1 I_2W_1) - (\mu + \delta_{12} + \gamma)I_{12} \\ (I_1 + I_{12})\xi_1 - (d_1 + \phi_1)W_1 \\ (I_2 + I_{12})\xi_2 - (d_2 + \phi_2)W_2 \end{bmatrix}.$$

Thus, we have

$$\frac{\partial G}{\partial X_2}(X_1, X_2) = \begin{bmatrix} g_{11} & -\beta_{22}I_1 & \beta_{01}S - \beta_{02}I_1 & \alpha_1 S & -\alpha_2 I_1 \\ \beta_{11}I_2 & g_{22} & \beta_{02}S - \beta_{01}I_2 & -\alpha_1 I_2 & \alpha_2 S \\ g_{31} & g_{32} & g_{33} & \alpha_1 E_2 & \alpha_2 I_1 \\ \xi_1 & 0 & \xi_1 & -(d_1 + \phi_1) & 0 \\ 0 & \xi_2 & \xi_2 & 0 & -(d_2 + \phi_2) \end{bmatrix},$$

where

$$g_{11} = \beta_{11}S - (\beta_{22}I_2 + \beta_{02}I_{12} + \alpha_2 W_2) - (\mu + \delta_{11} + \gamma),$$
$$g_{22} = \beta_{22}S - (\beta_{11}I_1 + \beta_{01}I_{12}\alpha_1 W_1) - (\mu + \delta_{22} + \gamma),$$
$$g_{31} = \beta_{22}I_2 + \beta_{02}I_{12} + \alpha_2 W_2 + \beta_{11}I_2,$$
$$g_{32} = \beta_{22}I_1 + \beta_{11}I_1 + \beta_{01}I_{12} + \alpha_1 W_1,$$
$$g_{33} = \beta_{02}I_1 + \beta_{01}I_2 - (\mu + \delta_{12} + \gamma).$$

Then, we get

$$A = \frac{\partial G}{\partial X_2}(X_1^*, 0)$$
$$= \begin{bmatrix} \frac{\beta_{11}\Lambda}{\mu} - (\mu + \delta_{11} + \gamma) & 0 & \frac{\beta_{01}\Lambda}{\mu} & \frac{\alpha_1\Lambda}{\mu} & 0 \\ 0 & \frac{\beta_{22}\Lambda}{\mu} - (\mu + \delta_{22} + \gamma) & \frac{\beta_{02}\Lambda}{\mu} & 0 & \frac{\alpha_2\Lambda}{\mu} \\ 0 & 0 & -(\mu + \delta_{12} + \gamma) & 0 & 0 \\ \xi_1 & 0 & \xi_1 & -(d_1 + \phi_1) & 0 \\ 0 & \xi_2 & \xi_2 & 0 & -(d_2 + \phi_2) \end{bmatrix}.$$

This matrix is an M-matrix, meaning it has non-negative in its off-diagonal elements. Furthermore, based on $(H2)$ we will show that $\widehat{G}(X_1, X_2)$ must be greater than or equal to zero. Thus, we consider

$$\widehat{G}(X_1, X_2) = AX_2 - G(X_1, X_2)$$
$$= \begin{bmatrix} \widehat{G}_1(X_1, X_2) \\ \widehat{G}_2(X_1, X_2) \\ \widehat{G}_3(X_1, X_2) \end{bmatrix}$$
$$= \begin{bmatrix} \beta_{11} I_1 \left(\frac{\Lambda}{\mu} - S\right) + \beta_{01} I_{12} \left(\frac{\Lambda}{\mu} - S\right) + \frac{\alpha_1}{\mu} W_1 \left(\frac{\Lambda}{\mu} - S\right) + (\beta_{22} I_1 I_2 + \beta_{02} I_1 I_{12} + \alpha_2 I_1 W_2) \\ \beta_{22} I_2 \left(\frac{\Lambda}{\mu} - S\right) + \beta_{02} I_{12} \left(\frac{\Lambda}{\mu} - S\right) + \frac{\alpha_2}{\mu} W_2 \left(\frac{\Lambda}{\mu} - S\right) + (\beta_{11} I_2 I_1 + \beta_{01} I_2 I_{12} + \alpha_1 I_2 W_1) \\ -(\beta_{22} I_1 I_2 + \beta_{02} I_1 I_{12} + \alpha_2 I_1 W_2) - (\beta_{11} I_2 I_1 + \beta_{01} I_2 I_{12} + \alpha_1 I_2 W_1) \end{bmatrix}.$$

Since $\widehat{G}_3(X_1, X_2) < 0$, which leads to $\widehat{G}(X_1, X_2) < 0$, that means the second condition (H2) is not satisfied. Consequently, the disease-free equilibrium E^0_{BT} may not be globally asymptotically stable in Ω for $R_{BT} < 1$, owing to the possibility of backward bifurcation. Hence, we shall only derive the bifurcation parameters for the full model. Let $S = x_1, I_1 = x_2, I_2 = x_3, I_{12} = x_4, W_1 = x_5$ and $W_2 = x_6$, so that $N = x_1 + x_2 + x_3 + x_4$. Further, by using notation $X = (x_1, x_2, x_3, x_4, x_5, x_6)^T$, the full brucellosis-bovine tuberculosis model can be written in the form $\frac{dX}{dt} = F(X)$, with $F = (f_1, f_2, f_3, f_4, f_5, f_6)^T$ as follow:

$$\begin{aligned}
\frac{dx_1}{dt} &= \Lambda - (\beta_{11} x_1 x_2 + \beta_{01} x_1 x_4 + \alpha_1 x_1 x_5) - (\beta_{22} x_1 x_3 + \beta_{02} x_1 x_4 + \alpha_2 x_1 x_6) - \mu x_1, \\
\frac{dx_2}{dt} &= (\beta_{11} x_1 x_2 + \beta_{01} x_1 x_4 + \alpha_1 x_1 x_5) - (\beta_{22} x_2 x_3 + \beta_{02} x_2 x_4 + \alpha_2 x_2 x_6) \\
&\quad - (\mu + \delta_{11} + \gamma) x_2, \\
\frac{dx_3}{dt} &= (\beta_{22} x_1 x_3 + \beta_{02} x_1 x_4 + \alpha_2 x_1 x_6) - (\beta_{11} x_3 x_2 + \beta_{01} x_3 x_4 + \alpha_1 x_3 x_5) \\
&\quad - (\mu + \delta_{22} + \gamma) x_3, \\
\frac{dx_4}{dt} &= (\beta_{22} x_2 x_3 + \beta_{02} x_2 x_4 + \alpha_2 x_2 x_6) + (\beta_{11} x_3 x_2 + \beta_{01} x_3 x_4 + \alpha_1 x_3 x_5) \\
&\quad - (\mu + \delta_{12} + \gamma) x_4, \\
\frac{dx_5}{dt} &= (x_2 + x_4)\xi_1 - (d_1 + \phi_1) x_5, \\
\frac{dx_6}{dt} &= (x_3 + x_4)\xi_2 - (d_2 + \phi_2) x_6.
\end{aligned} \tag{4.5.2}$$

The Jacobian of the above system at E^0_{BT} is given by,

$$J(E^0_{BT}) = \begin{bmatrix} -\mu & \frac{-\beta_{11}\Lambda}{\mu} & \frac{-\beta_{22}\Lambda}{\mu} & -(\beta_{01}+\beta_{02})\frac{\Lambda}{\mu} & \frac{-\alpha_1\Lambda}{\mu} & \frac{-\alpha_2\Lambda}{\mu} \\ 0 & \frac{\beta_{11}\Lambda}{\mu} - (\mu+\delta_{11}+\gamma) & 0 & \frac{\beta_{01}\Lambda}{\mu} & \frac{\alpha_1\Lambda}{\mu} & 0 \\ 0 & 0 & \frac{\beta_{22}\Lambda}{\mu} - (\mu+\delta_{22}+\gamma) & \frac{\beta_{02}\Lambda}{\mu} & 0 & \frac{\alpha_2\Lambda}{\mu} \\ 0 & 0 & 0 & -(\mu+\delta_{12}+\gamma) & 0 & 0 \\ 0 & \xi_1 & 0 & \xi_1 & -(d_1+\phi_1) & 0 \\ 0 & 0 & \xi_2 & \xi_2 & 0 & -(d_2+\phi_2) \end{bmatrix}, \tag{4.5.3}$$

Consider, the case when $R_{BT} = 1$ (that is, $R_B = 1$). Suppose, further, that $\beta_{11} = \beta^*_{11}$ is chosen as a bifurcation parameter. Solving for β_{11} from $R_B = 1$ gives,

$$\beta_{11} = \beta^*_{11} = \frac{\mu(\mu+\delta_{11}+\gamma)}{\Lambda} - \frac{\alpha_1\xi_1}{(d_1+\phi_1)}. \tag{4.5.4}$$

The eigenvalues of $J(E^0_{BT})$ are calculated using $\det(J(E^0_{BT}) - \lambda I) = 0$, then we obtain that

$$0 = (-\mu-\lambda)\begin{vmatrix} \frac{\beta_{11}\Lambda}{\mu} - (\mu+\delta_{11}+\gamma) - \lambda & 0 & \frac{\beta_{01}\Lambda}{\mu} & \frac{\alpha_1\Lambda}{\mu} & 0 \\ 0 & \frac{\beta_{22}\Lambda}{\mu} - (\mu+\delta_{22}+\gamma) - \lambda & \frac{\beta_{02}\Lambda}{\mu} & 0 & \frac{\alpha_2\Lambda}{\mu} \\ 0 & 0 & -(\mu+\delta_{12}+\gamma) - \lambda & 0 & 0 \\ \xi_1 & 0 & \xi_1 & -(d_1+\phi_1) - \lambda & 0 \\ 0 & \xi_2 & \xi_2 & 0 & -(d_2+\phi_2) - \lambda \end{vmatrix}.$$

Thus, we get $\lambda_1 = -\mu$. Next, we consider

$$\begin{aligned} 0 &= \begin{vmatrix} \frac{\beta_{11}\Lambda}{\mu} - (\mu+\delta_{11}+\gamma) - \lambda & 0 & \frac{\beta_{01}\Lambda}{\mu} & \frac{\alpha_1\Lambda}{\mu} & 0 \\ 0 & \frac{\beta_{22}\Lambda}{\mu} - (\mu+\delta_{22}+\gamma) - \lambda & \frac{\beta_{02}\Lambda}{\mu} & 0 & \frac{\alpha_2\Lambda}{\mu} \\ 0 & 0 & -(\mu+\delta_{12}+\gamma) - \lambda & 0 & 0 \\ \xi_1 & 0 & \xi_1 & -(d_1+\phi_1) - \lambda & 0 \\ 0 & \xi_2 & \xi_2 & 0 & -(d_2+\phi_2) - \lambda \end{vmatrix} \\ &= \left(\left(\frac{\beta_{11}\lambda}{\mu} - (\mu+\delta_{11}+\gamma) - \lambda\right)(-(d+\phi_1) - \lambda) - \frac{\xi_1\alpha_1\Lambda}{\mu}\right) \\ &\quad \times \begin{vmatrix} \frac{\beta_{22}\Lambda}{\mu} - (\mu+\delta_{22}+\gamma) - \lambda & \frac{\beta_{02}\Lambda}{\mu} & \frac{\alpha_2\Lambda}{\mu} \\ 0 & -(\mu+\delta_{12}+\gamma) - \lambda & 0 \\ \xi_2 & \xi_2 & -(d_2+\phi_2) - \lambda \end{vmatrix}. \end{aligned}$$

Since $\beta_{11} = \frac{\mu(\mu+\delta_{11}+\gamma)}{\Lambda} - \frac{\alpha_1\xi_1}{(d_1+\phi_1)}$, then we obtain that

$$\begin{aligned} 0 &= \left(\left(\frac{-\alpha_1\xi_1\Lambda}{\mu(d_1+\phi_1)} - \lambda\right)(-(d+\phi_1) - \lambda) - \frac{\xi_1\alpha_1\Lambda}{\mu}\right) \begin{vmatrix} \frac{\beta_{22}\Lambda}{\mu} - (\mu+\delta_{22}+\gamma) - \lambda & \frac{\beta_{02}\Lambda}{\mu} & \frac{\alpha_2\Lambda}{\mu} \\ 0 & -(\mu+\delta_{12}+\gamma) - \lambda & 0 \\ \xi_2 & \xi_2 & -(d_2+\phi_2) - \lambda \end{vmatrix} \\ &= \lambda\left(\frac{\alpha_1\xi_1\Lambda}{\mu(d_1+\phi_1)} + d_1 + \phi_1 + \lambda\right) \begin{vmatrix} \frac{\beta_{22}\Lambda}{\mu} - (\mu+\delta_{22}+\gamma) - \lambda & \frac{\beta_{02}\Lambda}{\mu} & \frac{\alpha_2\Lambda}{\mu} \\ 0 & -(\mu+\delta_{12}+\gamma) - \lambda & 0 \\ \xi_2 & \xi_2 & -(d_2+\phi_2) - \lambda \end{vmatrix}. \end{aligned}$$

Hence, we get $\lambda_2 = 0$ and $\lambda_3 = -\left(\frac{\alpha_1\xi_1\Lambda}{\mu(d_1+\phi_1)} + d_1 + \phi_1\right)$. Next, we will consider

$$0 = \begin{vmatrix} \frac{\beta_{22}\Lambda}{\mu} - (\mu+\delta_{22}+\gamma) - \lambda & \frac{\beta_{02}\Lambda}{\mu} & \frac{\alpha_2\Lambda}{\mu} \\ 0 & -(\mu+\delta_{12}+\gamma) - \lambda & 0 \\ \xi_2 & \xi_2 & -(d_2+\phi_2) - \lambda \end{vmatrix}$$

$$= (-(\mu+\delta_{12}+\gamma) - \lambda) \begin{vmatrix} \frac{\beta_{22}\Lambda}{\mu} - (\mu+\delta_{22}+\gamma) - \lambda & \frac{\alpha_2\Lambda}{\mu} \\ \xi_2 & -(d_2+\phi_2) - \lambda \end{vmatrix}.$$

Therefore, we obtain $\lambda_4 = -(\mu+\delta_{12}+\gamma)$. Next, we consider

$$0 = \begin{vmatrix} \frac{\beta_{22}\Lambda}{\mu} - (\mu+\delta_{22}+\gamma) - \lambda & \frac{\alpha_2\Lambda}{\mu} \\ \xi_2 & -(d_2+\phi_2) - \lambda \end{vmatrix}$$

$$= \lambda^2 + \left(\mu+\delta_{22}+\gamma+d_2+\phi_2 - \frac{\beta_{22}\Lambda}{\mu}\right)\lambda$$

$$+ \left[(\mu+\delta_{22}+\gamma)(d_2+\phi_2) - \frac{\Lambda}{\mu}(\xi_2\alpha_2 + \beta_{22}(d_2+\phi_2))\right].$$

Since $R_T < 1$, then we obtain that

$$\mu+\delta_{22}+\gamma+d_2+\phi_2 - \frac{\beta_{22}\Lambda}{\mu} > 0$$

$$(\mu+\delta_{22}+\gamma)(d_2+\phi_2) - \frac{\Lambda}{\mu}(\xi_2\alpha_2 + \beta_{22}(d_2+\phi_2)) > 0.$$

According to the Routh-Hurwitz Criterion, it follows that two eigenvalues of the characteristic equation have negative real parts.

It follows that the Jacobian matrix at the disease-free equilibrium with $\beta_{11} = \beta_{11}^*$ has a simple zero eigenvalues (with all other eigenvalues having negative real part). Therefore, the Centre Manifold theory can be used to analyze the dynamics of system (4.5.2). By applying the Center Manifold theory in Castillo-Chavez and Song [50], left and right eigenvectors of the Jacobian matrix $J(E_{BT}^0)$ are computed first. For case $R_{BT} = 1$, It can be shown that the Jacobian of (4.5.3) at $\beta_{11} = \beta_{11}^*$ has a right eigenvector (associated with the zero eigenvalue) given by $w = [w_1, w_2, w_3, w_4, w_5, w_6]^T$, such that

$$-\mu w_1 - \frac{\beta_{11}\Lambda}{\mu}w_2 - \frac{\beta_{22}\Lambda}{\mu}w_3 - (\beta_{01}+\beta_{02})\frac{\Lambda}{\mu}w_4 - \frac{\alpha_1\Lambda}{\mu}w_5 - \frac{\alpha_2\Lambda}{\mu}w_6 = 0 \qquad (4.5.5)$$

$$\left(\frac{\beta_{11}\Lambda}{\mu} - (\mu+\delta_{11}+\gamma)\right)w_2 + \frac{\beta_{01}\Lambda}{\mu}w_4 + \frac{\alpha_1\Lambda}{\mu}w_5 = 0 \qquad (4.5.6)$$

$$\left(\frac{\beta_{22}\Lambda}{\mu} - (\mu + \delta_{22} + \gamma)\right)w_3 + \frac{\beta_{02}\Lambda}{\mu}w_4 + \frac{\alpha_2\Lambda}{\mu}w_6 = 0 \quad (4.5.7)$$

$$-(\mu + \delta_{12} + \gamma)w_4 = 0 \quad (4.5.8)$$

$$\xi_1 w_2 + \xi_1 w_4 - (d_1 + \phi_1)w_5 = 0 \quad (4.5.9)$$

$$\xi_2 w_3 + \xi_2 w_4 - (d_2 + \phi_2)w_6 = 0. \quad (4.5.10)$$

Considering equation (4.5.8), we can observe that

$$w_4 = 0. \quad (4.5.11)$$

Substituting equation (4.5.11) into equation (4.5.9) and (4.5.10), we obtain that

$$w_5 = \frac{\xi_1 w_2}{d_1 + \phi_1}, \quad (4.5.12)$$

$$w_6 = \frac{\xi_2 w_3}{d_2 + \phi_2}. \quad (4.5.13)$$

Substituting equation (4.5.11) and (4.5.12) into equation (4.5.6), we obtain that

$$\left(\frac{\beta_{11}\Lambda}{\mu} - (\mu + \delta_{11} + \gamma)\right)w_2 + + \frac{\alpha_1\Lambda}{\mu}\left(\frac{\xi_1 w_2}{d_1 + \phi_1}\right) = 0.$$

Since $\beta_{11} = \frac{\mu(\mu+\delta_{11}+\gamma)}{\Lambda} - \frac{\alpha_1\xi_1}{d_1+\phi_1}$, then we can deduce that

$$(0)w_2 = 0.$$

As a consequence, w_2 can take any value. Therefore, we choose $w_2 > 0$. Next, substituting equation (4.5.11) and (4.5.13) into equation (4.5.7), we have

$$\left(\frac{\beta_{22}\Lambda}{\mu} - (\mu + \delta_{22} + \gamma)\right)w_3 + \frac{\alpha_2\Lambda}{\mu}\left(\frac{\xi_2 w_3}{d_2 + \phi_2}\right) = 0$$

$$\left(\frac{\beta_{22}(d_2 + \phi_2)\Lambda + \alpha_2\Lambda\xi_2 - \mu(\mu + \delta_{22} + \gamma)(d_2 + \phi_2)}{\mu(d_2 + \phi_2)}\right)w_3 = 0.$$

Assuming $\beta_{22}(d_2 + \phi_2)\Lambda + \alpha_2\Lambda\xi_2 = \mu(\mu + \delta_{22} + \gamma)(d_2 + \phi_2)$, we can derive

$$(0)w_3 = 0.$$

Consequently, w_3 can vary across a range of values. Therefore, we specifically select w_3 to be greater than 0.

Substituting equation $w_4 = 0$, (4.5.12) and (4.5.13) into equation (4.5.5) , we obtain that

$$-\mu w_1 - \frac{\beta_{11}\Lambda}{\mu}w_2 - \frac{\beta_{22}\Lambda}{\mu}w_3 - \frac{\alpha_1\Lambda}{\mu}\left(\frac{\xi_1 w_2}{d_1 + \phi_1}\right) - \frac{\alpha_2\Lambda}{\mu}\left(\frac{\xi_2 w_3}{d_2 + \phi_2}\right) = 0$$

$$-\mu w_1 - \frac{\Lambda}{\mu}\left(\beta_{11} + \frac{\alpha_1\xi_1}{d_1+\phi_1}\right)w_2 - \frac{\Lambda}{\mu}\left(\beta_{22} + \frac{\alpha_2\xi_2}{d_2+\phi_2}\right)w_3 = 0$$

Since $\beta_{11} = \frac{\mu(\mu+\delta_{11}+\gamma)}{\Lambda} - \frac{\alpha_1\xi_1}{d_1+\phi_1}$, then we get that

$$-\mu w_1 - (\mu + \delta_{11} + \gamma)w_2 - -\frac{\Lambda}{\mu}\left(\beta_{22} + \frac{\alpha_2\xi_2}{d_2+\phi_2}\right)w_3 = 0.$$

Therefore, we obtain that

$$w_1 = -\frac{1}{\mu}\left[(\mu + \delta_{11} + \gamma)w_2 + \frac{\Lambda}{\mu}\left(\beta_{22} + \frac{\alpha_2\xi_2}{(d_2+\phi_2)}\right)w_3\right]. \tag{4.5.14}$$

Furthermore, the Jacobian matrix has a left eigenvector (associated with the zero eigenvalue) represented by $v = [v_1, v_2, v_3, v_4, v_5, v_6]$, where

$$-\mu v_1 = 0 \tag{4.5.15}$$

$$-\frac{\beta_{11}\Lambda}{\mu}v_1 + \left(\frac{\beta_{11}\Lambda}{\mu} - (\mu + \delta_{11} + \gamma)\right)v_2 + \xi_1 v_5 = 0 \tag{4.5.16}$$

$$-\frac{\beta_{22}\Lambda}{\mu}v_1 + \left(\frac{\beta_{22}\Lambda}{\mu} - (\mu + \delta_{11} + \gamma)\right)v_3 + \xi_2 v_6 = 0 \tag{4.5.17}$$

$$-(\beta_{01}+\beta_{02})\frac{\Lambda}{\mu}v_1 + \frac{\beta_{01}\Lambda}{\mu}v_2 + \frac{\beta_{02}\Lambda}{\mu}v_3 - (\mu + \delta_{12} + \gamma)v_4 + \xi_1 v_5 + \xi_2 v_6 = 0 \tag{4.5.18}$$

$$-\frac{\alpha_1\Lambda}{\mu}v_1 + \frac{\alpha_1\Lambda}{\mu}v_2 - (d_1+\phi_1)v_5 = 0 \tag{4.5.19}$$

$$-\frac{\alpha_2\Lambda}{\mu}v_1 + \frac{\alpha_1\Lambda}{\mu}v_3 - (d_2+\phi_2)v_6 = 0 \tag{4.5.20}$$

Considering equation (4.5.15), we find that $v_1 = 0$.

When substituting the equation $v_1 = 0$ into equation (4.5.19) and (4.5.20), we obtain that

$$v_5 = \frac{\alpha_1\Lambda v_2}{\mu(d_1+\phi_1)}, \tag{4.5.21}$$

$$v_6 = \frac{\alpha_2\Lambda v_3}{\mu(d_2+\phi_2)}. \tag{4.5.22}$$

Next, substituting equation $v_1 = 0$ and (4.5.21) into equation (4.5.16), we have

$$\left(\frac{\beta_{11}\Lambda}{\mu} - (\mu + \delta_{11} + \gamma) + \frac{\xi_1\alpha_1\Lambda}{\mu(d_1+\phi_1)}\right)v_2 = 0$$

Since $\beta_{11} = \frac{\mu(\mu+\delta_{11}+\gamma)}{\Lambda} - \frac{\alpha_1\xi_1}{d_1+\phi_1}$, then we obtain that

$$(0)v_2 = 0.$$

As a result, v_2 can assume any value. Hence, we opt for v_3 to be greater than 0. Substituting equation $v_1 = 0$ and (4.5.22) into equation (4.5.17), we have

$$\left(\frac{\beta_{22}(d_2+\phi_2)\Lambda + \alpha_2\Lambda\xi_2 - \mu(\mu+\delta_{22}+\gamma)(d_2+\phi_2)}{\mu(d_2+\phi_2)}\right)v_3 = 0.$$

Since $\beta_{22}(d_2+\phi_2)\Lambda + \alpha_2\Lambda\xi_2 = \mu(\mu+\delta_{22}+\gamma)(d_2+\phi_2)$, then we can deduce that

$$(0)v_3 = 0.$$

Consequently, v_3 can take any value. Therefore, we choose $v_3 > 0$.

Substituting equation $v_1 = 0$, (4.5.21) and (4.5.22) into equation (4.5.18), we have

$$\frac{\beta_{01}\Lambda}{\mu}v_2 + \frac{\beta_{02}\Lambda}{\mu}v_3 - (\mu+\delta_{12}+\gamma)v_4 + \xi_1\left(\frac{\alpha_1\Lambda v_2}{\mu(d_1+\phi_1)}\right) + \xi_2\left(\frac{\alpha_2\Lambda v_3}{\mu(d_2+\phi_2)}\right) = 0.$$

Therefore, we get

$$v_4 = \frac{\Lambda}{\mu(\mu+\delta_{12}+\gamma)}\left[\left(\beta_{01} + \frac{\xi_1\alpha_1}{d_1+\phi_1}\right)v_2 + \left(\beta_{02} + \frac{\xi_2\alpha_2}{d_2+\phi_2}\right)v_3\right]. \qquad (4.5.23)$$

Computation of a and b:

Algebraic calculations show that

$$\frac{\partial^2 f_1}{\partial x_1\partial x_2} = \frac{\partial^2 f_1}{\partial x_2\partial x_1} = -\beta_{11}, \quad \frac{\partial^2 f_1}{\partial x_1\partial x_3} = \frac{\partial^2 f_1}{\partial x_3\partial x_1} = -\beta_{22}, \quad \frac{\partial^2 f_1}{\partial x_1\partial x_4} = \frac{\partial^2 f_1}{\partial x_4\partial x_1} = -\beta_{01}-\beta_{02},$$
$$\frac{\partial^2 f_1}{\partial x_1\partial x_5} = \frac{\partial^2 f_1}{\partial x_5\partial x_1} = -\alpha_1, \quad \frac{\partial^2 f_1}{\partial x_1\partial x_6} = \frac{\partial^2 f_1}{\partial x_6\partial x_1} = -\alpha_2, \quad \frac{\partial^2 f_2}{\partial x_1\partial x_2} = \frac{\partial^2 f_2}{\partial x_2\partial x_1} = \beta_{11},$$
$$\frac{\partial^2 f_2}{\partial x_1\partial x_4} = \frac{\partial^2 f_2}{\partial x_4\partial x_1} = \beta_{01}, \quad \frac{\partial^2 f_2}{\partial x_1\partial x_5} = \frac{\partial^2 f_2}{\partial x_5\partial x_1} = \alpha_1, \quad \frac{\partial^2 f_2}{\partial x_2\partial x_3} = \frac{\partial^2 f_2}{\partial x_3\partial x_2} = -\beta_{22},$$
$$\frac{\partial^2 f_2}{\partial x_2\partial x_4} = \frac{\partial^2 f_2}{\partial x_4\partial x_2} = -\beta_{02}, \quad \frac{\partial^2 f_2}{\partial x_2\partial x_6} = \frac{\partial^2 f_2}{\partial x_6\partial x_2} = -\alpha_2, \quad \frac{\partial^2 f_3}{\partial x_1\partial x_3} = \frac{\partial^2 f_3}{\partial x_3\partial x_1} = \beta_{22},$$
$$\frac{\partial^2 f_3}{\partial x_1\partial x_4} = \frac{\partial^2 f_3}{\partial x_4\partial x_1} = \beta_{02}, \quad \frac{\partial^2 f_3}{\partial x_1\partial x_6} = \frac{\partial^2 f_3}{\partial x_6\partial x_1} = \alpha_2, \quad \frac{\partial^2 f_3}{\partial x_2\partial x_3} = \frac{\partial^2 f_3}{\partial x_3\partial x_2} = -\beta_{11},$$
$$\frac{\partial^2 f_3}{\partial x_3\partial x_4} = \frac{\partial^2 f_3}{\partial x_4\partial x_3} = -\beta_{01}, \quad \frac{\partial^2 f_3}{\partial x_3\partial x_5} = \frac{\partial^2 f_3}{\partial x_5\partial x_3} = -\alpha_1, \quad \frac{\partial^2 f_4}{\partial x_2\partial x_3} = \frac{\partial^2 f_4}{\partial x_3\partial x_2} = \beta_{22}+\beta_{11},$$
$$\frac{\partial^2 f_4}{\partial x_2\partial x_4} = \frac{\partial^2 f_4}{\partial x_4\partial x_2} = \beta_{02}, \quad \frac{\partial^2 f_4}{\partial x_2\partial x_6} = \frac{\partial^2 f_4}{\partial x_6\partial x_2} = \alpha_2, \quad \frac{\partial^2 f_4}{\partial x_3\partial x_4} = \frac{\partial^2 f_4}{\partial x_4\partial x_3} = \beta_{01},$$
$$\frac{\partial^2 f_4}{\partial x_3\partial x_5} = \frac{\partial^2 f_4}{\partial x_5\partial x_3} = \alpha_1, \quad \frac{\partial^2 f_1}{\partial x_1\partial \beta_{11}} = -\frac{\Lambda}{\mu}, \quad \frac{\partial^2 f_2}{\partial x_2\partial \beta_{11}} = \frac{\Lambda}{\mu}.$$

It follows from the above expression that

$$a = \sum_{k,i,j=1}^{n} v_k w_i w_j \frac{\partial^2 f_k}{\partial x_i\partial x_j}(0,0)$$
$$= 2v_1w_1w_2(-\beta_{11}) + 2v_1w_1w_4(-\beta_{01}-\beta_{02}) + 2v_1w_1w_5(-\alpha_1) + 2v_1w_1w_3(-\beta_{22})$$

$$
\begin{aligned}
&+ 2v_1w_1w_6(-\alpha_2) + 2v_2w_1w_2(\beta_{11}) + 2v_2w_1w_4(\beta_{01}) + 2v_2w_1w_5(\alpha_1) \\
&+ 2v_2w_2w_3(-\beta_{22}) + 2v_2w_2w_4(-\beta_{02}) + 2v_2w_2w_6(-\alpha_2) + 2v_3w_1w_3(\beta_{22}) \\
&+ 2v_3w_1w_4(\beta_{02}) + 2v_3w_1w_6(\alpha_2) + 2v_3w_2w_3(-\beta_{11}) + 2v_3w_3w_4(-\beta_{01}) \\
&+ 2v_3w_3w_5(-\alpha_1) + 2v_4w_2w_3(\beta_{22}+\beta_{11}) + 2v_4w_2w_4(\beta_{02}) + 2v_4w_2w_6(\alpha_2) \\
&+ 2v_4w_3w_4(\beta_{01}) + 2v_4w_3w_5(\alpha_1) \\
= {} & 2\beta_{11}v_2w_1w_2 + 2\alpha_1v_2w_1w_5 - 2\beta_{22}v_2w_2w_3 - 2\alpha_2v_2w_2w_6 \\
&+ 2\beta_{22}v_3w_1w_3 + 2\alpha_2v_3w_1w_6 - 2\beta_{11}v_3w_3w_2 - 2\alpha_1v_3w_3w_5 \\
&+ 2(\beta_{22}+\beta_{11})v_4w_2w_3 + 2\alpha_2v_4w_2w_6 + 2\alpha_1v_4w_3w_5,
\end{aligned}
$$

and

$$
b = \sum_{k,i=1}^{n} v_k w_i \frac{\partial^2 f_k}{\partial x_i \partial \phi}(0,0) = v_1w_2\left(-\frac{\Lambda}{\mu}\right) + v_2w_2\left(\frac{\Lambda}{\mu}\right) = v_2\dot{w}_2\left(\frac{\Lambda}{\mu}\right) > 0.
$$

Therefore, it follows from Theorem 2.1.2 that the full brucellosis-bovine tuberculosis model 4.1.1 undergoes backward bifurcation at $R_{BT} = 1$ whenever

$$
a > 0. \tag{4.5.24}
$$

This result is summarized below.

Theorem 4.5.2. *The full brucellosis-bovine tuberculosis model* (4.1.1) *undergoes backward bifurcation at* $R_{BT} = 1$ *whenever inequality* (4.5.24) *is satisfied.*

Figure 26 depicts the simulation of model (4.1.1), highlighting the presence of the backward bifurcation phenomenon. This phenomenon typically arises when a stable disease-free equilibrium coexists with a stable endemic equilibrium, occurring when the associated basic reproduction number is below unity. This signifies that eradication of the disease might not be feasible despite having a basic reproduction number lower than unity. Additionally, Figure 26 validates the analytical findings by confirming the emergence of the endemic equilibrium when the basic reproduction number exceeds 1.

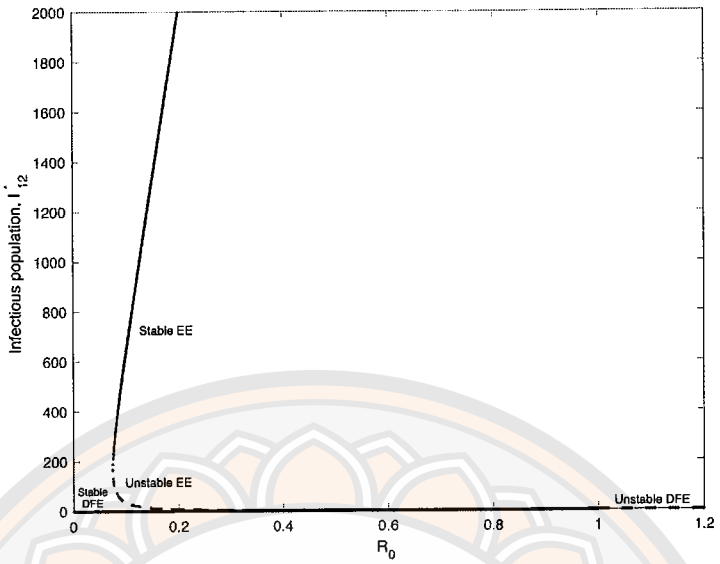

Figure 26 Illustration of the co-infection model's simulation, revealing the presence of a backward bifurcation. Employing the following parameters: $\Lambda = 16.6667, \alpha_1 = 1 \times 10^{-5}, \alpha_2 = 1 \times 10^{-5}, \beta_{01} = 3 \times 10^{-4}, \beta_{02} = 9 \times 10^{-4}, d_1 = 5 \times 10^{-5}, d_2 = 5 \times 10^{-5}, \delta_{11} = 0.0125, \delta_{12} = 0.0292, \delta_{22} = 0.0167, \gamma = 0.0333, \mu = 0.0058, \phi_1 = 0.0833, \phi_2 = 0.0833, \xi_1 = 0.1200$ and $\xi_2 = 0.1$.

Furthermore, the disease-free equilibrium of the brucellosis submodel is globally asymptotically stable when $R_B < 1$, and the endemic equilibrium attains global asymptotic stability for R_B exceeding unity. Similarly, the bovine tuberculosis submodel features a globally asymptotically stable disease-free equilibrium when $R_T < 1$. Additionally, the endemic equilibrium for bovine tuberculosis alone achieves global asymptotic stability when $R_T > 1$. Given that $R_{BT} = \max\{R_B, R_T\}$, in scenarios where both $R_B > 1$ and $R_T > 1$ (i.e., $R_{BT} > 1$), a coexistence of both diseases inevitably emerges, regardless of which of the basic reproduction numbers is higher.

4.6 Sensitivity Analysis

Within this section, we conduct a sensitivity analysis to discern the relative impact of each parameter on disease transmission. The sensitivity index of the basic

reproduction number (R_0) is determined using the normalized forward sensitivity index (refer to Section 2.1.8). The parameter values provided in Table 3 will be employed for calculating the sensitivity indices as well as for conducting the model simulations. The sensitivity analysis for each parameter influencing R_B has been computed and is presented in Table 4. Moreover, Table 5 displays the sensitivity indices of R_T with respect to each parameter.

Table 3 Parameter values of the Brucellosis-Bovine Tuberculosis model

Symbol	Value	Unit	Reference
Λ	16.6667	animals	[42]
μ	0.0058	month^{-1}	[17]
δ_{11}	0.0125	month^{-1}	[48]
δ_{22}	0.0167	month^{-1}	[48]
δ_{12}	0.0292	month^{-1}	[48]
γ	0.0333	month^{-1}	[17]
ξ_1	0.8333	month^{-1}	[14]
ξ_2	0.5833	month^{-1}	Assumed
d_1	0.00005	month^{-1}	Assumed
d_2	0.00005	month^{-1}	Assumed
ϕ_1	8.3333×10^{-5}	month^{-1}	Assumed
ϕ_2	8.3333×10^{-5}	month^{-1}	Assumed
β_{11}	9.1667×10^{-5}	month^{-1}	[14]
β_{01}	9.1667×10^{-5}	month^{-1}	Assumed
β_{22}	1.0995×10^{-5}	month^{-1}	[38]
β_{02}	1.0995×10^{-5}	month^{-1}	Assumed
α_1	2.9167×10^{-5}	month^{-1}	[14]
α_2	2.9167×10^{-5}	month^{-1}	Assumed

Table 4 Numerical values of sensitivity indices of R_B.

Parameter	Sensitivity index	Parameter	Sensitivity index
Λ	$+1$	μ	-1.0066
δ_{11}	-0.0141	γ	-0.0377
ξ_1	$+0.0579$	d_1	-0.3748
ϕ_1	-0.6247	β_{11}	$+5.0260 \times 10^{-4}$
α_1	$+0.9995$		

Table 5 Numerical values of sensitivity indices of R_T.

Parameter	Sensitivity index	Parameter	Sensitivity index
Λ	$+1$	μ	-1.0091
δ_{22}	-0.0141	γ	-0.0522
ξ_2	$+0.0873$	d_2	-0.3750
ϕ_2	-0.6249	β_{22}	$+8.6157 \times 10^{-5}$
α_2	$+0.9999$		

As depicted in Table 4, parameters such as Λ, ξ_1, α_1, and β_{11} exhibit a positive sensitivity index. Conversely, parameters including δ_{11}, ϕ_1, μ, γ, and d_1 possess a negative sensitivity index. Positive sensitivity indices associated with parameters indicate that an increase in these parameters leads to a higher value of the basic reproduction number. Thus, investigating these parameters could aid in mitigating the basic reproduction number.

Conversely, parameters with negative sensitivity indices demonstrate that raising their values results in a decrease in the basic reproduction number. The most negatively sensitive parameter is the natural mortality rate, μ. Another significant parameter with a negative sensitivity index is the elimination rate of *Brucella* in the environment, ϕ_1. Notably, $\Upsilon_{\phi_1}^{R_B} = -0.6247$, indicating that a 10% increase (or decrease) in the parameter ϕ_1 results in a 6.247% reduction (or increase) in the value of R_B.

Similarly, Table 5 reveals the most negatively sensitive parameter as the natural mortality rate, μ. Another noteworthy parameter exhibiting a negative sensitivity index is the elimination rate of *Mycobacterium bovis* in the environment, ϕ_2. Given that $\Upsilon_{\phi_2}^{R_T} = -0.6249$, a 10% increase (or decrease) in ϕ_2 results in a reduction (or increase) of the basic reproduction number R_T by 6.249.

It is evident that the most negatively sensitive parameter for the brucellosis and bovine tuberculosis model is μ. However, since μ is contingent on other uncontrollable factors, our focus will shift to investigating the control parameters instead. This signifies that control strategies will primarily concentrate on adjusting the elimination rates of *Brucella* and *Mycobacterium bovis* in the environment. Additionally, in the study conducted by Lolika et al. [48], an optimal control analysis was performed to assess how culling infectious animals would impact the prevalence of the two infections. Consequently, optimal control measures could effectively reduce the population of infected animals. Therefore, we also intend to formulate an optimal control problem encompassing culling strategies to explore the dynamics of the diseases.

4.7 Optimal control

In this section, we focus on determining the optimal implementation of control strategies involving the culling of infected animals ($u_1(t)$) and the reduction of *Brucella* ($u_2(t)$) and *Mycobacterium bovis* ($u_3(t)$) in the environment. These strategies aim to minimize the transmission of the aforementioned diseases. A successful control strategy simultaneously reduces the population of infectious animals while minimizing the associated control costs. To adapt model (4.1.1), we incorporate the time-dependent control variables $\gamma = u_1(t)$, $\phi_1 = u_2(t)$, and $\phi_2 = u_3(t)$. This leads to the formulation of the time-dependent brucellosis-bovine tuberculosis model (4.1.1) with control variables:

$$
\begin{aligned}
\frac{dS}{dt} &= \Lambda - (\beta_{11}SI_1 + \beta_{01}SI_{12} + \alpha_1 SW_1) - (\beta_{22}SI_2 + \beta_{02}SI_{12} + \alpha_2 SW_2) - \mu S, \\
\frac{dI_1}{dt} &= (\beta_{11}SI_1 + \beta_{01}SI_{12} + \alpha_1 SW_1) - (\beta_{22}I_1I_2 + \beta_{02}I_1I_{12} + \alpha_2 I_1W_2) \\
&\quad - (\mu + \delta_{11} + u_1(t))I_1, \\
\frac{dI_2}{dt} &= (\beta_{22}SI_2 + \beta_{02}SI_{12} + \alpha_2 SW_2) - (\beta_{11}I_2I_1 + \beta_{01}I_2I_{12} + \alpha_1 I_2W_1) \\
&\quad - (\mu + \delta_{22} + u_1(t))I_2, \\
\frac{dI_{12}}{dt} &= (\beta_{22}I_1I_2 + \beta_{02}I_1I_{12} + \alpha_2 I_1W_2) + (\beta_{11}I_2I_1 + \beta_{01}I_2I_{12} + \alpha_1 I_2W_1) \\
&\quad - (\mu + \delta_{12} + u_1(t))I_{12}, \\
\frac{dW_1}{dt} &= (I_1 + I_{12})\xi_1 - (d_1 + u_2(t))W_1, \\
\frac{dW_2}{dt} &= (I_2 + I_{12})\xi_2 - (d_2 + u_3(t))W_2.
\end{aligned}
\tag{4.7.1}
$$

We examine the system over a time interval of $[0, T]$. The functions $u_1(t)$, $u_2(t)$, and $u_3(t)$ are assumed to possess at least Lebesgue measurability on the interval $[0, T]$. Our aim is to minimize both the total count of infectious animals and the associated control expenses throughout the time span of $[0, T]$. To achieve this goal, we consider the following objective function:

$$
\begin{aligned}
J(u_1^*, u_2^*, u_3^*) = \min \int_0^T \Big[& I_1 + I_2 + I_{12} + c_1u_1(t)I_1 + c_2u_1(t)I_2 + c_3u_1(t)I_{12} \\
& + c_4u_2(t)W_1 + c_5u_3(t)W_2 + \frac{1}{2}\left(c_6u_1^2(t) + c_7u_2^2(t) + c_8u_3^2(t)\right) \Big] dt,
\end{aligned}
\tag{4.7.2}
$$

where c_i $(i = 1, 2, 3, 4, 5)$ denotes the respective positive balancing constants, while the terms $c_6u_1^2(t)$, $c_7u_2^2(t)$, and $c_8u_3^2(t)$ represent the costs associated with culling infected animals, eliminating *Brucella* in the environment, and eliminating *Mycobacterium bovis*, respectively. Furthermore, the values of $c_i (i = 1, 2, 3, \ldots, 8)$ are greater than or equal to zero. The control set is defined as:

$$
\begin{aligned}
\Gamma = \{u_1(t), u_2(t), u_3(t) | & 0 \le u_1(t) \le u_{1max}, \\
& 0 \le u_2(t) \le u_{2max}, \\
& 0 \le u_3(t) \le u_{3max}\},
\end{aligned}
\tag{4.7.3}
$$

where u_{1max}, u_{2max}, and u_{3max} represent the upper limits for the efforts exerted in culling infected animals, eliminating *Brucella*, and eliminating *Mycobacterium bovis*, respectively. The Hamiltonian (H) corresponding to the objective J is deduced using Pontryagin's Minimum Principle, similar to the methodology outlined

in section 2.1.9. It can be expressed as follows:

$$
\begin{aligned}
H &= I_1 + I_2 + I_{12} + +c_1u_1(t)I_1 + c_2u_1(t)I_2 + c_3u_1(t)I_{12} \\
&\quad + c_4u_2(t)W_1 + c_5u_3(t)W_2 + \frac{1}{2}\left(c_6u_1^2(t) + c_7u_2^2(t) + c_8u_3^2(t)\right) \\
&\quad + \lambda_S\Big[\Lambda - (\beta_{11}SI_1 + \beta_{01}SI_{12} + \alpha_1SW_1) - (\beta_{22}SI_2 + \beta_{02}SI_{12} + \alpha_2SW_2) - \mu S\Big] \\
&\quad + \lambda_{I_1}\Big[(\beta_{11}SI_1 + \beta_{01}SI_{12} + \alpha_1SW_1) - (\beta_{22}I_1I_2 + \beta_{02}I_1I_{12} + \alpha_2I_1W_2) \\
&\qquad\quad - (\mu + \delta_{11} + u_1(t))I_1\Big] \\
&\quad + \lambda_{I_2}\Big[(\beta_{22}SI_2 + \beta_{02}SI_{12} + \alpha_2SW_2) - (\beta_{11}I_2I_1 + \beta_{01}I_2I_{12} + \alpha_1I_2W_1) \\
&\qquad\quad - (\mu + \delta_{22} + u_1(t))I_2\Big] \\
&\quad + \lambda_{I_{12}}\Big[(\beta_{22}I_1I_2 + \beta_{02}I_1I_{12} + \alpha_2I_1W_2) + (\beta_{11}I_2I_1 + \beta_{01}I_2I_{12} + \alpha_1I_2W_1) \\
&\qquad\quad - (\mu + \delta_{12} + u_1(t))I_{12}\Big] \\
&\quad + \lambda_{W_1}\Big[(I_1 + I_{12})\xi_1 - (d_1 + u_2(t))W_1\Big] + \lambda_{W_2}\Big[(I_2 + I_{12})\xi_2 - (d_2 + u_3(t))W_2\Big].
\end{aligned}
$$

Given an optimal control $u_1^*(t), u_2^*(t)$, and $u_3^*(t)$, there exist adjoint functions, $\lambda_S, \lambda_{I_1}, \lambda_{I_2}, \lambda_{I_{12}}, \lambda_{W_1}$, and λ_{W_2}, corresponding to the state S, I_1, I_2, I_{12}, W_1 and W_2, respectively satisfying

$$
\begin{aligned}
\frac{d\lambda_S}{dt} &= -\frac{\partial H}{\partial S} \\
&= -\Big[\lambda_S(-\beta_{11}I_1 - \beta_{01}I_{12} - \alpha_1W_1 - \beta_{22}I_2 - \beta_{02}I_{12} - \alpha_2W_2 - \mu) \\
&\qquad + \lambda_{I_1}(\beta_{11}I_1 + \beta_{01}I_{12} + \alpha_1W_1) + \lambda_{I_2}(\beta_{22}I_2 + \beta_{02}I_{12} + \alpha_2W_2)\Big] \qquad (4.7.4)
\end{aligned}
$$

$$
\begin{aligned}
\frac{d\lambda_{I_1}}{dt} &= -\frac{\partial H}{\partial I_1} \\
&= -\Big[1 + c_1u_1(t) + \lambda_S(-\beta_{11}S) + +\lambda_{I_1}(\beta_{11}S - \beta_{22}I_2 - \beta_{02}I_{12} - \alpha_2W_2 \\
&\qquad - \mu - \delta_{11} - u_1(t)) + \lambda_{I_2}(-\beta_{11}I_2) + \lambda_{I_{12}}(\beta_{22}I_2 + \beta_{02}I_{12} + \alpha_2W_2 + \beta_{11}I_2) \\
&\qquad + \lambda_{W_1}\xi_1\Big] \qquad (4.7.5)
\end{aligned}
$$

$$
\begin{aligned}
\frac{d\lambda_{I_2}}{dt} &= -\frac{\partial H}{\partial I_2} \\
&= -\Big[1 + c_2u_1(t) + \lambda_S(-\beta_{22}S) + +\lambda_{I_1}(-\beta_{22}I_1) + \lambda_{I_2}(\beta_{22}S - \beta_{11}I_1 - \beta_{01}I_{12} \\
&\qquad - \alpha_1W_1 - \mu - \delta_{22} - u_1(t)) + \lambda_{I_{12}}(\beta_{22}I_1 + \beta_{11}I_1 + \beta_{01}I_{12} + \alpha_1W_1) \\
&\qquad + \lambda_{W_2}\xi_2\Big] \qquad (4.7.6)
\end{aligned}
$$

$$
\frac{d\lambda_{I_{12}}}{dt} = -\frac{\partial H}{\partial I_{12}}
$$

$$= -\Big[1 + c_3u_1(t) + \lambda_S(-\beta_{01}S - \beta_{02}S) + \lambda_{I_1}(\beta_{01}S - \beta_{02}I_1) + \lambda_{I_2}(\beta_{02}S - \beta_{01}I_2) + \lambda_{I_{12}}(\beta_{02}I_1 + \beta_{01}I_2 - \mu - \delta_{12} - u_2(t)) + \lambda_{W_1}\xi_1 + \lambda_{W_2}\xi_2\Big] \tag{4.7.7}$$

$$\frac{d\lambda_{W_1}}{dt} = -\frac{\partial H}{\partial W_1} = -\Big[c_4u_2(t) + \lambda_S(-\alpha_1 S) + \lambda_{I_1}(\alpha_1 S) + \lambda_{I_2}(-\alpha_1 I_2) + \lambda_{I_{12}}(\alpha_1 I_2) + \lambda_{W_1}(-d - u_2(t))\Big] \tag{4.7.8}$$

$$\frac{d\lambda_{W_2}}{dt} = -\frac{\partial H}{\partial W_2} = -\Big[c_5u_3(t) + \lambda_S(-\alpha_2 S) + \lambda_{I_1}(-\alpha_2 I_1) + \lambda_{I_2}(\alpha_2 S) + \lambda_{I_{12}}(\alpha_2 I_1) + \lambda_{W_1}(-d - u_3(t))\Big], \tag{4.7.9}$$

The transversality conditions are

$$\lambda_S(T) = 0,\ \lambda_{I_1}(T) = 0,\ \lambda_{I_2} = 0,\ \lambda_{I_{12}}(T) = 0,\ \lambda_{W_1}(T) = 0,\ \lambda_{W_2}(T) = 0.$$

The characterizations of the optimal controls $u_1(t), u_2(t)$, and $u_3(t)$ are then based on the conditions

$$\frac{\partial H}{\partial u_1} = 0,\ \frac{\partial H}{\partial u_2} = 0,\ \text{and}\ \frac{\partial H}{\partial u_3} = 0,$$

subject to the constraints $0 \le u_1(t) \le u_{1max}$, $0 \le u_2(t) \le u_{2max}$, and $0 \le u_3(t) \le u_{3max}$. Furthermore, the optimal controls are characterized by the optimality conditions:

$$u_1^*(t) = \max\{0, \min\{u_1(t), u_{1max}\}\},$$
$$u_2^*(t) = \max\{0, \min\{u_2(t), u_{2max}\}\},$$
$$u_3^*(t) = \max\{0, \min\{u_3(t), u_{3max}\}\},$$

where

$$u_1(t) = \frac{\lambda_{I_1}I_1 + \lambda_{I_2}I_2 + \lambda_{I_{12}}I_{12} - c_1I_1 - c_2I_2 - c_3I_{12}}{c_6}, \tag{4.7.10}$$

$$u_2(t) = \frac{\lambda_{W_1}W_1 - c_4W_1}{c_7}, \tag{4.7.11}$$

$$u_3(t) = \frac{\lambda_{W_2}W_2 - c_5W_2}{c_8}. \tag{4.7.12}$$

4.8 Numerical simulations

To visually elucidate certain analytical findings presented in this paper, numerical simulations of the co-infection model have been executed. The model is

subjected to optimal control theory to ascertain optimal strategies for culling infected animals, eliminating *Brucella*, and reducing *Mycobacterium bovis* levels in the environment. The parameter values used for these simulations are provided in Table 3. Initial conditions $(S(0), I_1(0), I_2(0), I_{12}(0), W_1(0), W_2(0))$ are set as $(650, 150, 100, 50, 10000, 10000)$, with weighting constants $c_1 = 1$, $c_2 = 1$, $c_3 = 1$, $c_4 = 0.0001$, $c_5 = 0.0001$, $c_6 = 0.01$, $c_7 = 0.01$, and $c_8 = 0.01$. The corresponding basic reproduction number for this parameter set is approximately 588.81. We shall investigate four control strategies, detailed as follows:

Strategy A: $u_1(t) \neq 0, u_2(t) \neq 0$ and $u_3(t) \neq 0$.

Strategy B: $u_1(t) \neq 0, u_2(t) \neq 0$ and $u_3(t) = 0$.

Strategy C: $u_1(t) \neq 0, u_2(t) = 0$ and $u_3(t) \neq 0$.

Strategy D: $u_1(t) = 0, u_2(t) \neq 0$ and $u_3(t) \neq 0$.

4.8.1 Strategy A: Using all the control variables

This strategy employs controls u_1, u_2, and u_3 to optimize the objective function. It is evident from Fig. 27 (a) that, through control, the count of brucellosis-infected animals (I_1) decreases and approaches zero around the eighth month. In contrast, without control, the infection curve remains persistently nonzero. Similarly, the outcomes depicted in Fig. 27 (b) and (c) reveal reductions in the numbers of bovine tuberculosis cases (I_2) and co-infection animals (I_{12}) when compared to the scenario without control. In Fig. 27 (c), it is evident that in the absence of control, the number of co-infection cases reaches a peak of approximately 55 cases around the fifth month before declining. Conversely, with controls, the curve initiates at 50 cases and diminishes to zero a few months following the onset of the disease outbreak. Additionally, Figs. 27 (d) and (e) display the concentrations of *Brucella* (W_1) and *Mycobacterium bovis* (W_2) in the environment.

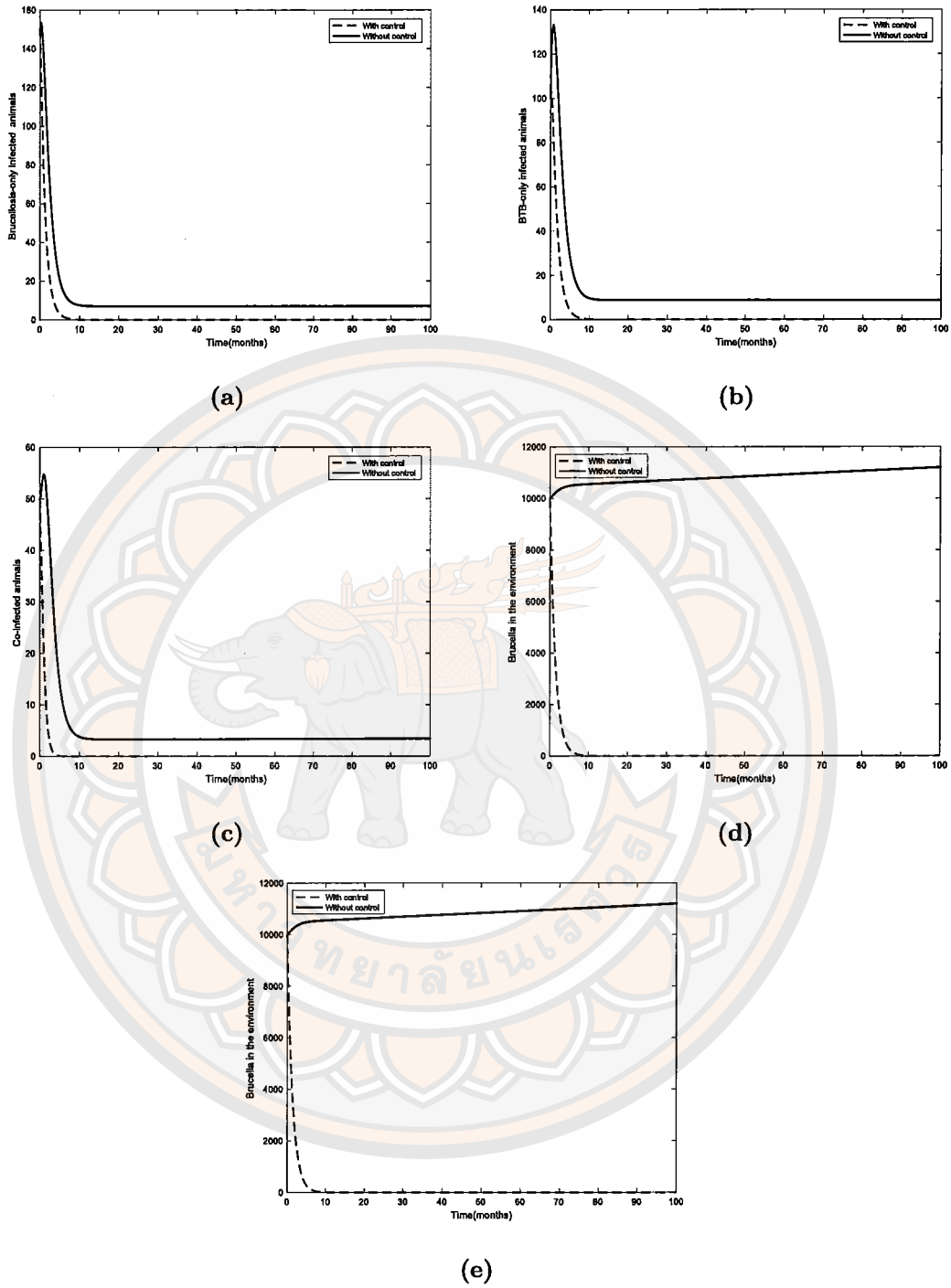

Figure 27 The numerical simulations depict the optimal control model with the utilization of controls u_1, u_2, and u_3. The panels illustrate: (a) Brucellosis-infected animals, (b) Bovine tuberculosis animals (BTB), (c) Co-infection cases, (d) Concentration of *Brucella* in the environment, and (e) Concentration of *Mycobacterium bovis* in the environment.

Figure 28 (a)-(c) illustrates that the implementation of comprehensive controls, including culling and environmental decontamination, should be initiated for around 70% of the infected animals or regions over a span of 5 months. Subsequently, the control rates should be gradually scaled down, reaching zero by the 25th month.

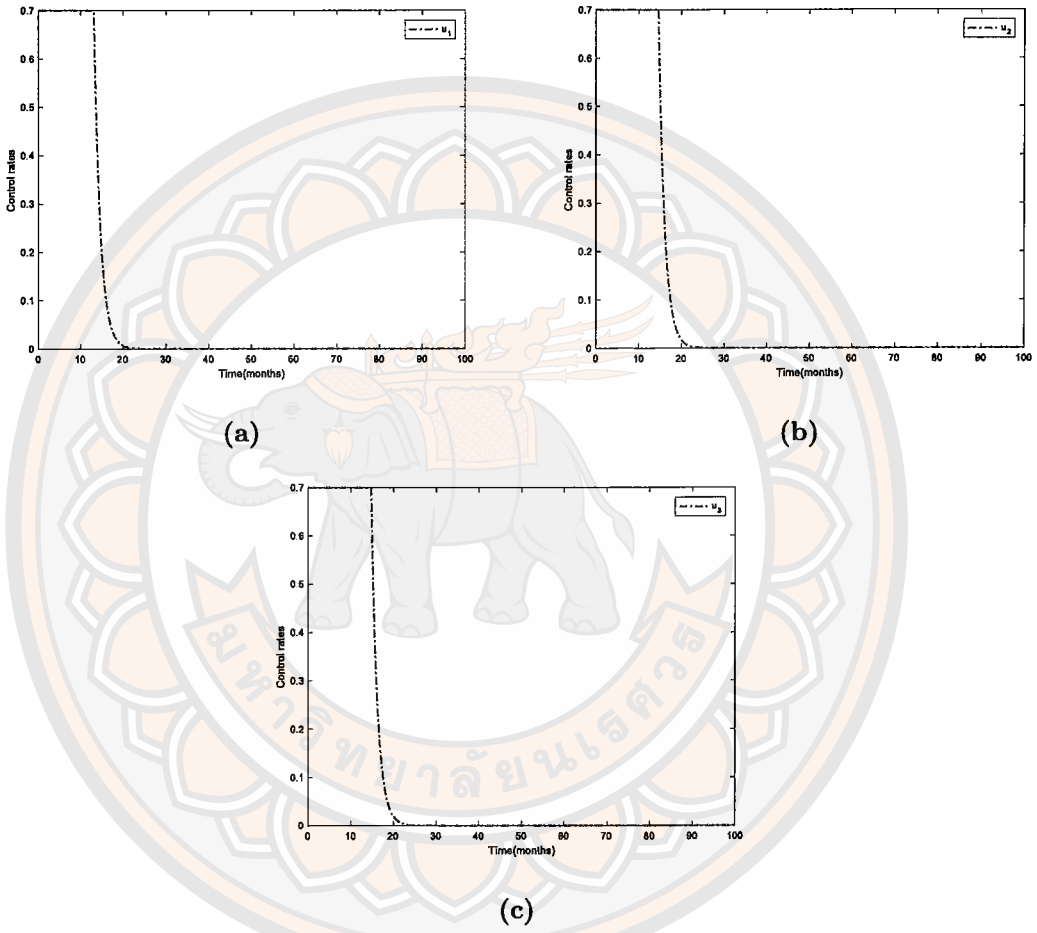

Figure 28 Dynamics of controls (a) Culling infected animals ($u_1(t)$), (b) Elimination of *Brucella* in the environment ($u_2(t)$) and (c) Elimination of *Mycobacterium bovis* in the environment ($u_3(t)$).

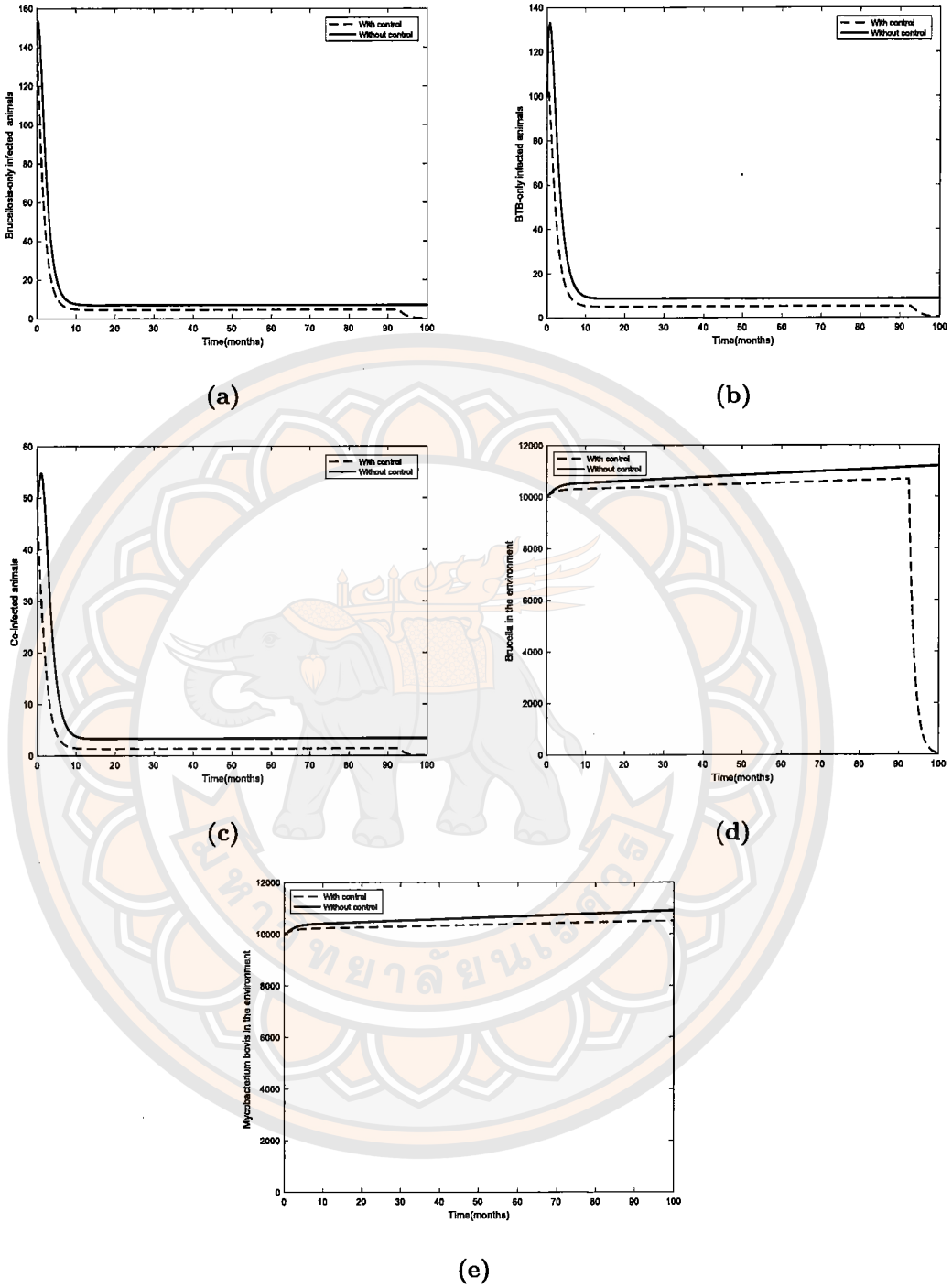

Figure 29 The numerical simulations showcase the optimal control model with the utilization of controls u_1 and u_2. The panels illustrate: (a) Brucellosis-infected animals, (b) Bovine tuberculosis animals (BTB), (c) Co-infection cases, (d) Concentration of *Brucella* in the environment, and (e) Concentration of *Mycobacterium bovis* in the environment.

4.8.2 Strategy B: Control with culling of infected animals and elimination of *Brucella* in the environment.

In this scenario, the controls u_1 and u_2 are employed to optimize the objective function, while u_3 is maintained at zero. As depicted in Fig. 29 (a)-(c), the utilization of controls results in reductions in the numbers of brucellosis animals (I_1), bovine tuberculosis animals (I_2), and co-infection cases (I_{12}) right from the onset of the outbreak. However, these reductions are not substantial enough to drive the numbers down to zero within the initial months. Nevertheless, this strategy guarantees eventual disease elimination. Moreover, Fig. 29 (d) illustrates that relying solely on the elimination of *Brucella* may not suffice to maintain the agent count at low levels. Figure 30 illustrates the control profiles involving culling infected animals and eliminating *Brucella*.

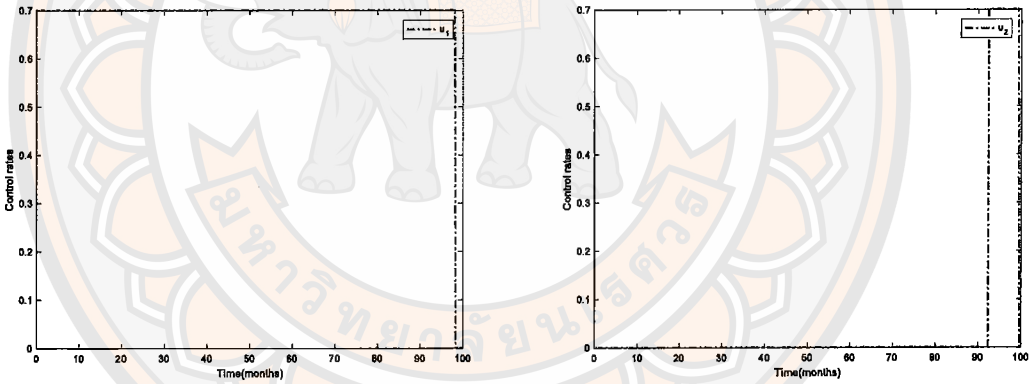

(a) (b)

Figure 30 Dynamics of controls (a) Culling control ($u_1(t)$), (b) Elimination of *Brucella* in the environment ($u_2(t)$).

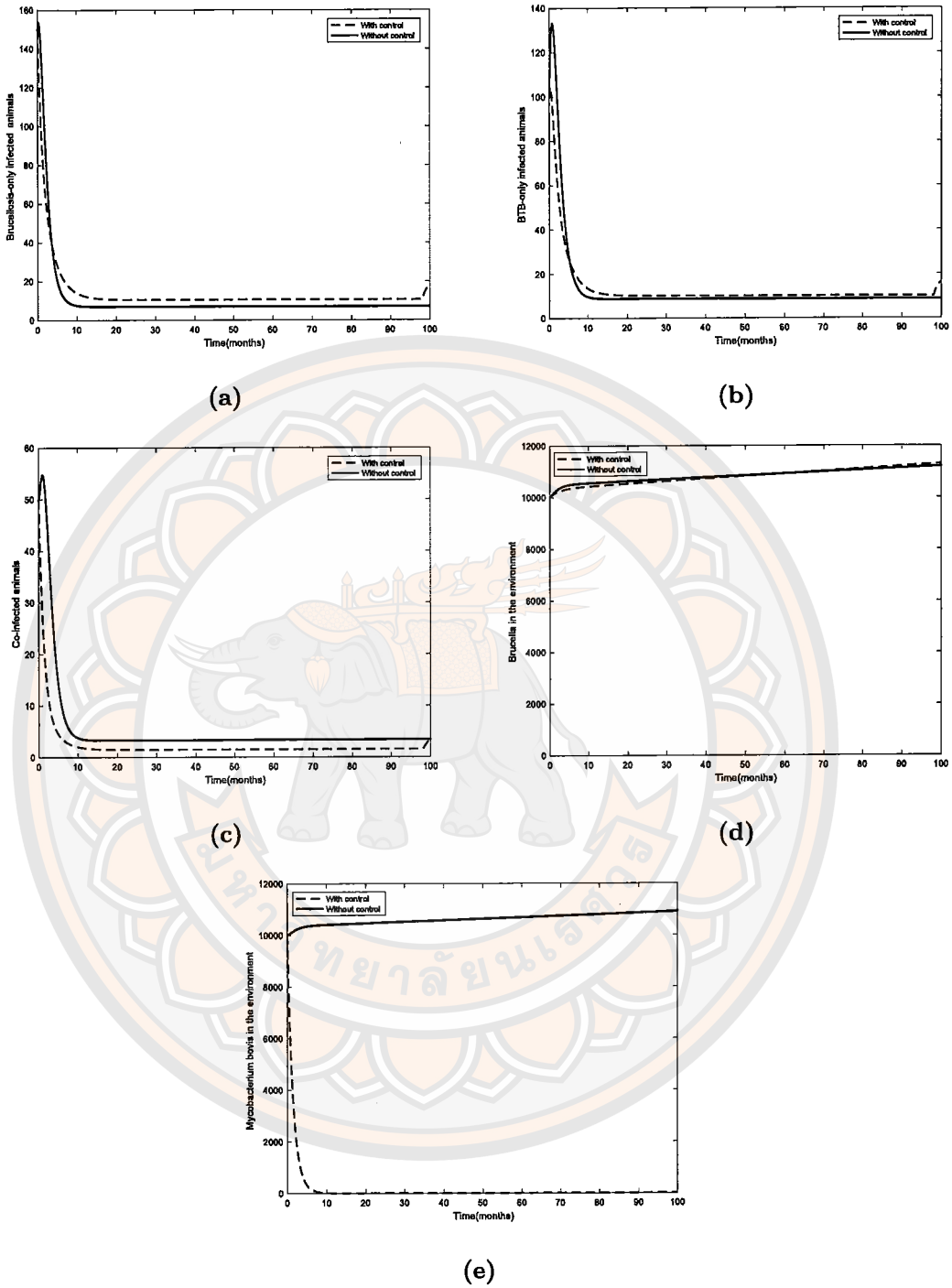

Figure 31 The numerical simulations illustrate the optimal control model utilizing controls u_1 and u_3. The panels display: (a) Brucellosis-infected animals, (b) Bovine tuberculosis animals, (c) Co-infection cases, (d) Concentration of *Brucella* in the environment, and (e) Concentration of *Mycobacterium bovis* in the environment.

4.8.3 Strategy C: Control with culling of infected animals and elimination of *Mycobacterium bovis* in the environment.

Subsequently, we explore the optimization of the objective function using solely u_1 and u_3. Figure 31 (a), (b), and (d) illustrate the quantities of brucellosis-infected animals, bovine tuberculosis-infected animals, and *Brucella* in the environment, respectively. The infection curves for brucellosis and bovine tuberculosis animals exhibit slightly higher levels compared to the uncontrolled scenario in certain segments. However, on average, the two curves seem to display similar trends. Notably, the uncontrolled curves reach higher peaks than those under control measures. Figures 31 (c) and (e) depict the counts of co-infection cases and the concentration of *Mycobacterium bovis* in the environment. The control profile for this strategy is presented in Figure 32. The findings suggest that implementing a culling process is imperative, with subsequent deployment of bovine tuberculosis decontamination measures in the environment.

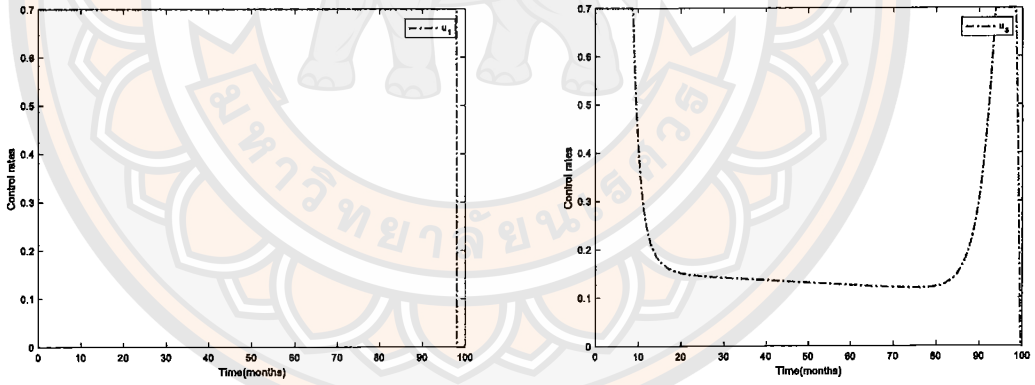

(a) (b)

Figure 32 Control Dynamics: (a) Culling Rate ($u_1(t)$), and (b) Elimination of *Mycobacterium bovis* in the Environment ($u_3(t)$).

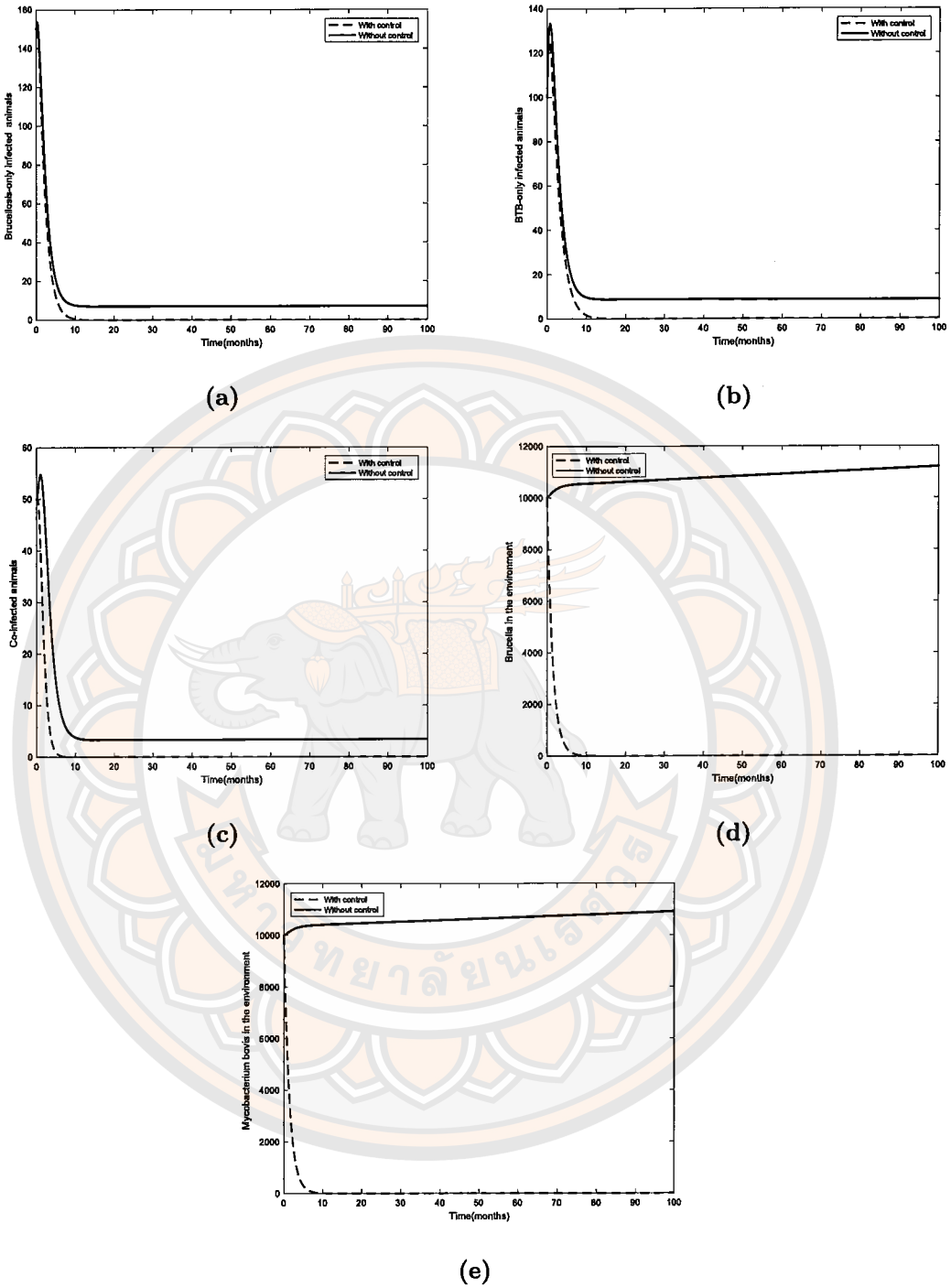

Figure 33 Numerical simulations of the optimal control model utilizing u_2 and u_3 controls. (a) Brucellosis-infected animals, (b) Bovine Tuberculosis animals, (c) co-infection animals, (d) *Brucella* in the environment, and (e) *Mycobacterium bovis* in the environment.

4.8.4 Strategy D: Control with elimination of *Brucella* and *Mycobacterium bovis* in the environment.

Figure 33(a)-(c) indicates that the decline in the number of brucellosis-infected animals, bovine tuberculosis-infected animals, and co-infection animals is slower compared to strategy A, yet the outcomes are more favorable than other strategies. In Fig. 33(d)-(e), the control profiles are displayed, showing similarities to strategy A. The control measures are depicted in Fig 34, revealing that the utilization of only these two controls can substantially reduce the number of agents in the environments.

Based on the aforementioned numerical results, it can be concluded that the synergistic utilization of all control strategies proves notably more effective in mitigating the disease's propagation. Alternatively, if culling is deemed less favorable, solely implementing the process of cleaning contaminated habitats can sufficiently halt the disease's spread over time.

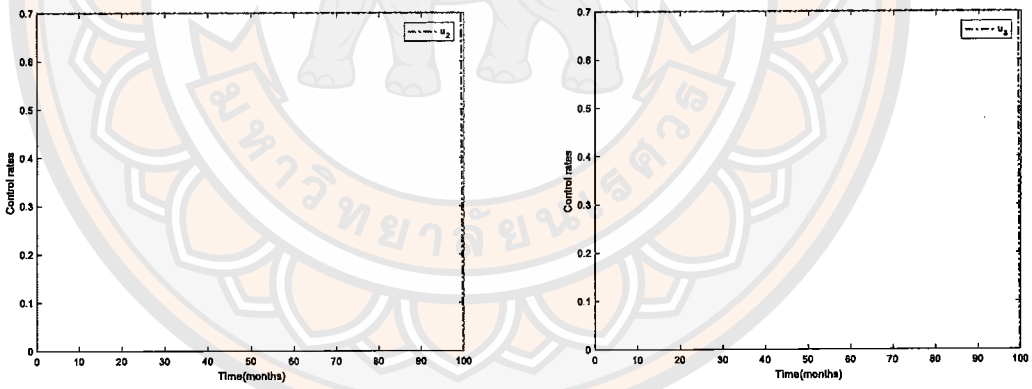

(a) (b)

Figure 34 Dynamics of controls (a) Elimination of *Brucella* in the environment ($u_2(t)$) and (b) Elimination of *Mycobacterium bovis* in the environment ($u_3(t)$).

4.9 Cost-effectiveness analysis

Cost-effectiveness analysis is employed to decide on the most cost-effective control intervention strategy from other strategies. Thus, we calculate two quantities to distinguish between interventions strategies, Average Cost-Effectiveness Ratio (ACER) and Incremental Cost-Effectiveness Ratio (ICER) [62]. The ACER formula is given by

$$\text{ACER} = \frac{\text{Total cost of intervention}}{\text{Total number of infection averted}}.$$

The total number of infections averted above is given as the difference between total infectious animals without control and the total infectious animals with controls. Furthermore, the total cost implemented during the entire period is estimated from

$$C(u) := \int_0^T \left(\frac{c_6 u_1^2 + c_7 u_2^2 + c_8 u_3^2}{2} \right) dt.$$

Table 6 Total infection averted, total cost and ACER.

Strategy	Total infection averted	Cost	ACER
Strategy A	2.4407×10^4	1.0959	4.49×10^{-5}
Strategy B	1.2716×10^4	2.5787	2.0278×10^{-4}
Strategy C	515.6911	2.8960	0.0056
Strategy D	2.0179×10^4	4.8735	2.4152×10^{-4}

Table 6 summarizes the ACER for each strategy. The result shows that the most cost-effective strategy is Strategy A, followed by Strategy B, then Strategy D. The least cost-effective strategy is Strategy C. To further investigate the cost-effectiveness of the various control strategies, we calculate the Incremental Cost-Effectiveness Ratio (ICER). The ICER formula is given by

$$\text{ICER} = \frac{\text{Difference in costs in strategies i and j}}{\text{Difference in infected averted in strategies i and j}}$$

In Table 6, we have that Strategy C averted the least number of infections, followed by Strategy B, Strategy D and Strategy A. Thus, ICER is computed as follow

$$\text{ICER(C)} = \frac{2.8960}{515.6911} = 0.0056$$
$$\text{ICER(B)} = \frac{2.5787 - 2.8960}{1.2716 \times 10^4 - 515.6911} = -2.6008 \times 10^{-5}$$
$$\text{ICER(D)} = \frac{4.8735 - 2.5787}{2.0179 \times 10^4 - 1.2716 \times 10^4} = 3.0749 \times 10^{-4}$$
$$\text{ICER(A)} = \frac{1.0959 - 4.8735}{2.4407 \times 10^4 - 2.0179 \times 10^4} = -8.9347 \times 10^{-4}$$

Table 7 Total infection averted, total cost, and ICER for Strategy C, B, D, and A.

Strategy	Total infection averted	Cost	ICER
Strategy C	515.6911	2.8960	0.0056
Strategy B	1.2716×10^4	2.5787	-2.6008×10^{-5}
Strategy D	2.0179×10^4	4.8735	3.0749×10^{-4}
Strategy A	2.4407×10^4	1.0959	-8.9347×10^{-4}

The computed results indicate that the Incremental Cost-Effectiveness Ratio (ICER) for Strategy C is higher than for Strategy B. This implies that Strategy C is both more expensive and less effective compared to Strategy B. As a result, Strategy C is eliminated from the list of alternative control strategies. Subsequently, a further comparison is made between Strategy B and both Strategy D and Strategy A.

The results for these comparisons are presented in Table 8. When comparing Strategy B to Strategy D, it is evident that ICER(B) is lower than ICER(D), indicating that Strategy D is more expensive and less effective than Strategy B. Consequently, Strategy D is ruled out, leaving Strategy B to be further compared with Strategy A. The outcomes of the ICER computations are detailed in Table 9. These results reveal that Strategy B is dominated by Strategy A, as ICER(B) surpasses ICER(A). This implies that Strategy B is both more costly and less

effective to implement than Strategy A. Therefore, among the four strategies considered, Strategy A, which combines culling infected animals with the elimination of *Brucella* and *Mycobacterium bovis* in the environment, emerges as the most cost-effective option.

Table 8 Total infection averted, total cost, and ICER for Strategy B, D, and A.

Strategy	Total infection averted	Cost	ICER
Strategy B	1.2716×10^4	2.5787	2.0279×10^{-4}
Strategy D	2.0179×10^4	4.8735	3.0749×10^{-4}
Strategy A	2.4407×10^4	1.0959	-8.9347×10^{-4}

Table 9 Total infection averted, total cost, and ICER for Strategy B and A.

Strategy	Total infection averted	Cost	ICER
Strategy B	1.2716×10^4	2.5787	2.0279×10^{-4}
Strategy A	2.4407×10^4	1.0959	-1.2683×10^{-4}

4.10 Applications to real-world data

In this section, we will apply our model using available real-world data. Despite our efforts, we encountered limited sources of data for brucellosis and tuberculosis, and unfortunately, no data on the co-infection of these diseases is available. Nevertheless, we did come across a research paper that discussed the detection of co-infection of these two diseases during animal slaughter screenings. As a result, we will present our analysis for brucellosis and tuberculosis infections individually and then address the aspect of co-infection.

To begin, Kabiru Akinyemi and colleagues conducted a comprehensive review of human and animal brucellosis in Nigeria spanning from 2001 to 2021, en-

compassing data collected from the six geopolitical zones [63]. The data obtained from this study is represented by star markers in Fig. 35. In order to fit this data, we have adjusted certain parameters as follows: $\Lambda = 410$, $\mu = 0.007$, $\delta_{11} = 0.0005$, $\delta_{22} = 0.002$, $\delta_{12} = 0.35$, $\gamma = 0.0004$, $\xi_1 = 0.7$, $\xi_2 = 2.2$, $d_1 = 0.00005$, $d_2 = 0.00005$, $\phi_1 = 0.01$, $\phi_2 = 0.01$, $\beta_{11} = 0.001$, $\beta_{01} = 0.00001$, $\beta_{22} = 1.00995 \times 10^{-2}$, $\beta_{02} = 1.00995 \times 10^{-5}$, $\alpha_1 = 0.00000000015$, and $\alpha_2 = 0.0000015$. These parameter values do not differ significantly from the initial values listed in Table 3.

In Fig. 35, the solid line illustrates the curve generated by our model without any control interventions. On the other hand, the dashed line represents the curve produced by the control model. Notably, the model exhibits a similar infection trend, and our control model demonstrates analogous behavior. However, for accurate alignment with actual data, some modifications to the model are necessary. This is due to our model being formulated based on simulation results from other research papers. Nonetheless, the depicted figure suggests that our model holds potential for predicting the brucellosis trend in Nigeria. This predictive capability can assist authorities in implementing effective measures to control the disease.

We proceeded to examine the occurrence of tuberculosis infection in animals in Great Britain [64]. The tuberculosis data pertaining to cattle covered the period from 1996 to 2023, as recorded by the Animal and Plant Health Agency (APHA) work management IT support system. To achieve alignment with this dataset, we made adjustments to our parameters as follows: $\Lambda = 400$, $\mu = 0.0007$, $\delta_{11} = 0.15$, $\delta_{22} = 0.002$, $\delta_{12} = 0.35$, $\gamma = 0.0004$, $\xi_1 = 1$, $\xi_2 = 2.42$, $d_1 = 0.00005$, $d_2 = 0.00005$, $\phi_1 = 0.001$, $\phi_2 = 0.001$, $\beta_{11} = 0$, $\beta_{01} = 0$, $\beta_{22} = 1.00995 \times 10^{-2}$, $\beta_{02} = 1.00995 \times 10^{-5}$, $\alpha_1 = 0.00035$, and $\alpha_2 = 0.00015$. Notably, these parameter adjustments do not deviate significantly from the initial values listed in Table 1.

The outcomes of this fitting process are illustrated in Fig. 36. Here, the solid line corresponds to our original model (without control), while the dashed line portrays the modified control model, which illustrates the infection trend when adhering to the control guidelines inferred from our simulations. It is evident that our model for tuberculosis infection in cattle within Great Britain closely resembles the actual data trend.

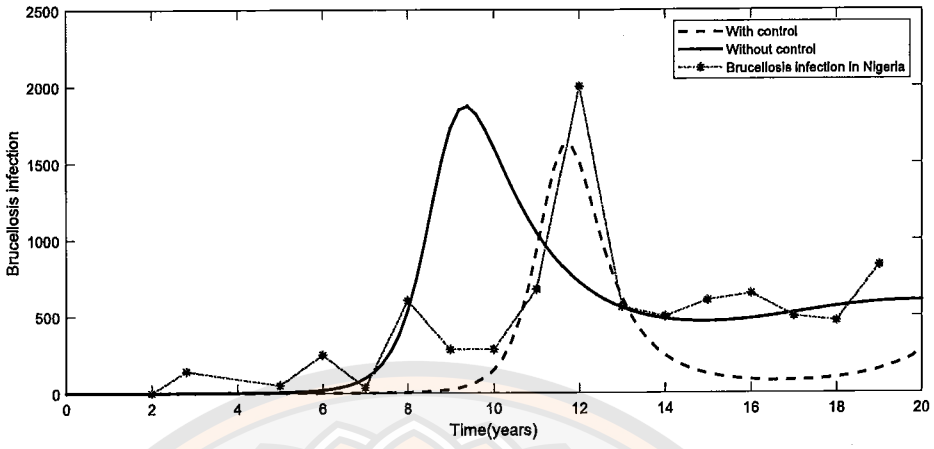

Figure 35 Brucellosis trends in Nigeria and model projections

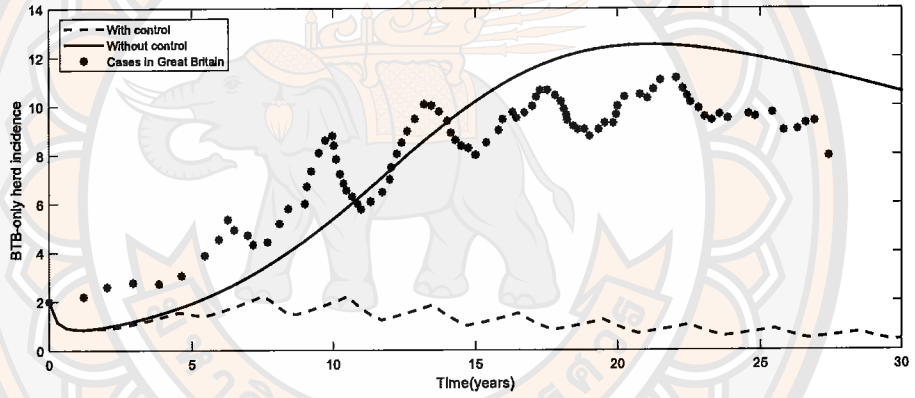

Figure 36 Tuberculosis patterns in Great Britain [64] and model predictions

Our search did not yield data on the co-infection of brucellosis and tuberculosis among animals. However, we did find information regarding the detection of co-infection of these two diseases in Nigeria during the screening of animals for slaughter. Simeon I.B. Cadmus, et al., presented a case report in *Veterinaria Italiana* [65] describing the discovery of co-infection of brucellosis and tuberculosis in slaughtered cattle in Ibadan, Nigeria. The study revealed that approximately 3 percent of the slaughtered animals were co-infected. Although the report lacked yearly data for co-infection cases, it indicated that the initially brucellosis-infected animals were co-infected with tuberculosis. Consequently, we assumed that 3 percent of animals infected with brucellosis were also co-infected with tuberculosis.

As depicted in Fig.35, we employed this available data to simulate the co-infection of these diseases, as illustrated in Fig.37. To align with the data, we adjusted certain parameter values as follows: $\Lambda = 320$, $\mu = 0.007$, $\delta_{11} = 0.0015$, $\delta_{22} = 0.002$, $\delta_{12} = 0.035$, $\gamma = 0.00004$, $\xi_1 = 1$, $\xi_2 = 2$, $d_1 = 0.0005$, $d_2 = 0.0005$, $\phi_1 = 0.2$, $\phi_2 = 0.0001$, $\beta_{11} = 0.01$, $\beta_{01} = 0.01$, $\beta_{22} = 1.00995 \times 10^{-5}$, $\beta_{02} = 1.00995 \times 10^{-5}$, $\alpha_1 = 0.0000035$, and $\alpha_2 = 0.00015$. Notably, our model demonstrates a trend similar to the real data, reinforcing its relevance and potential utility.

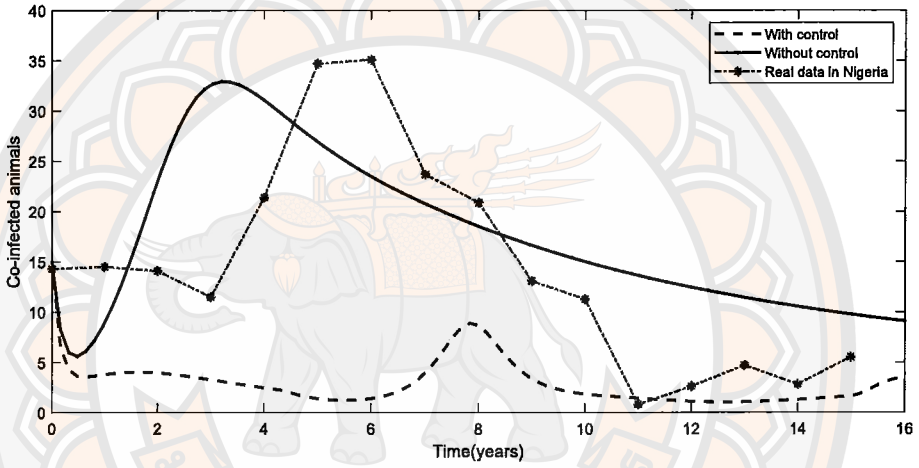

Figure 37 Co-infection data (3 percent of brucellosis cases) and our model

CHAPTER V

DISCUSSION AND CONCLUSION

This chapter presents all the results obtained in this dissertation. We have established and analyzed the mathematical model for Brucellosis infection in bison, as well as the mathematical model for the co-infection of brucellosis and bovine tuberculosis. The discussion and conclusion can be found below.

Mathematical model of brucellosis infection in bison

In Chapter 3, we presented a Brucellosis epidemiological model in bison that incorporates vaccination for susceptible individuals, elimination of Brucella in the environment, and culling of infected animals. First, the basic reproduction number R_0 of this model is determined. The numerical simulations of the reproduction numbers of the two models (with and without controls) are also compared. Then the two equilibrium points, the disease-free and the endemic are determined. From our analysis, the disease-free equilibrium point is both locally and globally asymptotically stable if $R_0 < 1$ while the endemic equilibrium exists uniquely and is globally asymptotically stable if $R_0 > 1$. Based on the sensitivity analysis of the basic reproduction number R_0 on the given parameters, we suggest that the vaccination rate for susceptible individuals is useful to control strategies in reducing the value of R_0. Finally, we have formulated the optimal control problem to minimize the total number of infected animals while also minimizing the cost of controls. Our results have interpreted that combining all three controls can significantly reduce the total number of chronic and infectious animals. Our several numerical simulations suggest that vaccination strategy is the best control if applicable. In some remote areas, the combination of sanitation or eliminating Brucella in the environment control and the culling strategy is an option. We also have investigated that only culling infected animals can reduce the number of total infections as well. This scenario was also observed in [17]. However, it will not prevent the second round of the disease outbreak. Therefore, a proper

and safe culling strategy is needed if only this control measure presents at a farm.

Mathematical model of brucellosis and bovine tuberculosis co-infection

In Chapter 4, we have developed a deterministic mathematical model to explore the spread of co-infection between brucellosis and bovine tuberculosis. Our model incorporates strategies such as culling of infected animals and the elimination of *Brucella* and *Mycobacterium bovis* from the environment. Through our analysis, we have determined that the brucellosis submodel and the bovine tuberculosis submodel exhibit both locally and globally asymptotically stable disease-free equilibria when their respective basic reproduction numbers are below unity. Conversely, when the basic reproduction numbers exceed unity, the endemic equilibrium points are found to be both locally and globally stable.

Furthermore, the complete brucellosis-bovine tuberculosis model displays a locally asymptotically stable disease-free equilibrium when the basic reproduction number is less than unity. Interestingly, the model also exhibits the phenomenon of backward bifurcation under specific conditions. This implies that the model demonstrates the coexistence of disease-free and endemic equilibria when the basic reproduction number is less than unity.

We have also conducted sensitivity analysis, which indicates that controlling the elimination rates of *Brucella* and *Mycobacterium bovis* in the environment plays a crucial role in reducing the values of R_B and R_T, respectively. Additionally, we formulated an optimal control problem to minimize the overall number of infected animals while simultaneously minimizing control implementation costs.

Our numerical simulations of optimal control strategies reveal that the most effective approach is to combine all controls, encompassing culling of infected animals and the elimination of *Brucella* and *Mycobacterium bovis* from the environments. This finding is supported by our cost-effectiveness analysis, where we calculated ACER and ICER. Consequently, Strategy A, which encompasses all controls, emerges as the most cost-effective strategy.

We have introduced our model and demonstrated its fitting capabilities

with real-world data. Throughout our study, we delved into related research papers, many of which were quite intriguing. Therefore, we will engage in a comparative analysis between those models and our own, using the real data presented in the preceding sections.

Model 1, proposed by Stephen A. et al. [19] in 2022, encompasses five equations and draws conclusions that align closely with our model's ideas. Model 2, presented by Emmanuel A. et al. [15] in 2015, aims to represent the dynamics of brucellosis among bison. Both of these models primarily focus on brucellosis infection, which led us to consider our model's applicability solely to this disease. The outcome is illustrated in Fig. 38, where the solid line represents our model and the dashed line signifies our optimal control model. Both curves exhibit trends similar to the actual data on brucellosis infection in Nigeria.

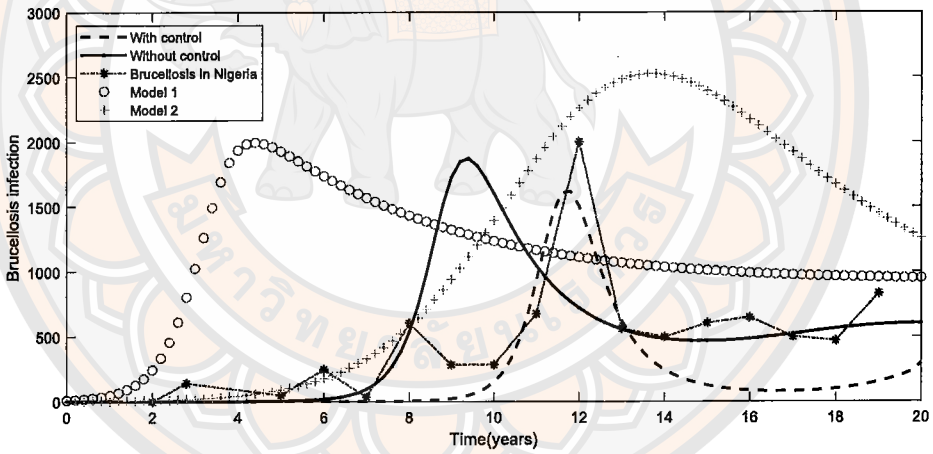

Figure 38 Brucellosis infection.

Subsequently, we undertake a comparison between our model and two alternative models focusing on tuberculosis infection. Model 1, introduced by Mahamat Fayiz A. et al. [47] in 2017, involves both human and cattle populations. However, since humans do not impact animals in this context, we can make relevant comparisons with our model. Model 2, devised by Tasmi et al. [46] in 2016, originally targeted the badger population with a vaccination strategy. We can conduct a comparison with our model to gain insights. The comparative analysis of these two models alongside ours is presented in Fig.39.

In an effort to align the parameter values of the other two models with actual tuberculosis data, adjustments were made. However, achieving a perfect fit for these models with our data remains challenging at present, and further modifications might be necessary. As illustrated in Fig. 39, our original model (depicted by the solid line) exhibits a similar trend to the actual data. Additionally, the optimal control model showcases the potential reduction in tuberculosis infection if one adheres to the guidelines proposed in the preceding sections.

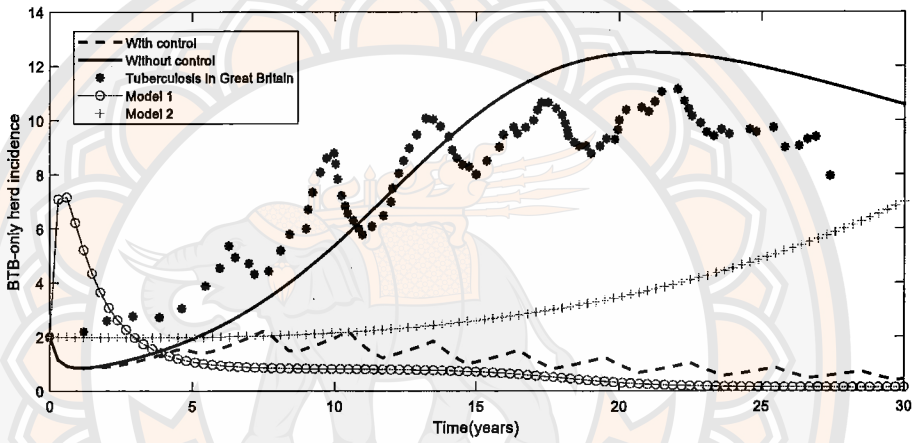

Figure 39 Tuberculosis infection.

Regarding co-infection models, we have identified just one mathematical model available for comparison. This model (Model 1), introduced by Paride O. Lolika et al. in 2021 [48], was designed within a periodic environment to study culling as a potential control measure. In an attempt to align the model with our data, we adjusted certain parameter values. However, despite our efforts, we were unable to achieve a perfect fit between the model and the data. Nevertheless, consistent with our findings in other instances, our model captures the infection trend, as demonstrated in Fig 40.

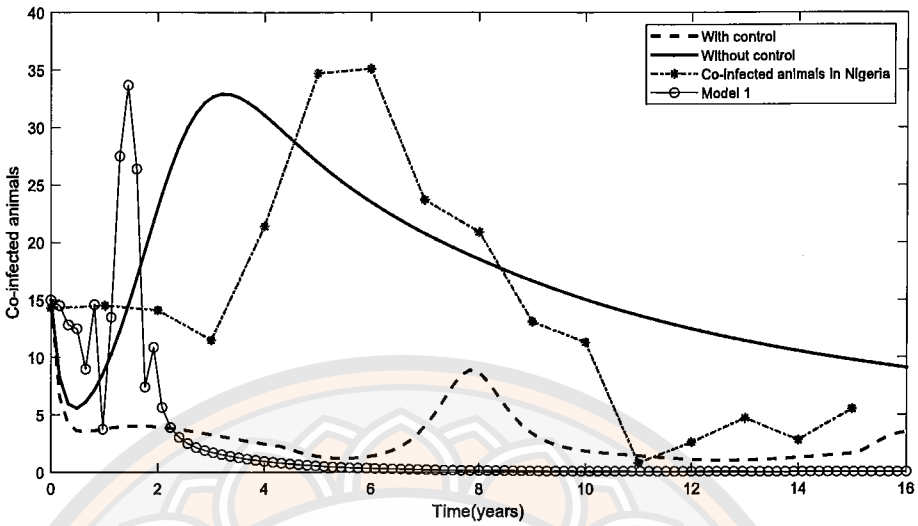

Figure 40 Co-infection of brucellosis and tuberculosis.

As demonstrated, our model can be adjusted to accommodate certain datasets. However, for enhanced accuracy, it is essential to initiate our work with actual data from specific locations. This will be the focus of our future endeavors in the realm of mathematical modeling, allowing us to gain deeper insights and refine our approach.

REFERENCES

REFERENCES

1. Zhou, K., Wu, B., Pan, H., Paudyal, N., Jiang, J., Zhang, L., Li, Y., Yue, M. ONE health approach to address zoonotic brucellosis: a spatiotemporal associations study between animals and humans. Frontiers in Veterinary Science. 2020;7(521):1-10.

2. Corbel, M. J. Brucellosis in humans and animals. Geneva: World Health Organization; 2006.

3. Millar, M., Stack, J. Brucellosis–what every practitioner should know. In Practice. 2012;34(9):532-539.

4. Brucellosis [Internet]. Paris: World Organisation for Animal Health; 1924 [cited 2022 Aug 1]. Available from: https://www.woah.org/en/disease/brucellosis/.

5. Spickler AR. Brucellosis [Internet]. United States: The Center for Food Security and Public Health; c2004-2024 [updated 2018 May 1; cited 2022 Aug 1]. Available from: http://www.cfsph.iastate.edu/Factsheets/pdfs/brucellosis.pdf.

6. Brucellosis Undulant Fever [Internet]. United States: The Center for Food Security and Public Health; c2004-2024 [updated 2018 Apr 1; cited 2022 Aug 1]. Available from: http://www.cfsph.iastate.edu/FastFacts/pdfs/brucellosis_F.pdf.

7. Richey, E.J., Harrell, C.D. Brucella abortus disease (brucellosis) in beef cattle. University of Florida Cooperative Extension Service, Institute of Food and Agriculture Sciences, EDIS; 1997.

8. Segwagwe, B.E., Samkange, A., Mushonga, B., Kandiwa, E., Ndazigaruye, G. Prevalence and risk factors for brucellosis seropositivity in cattle in Nyagatare District, Eastern Province, Rwanda. Journal of the South African Veterinary Association. 2018;89(1):1-8.

9. Akakpo, A.J., Têko-Agbo, A., Koné, P. The impact of brucellosis on the economy and public health in Africa. Compendium of technical items presented to the OIE World Assembly of Delegates or to OIE Regional Commissions. 2009;2010:85-98.

10. Kazak, E., Akalın, H., Yılmaz, E., Heper, Y., Mistik, R., Sinirtaş, M., Özakin, C., Göral, G., Helvaci, S., Brucellosis: a retrospective evaluation of 164 cases, Singapore medical journal. 2016;57(11):624-629.

11. Aitken, I.D. Diseases of Sheep. 4th ed. Oxford: Blackwell Publishing Ltd; 2007.

12. Hou, Q., Sun, X., Zhang, J., Liu, Y., Wang, Y., Jin, Z. Modeling the transmission dynamics of sheep brucellosis in Inner Mongolia Autonomous Region, China. Mathematical biosciences. 2013;242(1):51-58.

13. Sun, G. Q., Zhang, Z. K. Global stability for a sheep brucellosis model with immigration. Applied Mathematics and Computation. 2014;246:336-345.

14. Li, M., Sun, G., Zhang, J., Jin, Z. Transmission dynamics of a multi-group brucellosis model with mixed cross infection in public farm. Applied Mathematics and Computation. 2014;237:582-594.

15. Abatih, E., Ron, L., Speybroeck, N., Williams, B., Berkvens, D. Mathematical analysis of the transmission dynamics of brucellosis among bison. Mathematical Methods in the Applied Sciences, 2015;38(17):3818-3832.

16. Yang, C., Lolika, OP., Mushayabasa, S., Wang, J. Modeling the spatiotemporal variations in brucellosis transmission. Nonlinear Analysis: Real World Applications. 2017;38:49-67.

17. Lolika, P. O., Modnak, C., Mushayabasa, S. On the dynamics of brucellosis infection in bison population with vertical transmission and culling. Mathematical biosciences. 2018;305:42-54.

18. Nyerere, N., Luboobi, L.S., Mpeshe, S.C. and Shirima, G.M. Optimal control strategies for the infectiology of brucellosis. International Journal of Mathematics and Mathematical Sciences. 2020;2020:1-17.

19. Abagna, S., Seidu, B., Bornaa, C.S. A mathematical model of the transmission dynamics and control of bovine brucellosis in cattle. Abstract and Applied Analysis, Hindawi. 2022;2022:1-10.

20. World Health Organization, United Kingdom. Dept. for International Development. Animal Health Program, Food and Agriculture Organization of the United Nations & World Organisation for Animal Health. The control of neglected zoonotic diseases : a route to poverty alleviation : report of a joint WHO/DFID-AHP meeting, 20 and 21 September 2005. Geneva: World Health Organization; 2006.

21. Bovine Tuberculosis [Internet]. United States: The Center for Food Security and Public Health; c2004-2024 [updated 2009 Jul 1; cited 2022 Aug 1]. Available from: https://www.cfsph.iastate.edu/FastFacts/pdfs/bovine_tuberculosis.pdf.

22. Bovine tuberculosis [Internet]. Paris: World Organisation for Animal Health; 1924 [cited 2022 Aug 1]. Available from: https://www.woah.org/en/disease/ bovine-tuberculosis/.

23. World Health Organization. Global tuberculosis report 2017. Geneva: World Health Organization. 2017.

24. Bovine Tuberculosis (TB) [Internet]. United States: The Center for Food Security and Public Health; c2004-2024 [updated 2006 Jan 1; cited 2022 Aug 1]. Available from: https://www.cfsph.iastate.edu/FastFacts/pdfs/ bovine_tuberculosis_F.pdf.

25. Yahyaoui Azami, H., Ducrotoy, M.J., Bouslikhane, M., Hattendorf, J., Thrusfield, M., Conde-Alvarez, R., Moriyón, I., Zúñiga-Ripa, A., Muñoz Álvaro, P.M., Mick, V., Bryssinckx, W. The prevalence of brucellosis and bovine tuberculosis in ruminants in Sidi Kacem Province, Morocco. PloS one. 2018;13(9):1-17.

26. Tschopp, R., Abera, B., Sourou, S.Y., Guerne-Bleich, E., Aseffa, A., Wubete, A., Zinsstag, J. and Young, D. Bovine tuberculosis and brucellosis prevalence in cattle from selected milk cooperatives in Arsi zone, Oromia region, Ethiopia. BMC veterinary research. 2013;9:1-9.

27. Dahourou, L.D., Ouoba, L.B., Minoungou, L.B.G., Tapsoba, A.R.S., Savadogo, M., Yougbaré, B., Traoré, A., Alambédji, R.B. Prevalence and factors associated with brucellosis and tuberculosis in cattle from extensive husbandry systems in Sahel and Hauts-Bassins regions, Burkina Faso. Scientific African. 2023;19:e01570.

28. Cadmus, S.I., Adesokan, H.K., Stack, J.A. Co-infection of brucellosis and tuberculosis in slaughtered cattle in Ibadan, Nigeria: a case report. Vet Ital. 2008;44:557-558.

29. Gorsich, E.E. Disease invasion dynamics: brucellosis and tuberculosis in African buffalo (Syncerus caffer) [dissertation]. Corvallis (OR): Oregon State University; 2013.

30. Folitse, R., Boi-Kikimoto, B.B., Emikpe, B., Atawalna, J. The prevalence of Bovine tuberculosis and brucellosis in cattle from selected herds in Dormaa and Kintampo Districts, Brong Ahafo region, Ghana. Archives of Clinical Microbiology. 2014;5(2):1-6.

31. Tumwiine, J., Robert, G. A mathematical model for treatment of bovine brucellosis in cattle population. Journal of Mathematical Modeling. 2017;5(2):137-152.

32. Aïnseba, B.E., Benosman, C., Magal, P. A model for ovine brucellosis incorporating direct and indirect transmission. Journal of biological dynamics. 2010;4(1):2-11.

33. Li, C., Guo, Z.G., Zhang, Z.Y. Transmission dynamics of a brucellosis model: Basic reproduction number and global analysis. Chaos, Solitons & Fractals, 2017;104:161-172.

34. Hou, Q., Sun, X., Zhang, J., Liu, Y., Wang, Y., Jin, Z. Modeling the transmission dynamics of sheep brucellosis in Inner Mongolia Autonomous Region, China. Mathematical biosciences. 2013;242(1):51-58.

35. Li, M., Sun, G., Zhang, J., Jin, Z., Sun, X., Wang, Y., Huang, B. and Zheng, Y. Transmission dynamics and control for a brucellosis model in Hinggan League of Inner Mongolia, China. Mathematical Biosciences & Engineering. 2014;11(5):1115-1137.

36. Nyerere, N., Luboobi, L.S., Mpeshe, S.C., Shirima, G.M. Mathematical model for the infectiology of brucellosis with some control strategies. New Trends in Mathematical Sciences. 2010;7(4):387-405.

37. Assis, L.M.E.D., Massad, E., Assis, R.A.D., Martorano, S.R., Venturino, E. A mathematical model for bovine tuberculosis among buffaloes and lions in the Kruger National Park. Mathematical Methods in the Applied Sciences. 2018;41(2):525-543.

38. Liu, S., Li, A., Feng, X., Zhang, X., Wang, K. A dynamic model of human and livestock tuberculosis spread and control in Urumqi, Xinjiang, China, Computational and mathematical methods in medicine. 2016;2016:1-10.

39. Agusto, F.B., Lenhart, S., Gumel, A.B., Odoi, A. Mathematical analysis of a model for the transmission dynamics of bovine tuberculosis. Mathematical Methods in the Applied Sciences, 2011;34(15):1873-1887.

40. Hassan, A.S., Garba, S.M., Gumel, A.B., Lubuma, J.S.: Dynamics of Mycobacterium and bovine tuberculosis in a human-buffalo population. Computational and mathematical methods in medicine, 2014;2014:1-20.

41. Phepa, P.B., Chirove, F., Govinder, K.S. Modelling the role of multi-transmission routes in the epidemiology of bovine tuberculosis in cattle and buffalo populations. Mathematical Biosciences, 2016;277:47-58.

42. Shirima Sabini, T., Ismail Irunde, J., Kuznetsov, D. Modeling the transmission dynamics of bovine tuberculosis, International Journal of Mathematics and Mathematical Sciences. 2020;2020;1-14.

43. Silva, C.J., Torres, D.F. Optimal control for a tuberculosis model with reinfection and post-exposure interventions. Mathematical Biosciences, 2013;244(2):154-164.

44. Aldila, D., Latifah, S.L., Dumbela, P.A. Dynamical analysis of mathematical model for Bovine Tuberculosis among human and cattle population. Commun. Biomath. Sci. 2019;2(1):55-64.

45. Kasereka Kabunga, S., Doungmo Goufo, E.F., Ho Tuong, V. Analysis and simulation of a mathematical model of tuberculosis transmission in Democratic Republic of the Congo. Advances in Difference Equations. 2020;2020(1):1-19.

46. Tasmi, Aldila, D., Soewono, E., Nuraini, N. Mathematical model for transmission of tuberculosis in badger population with vaccination. AIP Conference Proceedings. 2016;1723(1):1-7.

47. Mahamat Fayiz, A., Hind Yahyaoui, A., Philipp Justus, B., Lisa, C., Petra, L., Mirjam, L., Nakul, C., Jakob Z. Transmission dynamics and elimination potential of zoonotic tuberculosis in morocco. PLOS Neglected Tropical Diseases. 2017;11(2):1-17.

48. Lolika, P.O., Bakhet, M.Y., Lagure, B.S. Modeling co-infection of bovine brucellosis and tuberculosis. Asian Research Journal of Mathematics. 2021;17(8): 1-13.

49. Van den Driessche, P., Watmough, J. Reproductive numbers and subthreshold endemic equilibria for compartment models of disease transmission. Math. Biosci. 2002;180:29-48.

50. Castillo-Chavez, C., Song, B. Dynamical models of tuberculosis and their applications. Mathematical Biosciences & Engineering. 2004;1(2):361-404.

51. Castillo-Chavez, C., Feng, Z., Huang, W. On the computation of R_0 and its role on global stability. Mathematical approaches for emerging and reemerging infectious diseases: an introduction. 2002;125:229-250.

52. Li, M.Y., Muldowney, J.S. A geometric approach to global-stability problems. SIAM Journal on Mathematical Analysis. 1996;27(4):1070-1083.

53. Li, M.Y., Wang, L. A criterion for stability of matrices. Journal of mathematical analysis and applications. 1998;225(1):249-264.

54. Chong, K. M. The arithmetic mean-Geometric mean inequality: A new proof. Mathematics Magazine. 1976;49(2):87-88.

55. Khalil, H. K. Nonlinear Systems. 3rd ed. United States: Prentice Hall, Upper Saddle River; 2002.

56. Hamby, D.M. A review of techniques for parameter sensitivity analysis of environmental models. Environmental monitoring and assessment. 1994;32(2):135-154.

57. Ngoteya, F. N., Gyekye, Y. N. Sensitivity analysis of parameters in a competition model. Applied and Computational Mathematics. 2015;4(5):363-368.

58. Chitnis, N., Hyman, J. M., Cushing, J. M. Determining important parameters in the spread of malaria through the sensitivity analysis of a mathematical model. Bulletin of mathematical biology. 2008;70(5):1272-1290.

59. Pontryagin, L. S., Boltyanskiy, V. G., Gamkrelidze, R. V., Mishchenko, E. F. Mathematical theory of optimal processes. Wiley Interscience, New York. 1962.

60. Lenhart S, Wortman J. Optimal control applied to biological models. Boca Raton: Crc Press; 2007.

61. Carr, J. Applications of center manifold theory. Berlin: springer-verlag; 1981.

62. Okosun, K.O., Rachid, O., Marcus, N. Optimal control strategies and cost-effectiveness analysis of a malaria model. BioSystems, 2013;111(2);83-101.

63. Akinyemi, K.O., Fakorede, C.O., Amisu, K.O., Wareth, G., Human and Animal Brucellosis in Nigeria: A Systemic Review and Meta-Analysis in the Last Twenty-One Years (2001-2021). Veterinary Sciences, MDPI. 2022;384(9): 1-24.

64. Guidance on the data and methodology used for the statistics on the Incidence TB in Cattle in GB [Internet]. London: Department for Environment, Food and Rural Affairs and Animal and Plant Health Agency; 2015 [updated 2022 Mar 9; cited 2023 Aug 1]. Available from: https://www.gov.uk/government/publications/data-and-methodology.

65. Cadmus, S.I., Adesokan, H.K., Stack, J.A. Co-infection of brucellosis and tuberculosis in slaughtered cattle in Ibadan, Nigeria: a case report. Vet Ital. 2008;44:557-558.